OAK RIDGE NATIONAL LABORATORY

operated by

UNION CARBIDE CORPORATION

for the

U.S. ATOMIC ENERGY COMMISSION

MARTIN MARIETTA ENERGY SYSYEMS LIBRARIES

3 4456 0323034 0

OAK RIDGE NATIONAL LABORATORY
CENTRAL RESEARCH LIBRARY
DOCUMENT COLLECTION
LIBRARY LOAN COPY
DO NOT TRANSFER TO ANOTHER PERSON
If you wish someone else to see this document, send in name with document and the library will arrange a loan.

CENTRAL RESEARCH LIBRARY
DOCUMENT COLLECTION

ORNL-RSIC-26
UC-34 — Physics

23

THE ATTENUATION PROPERTIES OF CONCRETE FOR SHIELDING OF NEUTRONS OF ENERGY LESS THAN 15 MeV

Fritz A. R. Schmidt

RADIATION SHIELDING INFORMATION CENTER

Printed in the United States of America. Available from Clearinghouse for Federal Scientific and Technical Information, National Bureau of Standards, U.S. Department of Commerce, Springfield, Virginia 22151
Price: Printed Copy $3.00; Microfiche $0.65

LEGAL NOTICE

This report was prepared as an account of Government sponsored work. Neither the United States, nor the Commission, nor any person acting on behalf of the Commission:

A. Makes any warranty or representation, expressed or implied, with respect to the accuracy, completeness, or usefulness of the information contained in this report, or that the use of any information, apparatus, method, or process disclosed in this report may not infringe privately owned rights; or

B. Assumes any liabilities with respect to the use of, or for damages resulting from the use of any information, apparatus, method, or process disclosed in this report.

As used in the above, "person acting on behalf of the Commission" includes any employee or contractor of the Commission, or employee of such contractor, to the extent that such employee or contractor of the Commission, or employee of such contractor prepares, disseminates, or provides access to, any information pursuant to his employment or contract with the Commission, or his employment with such contractor.

MARTIN MARIETTA ENERGY SYSYEMS LIBRARIES

3 4456 0323034 0

ORNL-RSIC-26

Contract No. W-7405-eng-26

Neutron Physics Division

Radiation Shielding Information Center

THE ATTENUATION PROPERTIES OF CONCRETE FOR SHIELDING OF NEUTRONS OF ENERGY LESS THAN 15 MeV

Fritz A. R. Schmidt*

NOTE:

This Work Partially Supported by
DEFENSE ATOMIC SUPPORT AGENCY
Under Subtask PE 055

AUGUST 1970

*Present address: Institut für Kernenergetik Universität Stuttgart, Germany

OAK RIDGE NATIONAL LABORATORY
Oak Ridge, Tennessee
operated by
UNION CARBIDE CORPORATION
for the
U.S. ATOMIC ENERGY COMMISSION

CONTENTS

Acknowledgement v

Abstract 1

I. Introduction. 1

II. Literature Review

1. Analytical Approximation of Radiation Transport in Concrete. . 6

A. Neutron Transmission 7

B. Secondary Gamma Rays 14

2. Neutron Transmission 18

3. Neutron Reflection-Albedos 34

4. Secondary Gamma Radiation 38

5. 14-MeV Neutrons 46

6. Special Concretes 50

7. Conclusions. 56

III. Cross Sections for Concrete

1. Removal Cross Sections 59

2. Intermediate- and Thermal-Neutron Cross Sections 63

3. Gamma-Ray Attenuation Data 66

A. Coefficients for Berger's Gamma-Ray Buildup Formula . . . 66

B. Values for the ψ_o and ψ_1 Functions 67

C. Gamma-Ray Attenuation Coefficients 68

4. Thermal-Neutron Capture Gamma-Ray Yields 68

5. Data Library

A. Neutron Data 74

B. Gamma-Ray Interaction Data 75

C. Thermal-Neutron Capture Gamma-Rays 75

D. Epithermal-Neutron Capture Gamma-Rays 75

E. Gamma Rays from Other Reactions 75

IV. Slab Transmission Factors for Neutron and Gamma-Ray Dose Equivalent

1. Calculations of the Transmission Factors 80

2. Use of the Transmission Factors 84

3. Results Obtained using the Transmission Factors and Comparisons with Various Other Calculations 87

References 105

Appendix A - Miscellaneous Data 114

Appendix B - Transmission Factors 138

ACKNOWLEDGMENT

The author wishes to acknowledge the assistance of many members of the Neutron Physics Division of the Oak Ridge National Laboratory. In particular, the following people should be singled out: H. C. Claiborne, D. C. Irving, Joe Lewin, R. E. Maerker, S. K. Penny, R. W. Roussin, M. Solomito, E. A. Straker, and K. J. Yost. Also, to N. M. Greene, W. E. Ford, III, and M. Gritzner, all of the Union Carbide Corporation Computing Technology Center in Oak Ridge, go many thanks for their valuable assistance in producing the group cross sections. The author wishes especially to thank D. K. Trubey, of the Radiation Shielding Information Center, for suggesting this state-of-the-art report and for his continuous support of the work. Finally, the author wishes to thank Mrs. Patti Gray, who very successfully fought his handwriting, R. P. Metcalf who carefully edited the manuscript after the author returned to Germany, Mrs. Margaret Elmore who typed most of the final manuscript and its many revisions, and Mrs. Mildred W. Landay who assisted in the preparation of the final manuscript.

THE ATTENUATION PROPERTIES OF CONCRETE FOR SHIELDING OF NEUTRONS OF ENERGY LESS THAN 15 MeV

Fritz A. R. Schmidt

ABSTRACT

A review of the literature concerning the attenuation properties of concrete for shielding neutrons of energies up to 15 MeV has been made and calculations of neutron transmission, including the secondary gamma rays, were carried out.

In connection with the literature review, analytical formulas were developed which are based on neutron removal-diffusion theory and gamma-ray buildup factors. They provide a reasonable tool to compare shielding properties of different concretes.

In view of the unsatisfactory state of available attenuation data, especially the lack of secondary gamma-ray results, calculations were performed by the discrete ordinates method and results are presented for various slab thicknesses, and incident energies and angles. The results show the great importance of the secondary gamma rays for large thicknesses.

In the course of the work extensive cross section and other data were compiled. The cross section data are available on computer tape from the Radiation Shielding Information Center. The other data are given in the tables of the report.

I. INTRODUCTION

It is likely that the only statement with which all the authors of the many documents concerning the use of concrete for radiation shielding may agree is that concrete is a very attractive shielding material. Reasons for this are: satisfactory mechanical strength, relatively low cost, and easy maintenance. From a shielding point of view, concrete is a mixture of light and heavy nuclei which gives it good neutron and gamma-ray attenuation properties.

Many types of concrete have been proposed for shielding purposes. They vary from light, strong neutron absorbers, such as boron containing concretes to the most common ones made with portland cement and a cheap aggregate (usually called ordinary concretes) to heavy concretes with densities up to over 9 g/cm^3. But the vast majority of shielding concretes are mixtures of cement, sand, gravel and water. Their average densities may be varied from 2 g/cm^3 to about 5 g/cm^3 by adding iron or barium in the form of ores, scrap, or punchings.

Because concrete is not primarily a shielding material, concretes are usually classified without having shielding in mind. Therefore, in shielding, a concrete should be described not only by its common name, which normally gives only a rough idea of its density and a few main constituents, but also by its chemical composition and density. Properties and composition of concrete can change with time.[1] This holds particularly for the water content. Therefore, in experiments over long periods of time, one should determine composition and density as a function of time.

Some basic properties of the most commonly used concretes can be described generally. For the mechanical aspects, one may refer to books such as those of A. M. Neville[2] or H. W. Taylor.[3] Information about new developments and their availability may be obtained from the American Concrete Institute[4] or similar institutions whose purposes are to collect and distribute all available information concerning concrete. Normally, as a small part of their activities, such institutions cover the field of shielding too. This may lead to publications such as Compilation No. 1 of the American Concrete Institute.[5] Articles

published between 1953 and 1959 in the ACI Journal are included in this compilation and provide a good survey of the knowledge available around 1960. Among the reprinted papers is the one by H. S. Davis entitled "High-Density Concrete for Shielding Atomic Energy Plants."[6]

Since 1960 much additional information has been made available. The Radiation Shielding Information Center (RSIC) has collected about 200 documents related to the use of concrete as a shielding material. Very few of them[7-9] combine engineering and shielding aspects. An exception is the book by Komarovskii[8] which was written in 1965. Most of the important Russian literature published prior to 1964 seems to be included in this work, but few American papers more recent than 1960 are cited. Reference 9 contains considerable nuclear information for most concretes which have been considered prior to 1961.

Much interesting American work has been presented at American Nuclear Society meetings. The Transactions[10] are a helpful guide to these programs. Mention should be made of the special sessions concerning concrete in nuclear shielding[11] held in 1965 which summarized the state-of-the art.

More general articles also may be found in the shielding handbooks. Blizard's paragraphs about concrete[12] are still valuable. His and Komarovskii's evaluations allow us access to most of the older literature by simply referring to their works.

Chapter 4 of the Weapons Radiation Shielding Handbook[13] deals extensively with concrete. In particular, it contains a detailed evaluation of available albedo data. We shall therefore take it as a source of most of our statements concerning albedos for concrete in Sec. II-3.

One of the main applications of concrete in shielding is in civil defense. This aspect of the subject is described in a compilation edited by William R. Kimel.[14]

There are two major areas which this report will cover: neutron transmission through concrete and secondary gamma-ray production in concrete. The literature review in Section II will show that considerable information is available on neutron transmission, but the secondary gamma-ray data are relatively poor. We shall therefore report additional new information in Sections III and IV.

In Section III we describe a combined neutron- and gamma-ray group cross-section library which was produced for RSIC in an energy structure suitable for ordinary concretes. This library is available from RSIC on computer tape. Also given are thermal-neutron capture gamma-ray yields for the most important elements of different concrete mixtures. In Section IV we give results of some discrete-ordinates calculations using this library and the ANISN computer code.[15] These include angle- and energy-dependent results from adjoint calculations for concrete slabs of several thicknesses. These results may be interpreted as Green's functions or more commonly as transmission coefficients for both neutron and gamma-ray tissue dose equivalent. Thus they may be used to determine primary neutron and gamma-ray dose equivalent, and the dose equivalent due to secondary gamma rays behind different thick slabs due to arbitrary angle- and energy dependent plane sources.

The contributions of two groups to the research on shielding with concrete should be mentioned in this introduction. The Neutron Physics Division of Oak Ridge National Laboratory used an ordinary

concrete called "Tower Shielding Facility (TSF) concrete". Because of the work of this group the "TSF concrete" probably is, in terms of shielding, the most thoroughly investigated concrete, with both experimental and theoretical data available. This concrete is made from an aggregate which contains an unusually large amount of CaO rather than the more common SiO_2.

The other group is the one of D. L. Broder in the USSR. This group applied simple analytical formulas, derived from a three-group removal-diffusion theory, to a wide variety of different concretes. Their formulas provide an easy way to estimate shielding properties of concretes by comparison with other concretes for which these properties are already known. Therefore we shall begin our literature review with a short sketch of this calculational procedure. The combined work of both groups should provide one with the tools to judge the more or less complete information given in papers originating elsewhere.

II. Literature Review

1. Analytical Approximations of Radiation Transport in Concrete*

Most of the systematic investigations done by Broder et al,[17,18] which we shall describe in more detail later in this report, are based on analytical solutions of the transport problem. The framework is the well-known Spinney method or removal-diffusion theory,[19] which is applicable at large distances from the source where the neutron spectrum has reached an approximate equilibrium. The calculations are done for three energy groups; a fast group with neutron energies greater than 1.5 MeV, an intermediate group, and a thermal group. The fast group determines the slope of the neutron attenuation curve. By age theory and diffusion theory, neutron "buildup factors" are calculated which connect the fast flux with the fluxes in the two other groups:

$$\varphi(E,z) = B_n(E,z)\ \varphi_f(z) \tag{1}$$

where $B_n(E,z)$ is the flux buildup factor for neutrons of energy E at space point z due to the fast-neutron flux $\varphi_f(z)$.

Equally simple equations exist to estimate gamma-ray attenuation and secondary gamma-ray dose rates behind a slab shield.

It seems reasonable that analytical expressions may be helpful in comparing different concretes. The results of such a comparison could be a guideline for the use of more sophisticated computer programs to obtain accurate transport data. In the remainder of this section we therefore report methods for the estimation of dose contributions behind concrete

---

* A condensed version of this section was published in Ref. 16

slabs. The results obtained may be compared with measured values or with the results of more accurate calculations.

A. Neutron Transmission

Reactor shields made from concrete generally fulfill the requirements that must be met to apply removal theory:[19]

1. They contain, in general, sufficient hydrogen to assure a very short characteristic transport length for intermediate-energy neutrons.

2. The high total content of oxygen, calcium, silicon, or iron guarantees enough inelastic scattering processes to shorten the transport distances in slowing down from the most penetrating energies into the intermediate energy range. In the case of fission-type sources, therefore, spatial equilibrium of all components with the high-energy part of the radiation is achieved close to the source. For other sources, such an approximate equilibrium may be achieved too, but in general at a greater distance from the source.

3. Reactor shields are very thick. This assures that over most of the range, the attenuation by the material can be fitted by an exponential. The slope of this exponential may be estimated using removal cross sections.

If Σ_{rj} is the total macroscopic removal cross section and σ_{rj} the microscopic cross section of an element j then:

$$\Sigma_{rj} = \frac{N}{A_j} \sigma_{rj} \rho_j , \qquad (2)$$

where $N = 6.02 \times 10^{23}$ (Avogadro's number) and A_j and ρ_j are atomic weight and partial density of the element j.

The macroscopic removal cross section of a compound or mixture is obtained by summing the individual microscopic removal cross section of its constituents:

$$\Sigma_r = \sum_j \rho_j \, (\Sigma_r/\rho)_j \tag{3}$$

where ρ_j is the partial density of constituent j (g/cm^3) and $(\Sigma_r/\rho)_j$ is the removal cross section per unit density of constituent j (cm^2/g).

The value of $(\Sigma_r/\rho)_j$ depends only on microscopic nuclear properties and varies smoothly with the atomic weight. Data, taken from Ref. 12, are shown in Fig. 1 where values of Σ_r/ρ are given as a function of the atomic number of the shielding material for fission sources.

Calculated and measured removal cross sections are presented in Table A-1 (Appendix A). They are taken from the compilation of Zoller[20] as reported in the Weapons Radiation Shielding Handbook.[21] With these cross sections one may approximate the transmitted dose at z due to fast neutrons per incident effective neutron as

$$P_f(z) \sim G\alpha_f e^{-\Sigma_r z} \quad . \tag{4}$$

where G is a geometry factor, equal to 1 for a parallel beam source, $1/(4\pi z^2)$ for a point source, and $1/(2\Sigma_r z)$ for a plane isotropic source. The quantity α_f is an averaged fluence-to-dose conversion factor, and z is the shield thickness. The absolute normalization (note word "effective") of this equation requires experimental data, and so removal cross sections are used mostly to estimate changes in dose with changes in Σ_r or z.

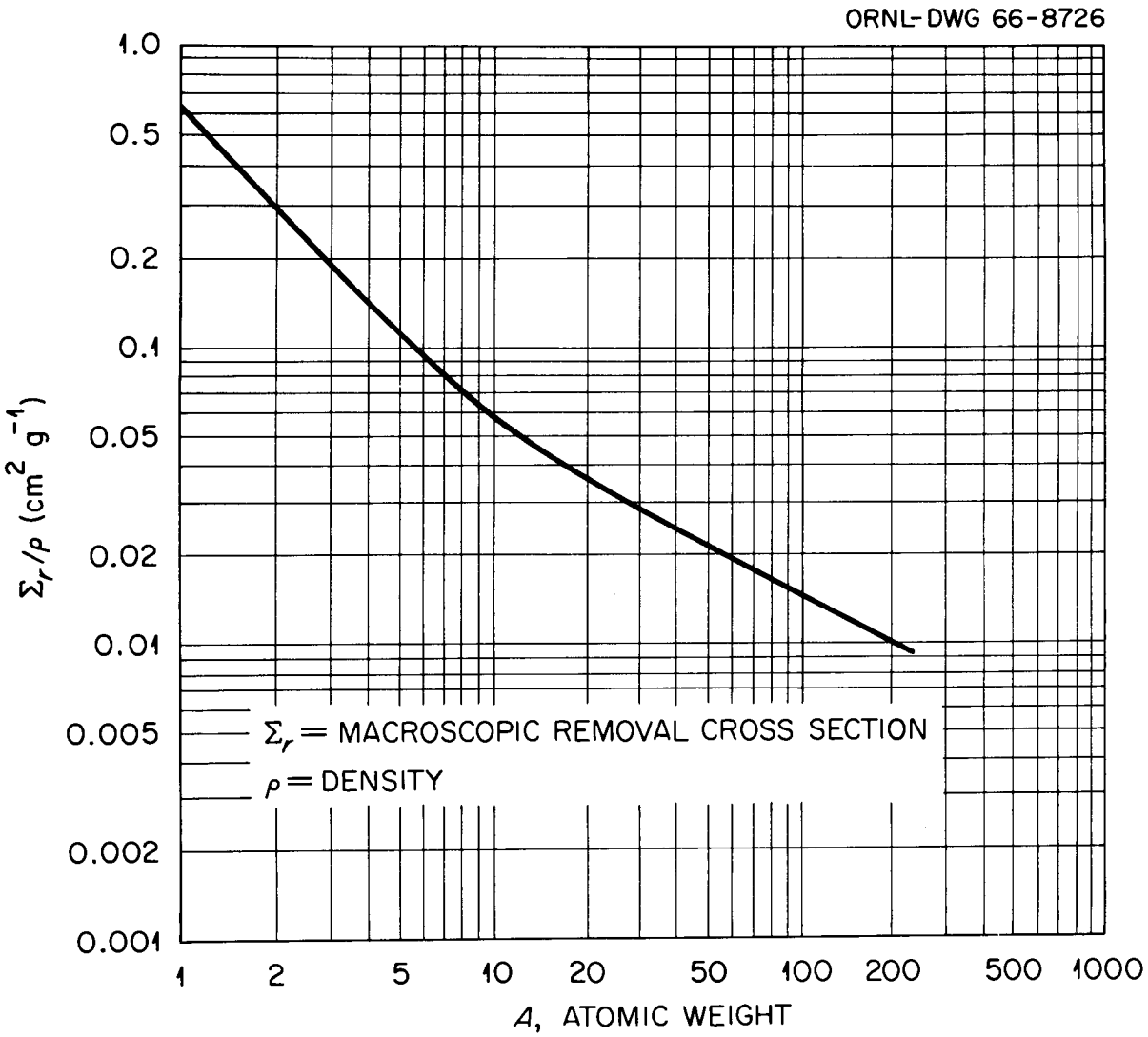

Fig. 1. Removal Cross Section per Unit Mass for Fission Neutrons as a Function of Atomic Weight (From Ref. 12).

A further refinement would require some sort of buildup factor to be included in (4). This factor should describe the approach to equilibrium. It depends, therefore, both on the composition of the concrete and on the spectrum of the source.

As was mentioned above, the fluxes in the intermediate and thermal groups may be related to the fast flux by an expression of the form of Eq. (1), i.e.

$$\varphi(E,z) = B_n(E,z)\ \varphi_f(z)\ . \tag{1}$$

For the intermediate energy neutron group the flux buildup factor $B_n(E,z)$ may be calculated by means of age theory. The neutrons removed from the fast group make up the source S of the intermediate group:

$$S(z) = \varphi_f(z)\ \Sigma_r\ . \tag{5}$$

The Fermi age τ of the intermediate neutrons is defined by

$$\tau = \tau_o + \int_E^{E_o} \frac{1}{3\xi\Sigma_s\Sigma_{tr}}\ \frac{dE'}{E'}\ , \tag{6}$$

where Σ_s and Σ_{tr} are the scattering and transport cross sections, respectively, ξ is the logarithmic energy decrement, and τ_o is the age at the source energy E_o. Normally τ_o is set equal to zero.

With (6) the age equation gives

$$\frac{d^2q}{dz^2} - \frac{dq}{d\tau} - 3\Sigma_{tr}\Sigma_a q = -\ \delta(\tau)\ S(z)\ , \tag{7}$$

where $\delta(\tau)$ is the delta function and the term $3\Sigma_{tr}\Sigma_a q$ takes absorption into account. Σ_{tr} and Σ_a are the transport and absorption cross sections in the intermediate group and q is the slowing-down density. It is connected with the flux at the same energy by

$$q(E,z) = \Sigma_s(E)\ \xi\ \varphi(E,z)\ . \tag{8}$$

Σ_s is the scattering cross section of the group under consideration.

At large distances and for small Σ_a, the solution of Eq. (7) is given by

$$q(E,z) = \varphi_f(z)\Sigma_r \exp\{\tau(E)\ \Sigma_r^2 - h(E)\}\ , \tag{9}$$

where

$$h(E) = \int_E^{E_o} \frac{\Sigma_a(E')}{\Sigma_s(E')\ \xi(E')}\ \frac{dE'}{E'}\ . \tag{10}$$

With Eq. (8) we finally get

$$\varphi(E,z) = \frac{\Sigma_r\varphi_f(z)}{\Sigma_s\xi} \exp\{\tau(E)\ \Sigma_r^2 - h(E)\}\ . \tag{11}$$

Combining with Eq. (1),

$$B_n(E,z) = \frac{\Sigma_r}{\Sigma_s\xi} \exp\{\tau(E)\ \Sigma_r^2 - h(E)\}\ . \tag{12}$$

Equation (12) is independent of z. This is mainly due to the way in which absorption was incorporated. It should be mentioned that Eq. (12) is restricted to phase-space regions where the conditions for age theory are valid. These conditions are given in Ref. 19 and are normally satisfied by concrete. Regions near a boundary, especially regions

adjacent to a vacuum, are excluded by these conditions. This means that the buildup factor is useful only for flux calculations within a medium; it does not describe the leakage flux at a boundary.

The slowing-down density at thermal energy may be used as the source term for the diffusion equation in the following form to determine the thermal neutron flux, $\varphi_{th}(z)$:

$$D\nabla^2\varphi_{th} - \Sigma_a\varphi_{th}(z) + \varphi_f(z)\ \Sigma_r\ \exp\{\tau_{th}\ \Sigma_r^2 - h(E_{th})\} = 0, \quad (13)$$

where $\tau_{th} = \tau(E_{th})$.

The diffusion constant D is given approximately by

$$D \approx (3\Sigma_{tr})^{-1} = L^2\ \Sigma_a\ , \quad (14)$$

where L is the diffusion length.

For $\Sigma_a/D > \Sigma_r^2$ and large z values, the solution of Eq. (13) is

$$\varphi_{th}(z) = \varphi_f(z)\ \frac{\Sigma_r\ \exp\left[\tau_{th}\Sigma_r^2 - h(E_{th})\right]}{\Sigma_a\left[1 - (L\Sigma_r)^2\right]}\ ; \quad (15a)$$

The thermal-neutron buildup factor, therefore, is

$$B_n(E_{th},z) = \frac{\Sigma_r}{\Sigma_a\left[1 - (L\Sigma_r)^2\right]}\ \exp\left[\tau_{th}\Sigma_r^2 - h(E_{th})\right]\ . \quad (16a)$$

For $\Sigma_a/D < \Sigma_r^2$ and large z values, the solution for the thermal-neutron flux may be approximated by

$$\varphi_{th}(z) = \frac{\varphi_f(z)\ \Sigma_r}{\Sigma_a(L\Sigma_r - 1)}\ \exp\left[\tau_{th}\Sigma_r^2 - h(E_{th})\right]\left[\exp\left[\left(\Sigma_r - \frac{1}{L}\right)z\right] - 1\right] \tag{15b}$$

which gives a buildup factor

$$B_n(E_{th},z) = \frac{\Sigma_r}{\Sigma_a(L\Sigma_r - 1)}\ \exp\left[\tau_{th}\Sigma_r^2 - h(E_{th})\right]\left[\exp\left[\left(\Sigma_r - \frac{1}{L}\right)z\right] - 1\right]\ . \tag{16b}$$

This form of the buildup factor will increase rapidly with z if $\Sigma_r > 1/L$. Because the thermal-neutron flux is the main source of capture gamma rays, this condition should be avoided by having enough capture to make $1/L \gg \Sigma_r$ which would mean that the neutrons would not diffuse far at thermal energy. In Section III-2 we shall show some of the implications of this condition for the selection of concretes to be used for shielding.

The crucial quantity in these formulas is the diffusion length L. Since thermal neutrons interact with molecules and groups of molecules rather than with single atoms independentally, the principle of additivity of atomic cross sections is invalid in the thermal range. In the case of scattering by hydrogen, Broder made the assumption that the thermal neutrons are scattered isotropically by water. Therefore he calculated diffusion lengths using the formula

$$\frac{1}{L^2} = 3\Sigma_a\ \Sigma_s\ (1 - \bar{\omega})\ ;$$

and for the mean cosine of the scattering angle he assumed $\bar{\omega} = 0$.

B. Secondary Gamma Rays

In describing the attenuation of gamma rays in concrete, the buildup factor concept is again quite useful. In the case of neutron buildup factors the reference quantity was the fast neutron flux, whose attenuation could be calculated by removal theory. In the case of gamma-ray buildup factors the fast-neutron flux has to be replaced by the uncollided gamma-ray flux. This means that the removal factor $e^{-\Sigma_r z}$ in Eq. (4) has to be replaced by the material attenuation factor $e^{-\mu(E)z}$. The attenuation coefficient $\mu(E)$ plays the same role for the uncollided gamma rays as the removal cross section Σ_r for the fast neutrons. Values of μ for elements that are important constituents of concrete are given in Table A-7.

For the uncollided gamma-ray dose $P_{u\gamma}(E,z)$, we may write an equation similar to Eq. (4) for fast neutrons:

$$P_{u\gamma}(E,z) = Ge^{-\mu z}S(E)\alpha_\gamma(E) \tag{17}$$

where $P_{u\gamma}$ is the uncollided gamma-ray dose which is the uncollided gamma-ray flux times the gamma-ray flux-to-dose conversion factor $\alpha_\gamma(E)$. The quantity S(E) is the source strength and G has the same meaning as in Eq. (4).

The total gamma-ray dose at z due to an incident gamma-ray source of energy E is then given by

$$P_\gamma(E,z) = B_\gamma(E,\mu z)\ P_{u\gamma}(E,z) \tag{18}$$

The quantity $B_\gamma(E,\mu z)$ is the dose buildup factor for gamma rays of energy E at a distance μz mean-free-paths away from the source. Empirical

fitting functions for $B_\gamma(E,\mu z)$ were evaluated by Trubey.[22] For the calculation of secondary gamma ray attenuation the two-parameter buildup formula proposed by Berger[23] seems to be the most efficient one. This formula is

$$B_\gamma(E,\mu z) = 1 + C(E)\ \mu z\ \exp[D(E)\mu z] \tag{19}$$

where C(E) and D(E) are energy-dependent parameters. Values for both quantities are reported in Section III-3 and in Table A-6.

To get the secondary gamma-ray dose at large thicknesses, including the contribution of neutron capture gamma rays, one has to substitute for S(E) in Eq. (17) the source strength of the capture gamma rays as a function of the source position z'. For a gamma-ray group i about energy E the source strength is the product of the thermal-neutron capture cross section Σ_a, the thermal-neutron flux at the plane at z', and n_i, the average number of gamma quanta in energy group i produced per neutron capture. For a plane collimated fast neutron source at z = 0 the thermal-neutron flux at the plane z = z' per incident effective fast neutron is, according to Eq. (1) and Eq. (4),

$$\varphi_{th}(z') = B_n(E_{th},z')\ e^{-\Sigma_r z'} . \tag{20}$$

No geometry factor is necessary for the transformation from a plane collimated source. Thus the source strength for capture gamma rays of energy E_i becomes

$$S(E_i,z') = \Sigma_a\ B_n(E_{th},z')\ e^{-\Sigma_r z'}\ n_i . \tag{21}$$

The dose of gamma rays with energy E_i at z and that result from a plane neutron source at z' is, according to Eqs. 17, 18, and 20,

$$P(E_i,z,z') \cong \alpha_\gamma(E_i)\ B_\gamma[E_i,\mu_i(z-z')]\ \Sigma_a\ B_n(E_{th},z')\ e^{-\Sigma_r z'}\ n_i\ \frac{e^{-\mu_i(z-z')}}{2\mu_i(z-z')}\ , \quad (22)$$

where μ_i is the attenuation coefficient for the gamma-ray energy E_i.

The total capture gamma-ray dose per incident fast neutron is obtained by integrating over z' (all source planes) and summing over i (all gamma-ray energies). For the position-independent neutron buildup factor, Eq. (16a), and the gamma-ray buildup factor of Berger, Eq. (19), the integration of Eq. (22) gives a combination of exponential functions and exponential integrals of the first order $E_1(x)$. The integration was also performed by Trubey.[22] For the attenuation of the isotropic gamma rays, which is described in Eq. (22) by

$$\exp\{-\mu_i(z - z')\} \Big/ [2\mu_i(z - z')]\ . \quad (23a)$$

he uses the more exact expression

$$1/2\ E_1[\mu_i(z - z')]\ . \quad (23b)$$

Actually Eq. (23a) is an approximation of Eq. (23b) that is valid for large arguments $\mu_i(z - z')$.

Trubey presented the result of his calculations in terms of the Claiborne[22b] functions $\psi_o(\mu z,a)$ and $\psi_1(\mu z,a')$. These functions, dependent on thickness in mean free paths, are defined in Section III-3B, p. 67. The parameter a is the ratio of the slope of the gamma ray source exponential function to the attenuation coefficient.

That is,

$$a = \Sigma_r/\mu_i \ . \tag{24}$$

The parameter a' is the sum of a and D, the second of the Berger coefficients.

With these functions the gamma-ray dose at z due to an effective fast neutron incident at z = 0 is:

$$P_{n\gamma}(z) = \sum_{i=1}^{k} \alpha_\gamma (E_i)\ n_i\ \Sigma_a\ B_n(E_{th})\ (\mu_i)^{-1}[\psi_o(\mu_i z,a) + \frac{C(E_i)}{1-D(E_i)} \exp\{D(E_i)\ \mu_i z\}\psi_1(\mu_i z,a')] \tag{25}$$

where

$$\mu_i = \mu(E_i)$$

$$a = \Sigma_r/\mu_i$$

and $$a' = a + D(E_i) \ .$$

In Section III-3 we show how the functions ψ_o and ψ_1 may be calculated. Equation (25), of course, can be used to compute gamma-ray doses due to other sources provided that the gamma-ray source distribution can be described by a sum of exponentials.

As was mentioned above, Eqs. (1) to (25) are not sufficiently exact to solve all attenuation problems in concrete. If the spectrum of the neutron source differs much from a fission spectrum, it even seems doubtful whether they predict the right order of magnitude. But they may be very useful in estimating the comparative shielding properties

of a given concrete. Broder used similar formulas to do a most complete and systematic investigation of some 60 different concrete mixtures. Therefore, throughout this literature review, we shall be confronted with results of Broder.[17,18] They may be compared with results of other authors which are in general more accurate but more specialized. Thus one may get some feeling for the use of concrete in reactor shielding.

2. Neutron Transmission

Most of Broder's calculations were done for 46 concretes which he indicates are the most widely used in the USSR. Their average chemical composition and hydrogen content are given in Table 1. In a paper by Zaitsev[24] the compositions of these concretes are described in terms of the cements and aggregates used to mix them. The hydrogen content was changed by varying the amount of cement or by using hydrated cement and fillers that contained hydrogen.

Tables 2 and 3 give results calculated with the methods discussed in Section II-1. The removal cross sections used are the same as in Table A-1. The source energy E_o of the intermediate neutrons was chosen to be 1.5 MeV. This is somewhat higher than the most probable energy of the fission spectrum, which is reasonable in view of the hydrogen content of concrete.[19] No information on the source of the gamma-ray attenuation coefficients was found. The dose conversion factors for intermediate neutrons were taken from Goldstein.[25] The corresponding values of fast- and thermal-neutron doses are respectively 0.135 and

+

TABLE 1

Hydrogen Content and Chemical Composition of Concretes, wt.%

Density, kg/m³	Hydrogen content at t = 85°C, number of concrete batch						Content of other elements for average amount of hydrogen						
	1	2	3	4	5	6	O	Al	Si	S	Ca	Fe	Ba
2300	0.10	0.35	0.61	0.81	0.84	0.94	52.90	4.41	30.95	0.15	7.66	2.03	—
2600	0.78	0.88	1.28	1.96	2.04	2.10	40.53	0.74	3.96	—	5.20	46.39	—
3200	0.30	0.46	0.54	0,62	0,70	0.85	32.82	0.89	11.10	—	4.94	48.81	—
3500	0.19	0.35	0.43	0.50	0.58	0.64	31.00	2.80	—	11.50	3.50	7.53	42.50
3600	0.25	0.33	0.43	0.49	0.61	0.89	32.05	3.26	12.38	0.38	3.69	50.13	—
4200	0.23	0.26	0.32	0.42	0.46	0.74	15.47	1.13	4.89	—	1.24	66.27	—
4600	0.18	0.28	0.33	0.50	0.60	0.65	9.36	1.54	0 69	—	1.67	75.25	—
5200	0.15	0.35	0.43	0.52	—	—	5.05	2.52	0.20	0 13	3.13	78.24	—

+

TABLE 2

Nuclear Constants for Concretes

Density, kg/m³	Relaxation length of gammas, cm, energy, MeV						Removal length of fast neutrons, cm, number of concrete batch					
	1	2	3	4	6	8	1	2	3	4	5	6
2300	6.4	9.7	11.9	13.7	16.2	18.0	13.1	12.6	12.2	11.8	11.5	11.4
2600	6.2	8.7	10.6	12.1	13.9	15.0	12.4	14.4	11.8	9.8	9.6	9.4
3200	5.1	7.2	8.5	9.6	10.5	11.8	10.7	10.2	10.1	10.0	9.9	9.7
3500	5.1	7.3	8.5	9.0	9.9	9.9	11.4	10.8	10.7	10.4	10.3	10.2
3600	4.3	6.6	7.4	8.3	9.5	10.1	9.8	9.5	9.4	9.3	8.9	8.7
4200	3.9	5.5	6.6	7.2	8.0	8.5	9.4	9.3	9.2	8.9	8.8	8.4
4600	3.6	5.0	6.0	6.5	7.3	7.6	9.0	8.8	8.6	8.3	8.2	8.1
5200	3.2	4.5	5.3	5.9	6.4	6.7	8.3	7.9	7.7	7.5	—	—

Neutron +

TABLE 3

Dose Buildup Factors*

Density, kg/m³	Intermediate neutrons (<1,5 MeV), number of concrete mix						Thermal neutrons, number of concrete mix					
	1	2	3	4	5	6	1	2	3	4	5	6
2300	10.3	3.4	2.3	1.9	1.8	1.6	205	2.80	0.95	0.61	0.58	0.50
2600	2.0	1.4	1.1	1.0	0.9	0.9	0.12	0.10	0.08	0.05	—	—
3200	4.2	3.0	2.7	2.3	2.1	1.9	0.11	0.07	0.06	0.05	0.04	0.03
3500	6.3	3.6	2.5	2.5	2.1	2.0	0.35	0.19	0.15	0.13	0.12	0.11
3600	5.2	4.3	3.4	3.0	2.4	1.8	0.10	0.08	0.07	0.06	0.03	—
4200	7.4	6.2	5.0	3.9	3.4	2.2	0.06	0.05	0.04	0.03	0.02	—
4600	11.7	6.1	5.4	3.4	2.8	2.3	0.11	0.08	0.05	0.03	0.02	—
5200	23.2	6.0	4.3	3.5	—	—	0.29	0.09	0.03	0.01	—	—

*Dose buildup factors were calculated for a shielding thickness greater than 1 m; for concrete mix No. 1 of density 2300 kg/m³ a thickness greater than 3 m. Excellent harmony is noted between the calculated buildup factors for concretes of 2300 kg/m³ density and the buildup factors cited in [26]

+ From Ref. 18

0.00375 mrem/hr per n/cm^2/sec. Dividing the thermal dose buildup factors by the ratio of thermal and fast dose factors leads to thermal-neutron flux buildup factors.

Most of the other reports that deal with neutron transmission through concrete shields are restricted to the fast-neutron component. Table 4 lists concretes for which we found measured or calculated values of the total removal cross section. Table 5 gives the chemical compositions of these concretes. Older results may be found in Ref. 9. The removal cross sections in Table 4 were mostly determined from the slope of the exponential part of the attenuation curves. In the case of the Hanford measurements,[27-31] a geometrical correction factor is given to correct for the influence of the reflector and the thermal shield. By applying these geometry corrections, values for the removal cross section could be obtained from parts of the attenuation curve that were not yet purely exponential. Descriptions of these corrections may be found in Ref. 29.

The differences between the removal cross sections as given in Table 4 and those which could be calculated from the combined data of Table 5 and Table A-1 are in general less than 10%. The problem in using one-velocity theory, or energy independent removal cross sections, is not associated with the exponential part of the attenuation curve, but the part just next to the source, where the neutron spectrum is not yet in equilibrium. Figure 2, which is taken from Ref. 36, is a typical example for attenuation curves in concrete.

To determine how the dose behaves near a specific source, one has to rely on more sophisticated calculational methods for dose transmission

TABLE 4

CONCRETE DEFINITION AND REMOVAL CROSS SECTIONS

CONCRETE		DENSITY (g/cm^3)	WATER CONTENT (wt.%)	REF.	Σ_r (cm^{-1})	COMMENTS
Ordinary	0-1	2.29	6	32	0.087	Slab geometry; fission source modified by 700 m of air, $S_{16}P_2$ ANISN calculation.
	0-2	2.3	6	33	0.0993	Slab geometry; fission source modified by 100 g/cm^2(≈760 m) of air; moments method RENUPAK calculation.
	0-3	2.3	7.5	34	0.0898	Slab geometry; fission source; moments method RENUPAK calculation.
	0-4	2.39	7.5	35	0.0884 0.087	Removal cross sections measured at ORNL Lid Tank Shielding Facility.
	0-5	2.357	7.6	36	0.092	Spherical geometry, unit-point-isotropic fission source; moments method RENUPAK calculation.
	0-6[a]	2.33	5.8	30	0.078	Measured at the Hanford Bulk Shielding Facility.
	0-7	2.4	7.6	37	~0.09	Measurement with reactor spectrum.
	0-8	2.43	6.9	40-42	~0.088	P activation measurements at the R2-0 reactor in Studsvik, Sweden.
	0-9	2.39	7.5	17	0.086	Russian concrete No. 10.
Limonite	L-1	2.731	11.22	36	0.103	See 0-5.
	L-2	2.7	10.8	37	~0.106	See 0-7.
Magnetite Limonite	L-3	3.39	6.1	27	0.104	See 0-6.
Limonite and Steel	L-4[b]	4.23	6	27	0.120	See 0-6.
Serpentine	S-1	2.2	11.3	38	~0.092	Measurements on a water-moderated, water-cooled research reactor; threshold detector.
Iron Serpentine	S-2	3.37	5.1	39	~0.105	See S-1.
Magnetite Serpentine	S-3	3.288	3.31	36	0.104	See 0-5.
Ferrophosphorus Serpentine	S-4[c]	3.396	5.5	36	0.1154	See 0-5.
Iron Serpentine 208	I-1	4.30	5.4	31	0.127	See 0-6.
Iron Serpentine 220	I-2	3.53	9.8	31	0.110	See 0-6.
Hydrous Iron Ore	I-3	3.522	5.5	36	0.109	See 0-5.
Ferrophosphorus	I-4	4.82	3.9	29	0.131	See 0-6.
Magnetite	M-1	3.74	3.6	40-42	0.109	See 0-8.

a. Identified as 0-HW1 by Walker and Grotenhuis [Ref. 9].
b. Identified as LS-HW1 by Walker and Grotenhuis [Ref. 9].
c. Identified as FP-HW1 by Walker and Grotenhuis [Ref. 9].

TABLE 5

ELEMENTAL COMPOSITION OF SELECTED CONCRETES

ELEMENT	Partial Densities (g/cm^3)										
	0-1	0-2	0-3	0-4	0-5	0-6*	0-7	0-8	0-9	L-1	L-2
H	0.015	0.0067	0.020	0.020	0.020	0.015	0.020	0.019	0.020	0.037	0.032
O	0.938	0.538	1.114	1.114	1.116	1.057	1.178	1.190	1.116	1.113	0.968
C	0.400		0.117	0.117	0.118				0.118		
Na	trace			0.011		0.048		0.041	0.011		
Mg	0.076			0.057		0.085		0.036	0.057		
Al	0.025			0.085		0.137	0.115	0.158	0.085		0.119
Si	0.079	0.235	0.484	0.342	0.612	0.487	0.822	0.660	0.342	0.165	0.113
P						0.002			0.007		
S						0.002	0.062		0.007		0.070
Cl						0.015					
K	0.003					0.295		0.061			
Ca	0.735	0.221	0.580	0.580		0.011	0.127	0.195	0.582	0.227	0.158
Ti											
V											
Cr											
Mn						0.003	0.022				0.121
Fe	0.018			0.026	0.491	0.178	0.055	0.073	0.026	1.189	1.190
Ni											
Cu											
Others				0.048			0.058		0.019		0.216
TOTAL	2.289	1.000	2.31	2.390	2.357	2.335	2.459	2.433	2.390	2.731	2.987

*Identified as 0-HW1 by Walker and Grotenhuis [Ref. 9]

TABLE 5 (cont.)

ELEMENTAL COMPOSITION OF SELECTED CONCRETES

ELEMENT	Partial Densities (g/cm^3)										
	L-3	L-4*	S-1	S-2	S-3	S-4	I-1	I-2	I-3	I-4**	M-1
H	0.023	0.028	0.0275	0.019	0.0122	0.0208	0.026	0.038	0.0215	0.021	0.015
O	1.343	0.806	1.036	0.653	1.180	0.7805	0.609	0.924	1.304	0.322	1.270
C				0.121						0.004	
Na				0.034							
Mg	0.156	0.039	0.341	0.188			0.140	0.303		0.006	0.045
Al			0.032	0.027			0.023	0.023		0.009	0.030
Si	0.117	0.078	0.440	0.239	0.457	1.044	0.151	0.263	0.108	0.090	0.135
P										1.049	0.026
S				0.008			0.004	0.003		0.004	
Cl											
K											
Ca	0.171	0.250	0.168	0.117	0.458	0.196	0.189	0.153	0.128	0.203	0.228
Ti										0.042	
V										0.084	
Cr										0.084	
Mn								0.011		0.013	
Fe	1.580	3.030	0.128	1.95	1.181	1.355	3.154	1.816	1.960	2.823	1.990
Ni							0.002			0.017	
Cu										0.008	
Other			0.029	0.008						0.042	
TOTAL	3.390	4.231	2.202	3.364	3.288	3.396	4.300	3.534	3.522	4.821	3.739

* Identified as LS-HW1 by Walker and Grotenhuis [Ref. 9]
** Identified as FP-HW1 by Walker and Grotenhuis [Ref. 9]

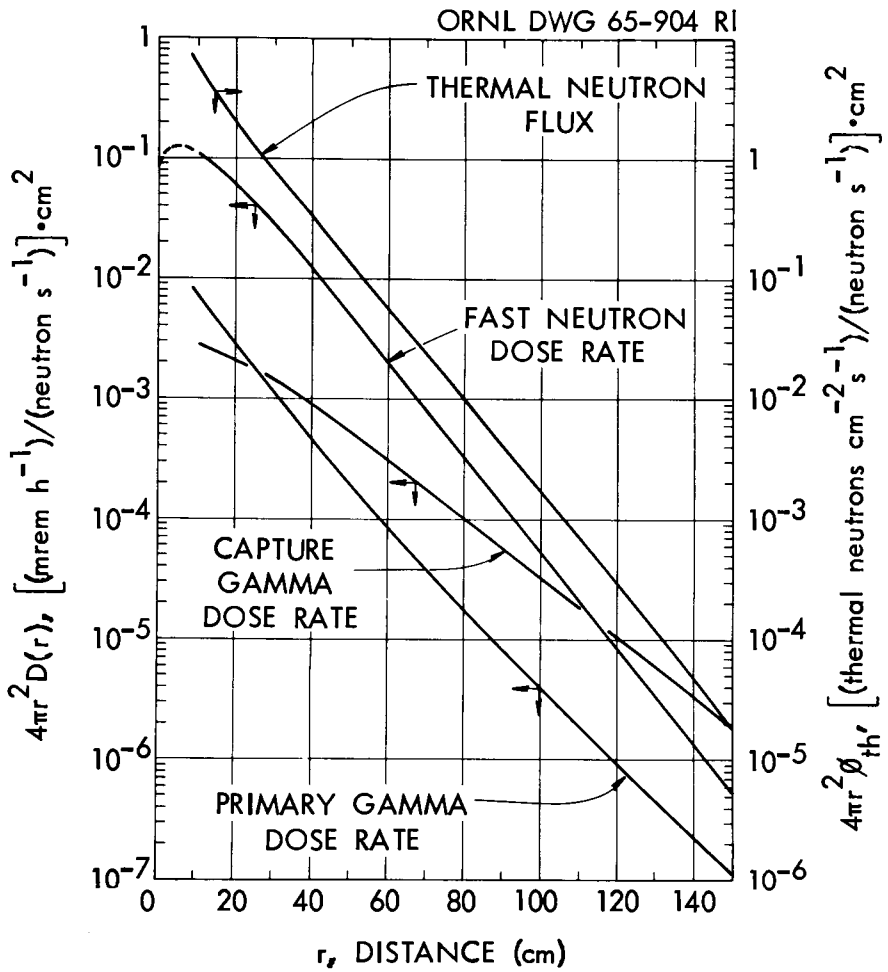

Fig. 2. Fast Neutron, Primary Gamma-Ray and Capture Gamma-Ray Dose Rates, and Thermal Neutron Flux in Ordinary Concrete for a Point Isotropic Fission Source of ^{235}U (From Ref. 36).

than we have described. Clark et al.[43] performed Monte Carlo calculations for monoenergetic beams of neutrons normally incident on a semi-infinite concrete similar to the TSF concrete. Data for slabs were also obtained. The neutron energies were 0.7, 1.2, 2, 3, 4, 6, 8, 10, 12, and 14 MeV. The density of the concrete was taken to be 2.43 g/cm^3 with the composition given in Table 6. The resulting dose attenuation curves are shown in Figs. 3 to 12. The difference between the slab and infinite medium half-space results for thickness 0 is based on the flux albedo values of Allen and Futterer[47] (as given in Sec. II-3) since the original Clark calculation did not determine this.

Allen and Futterer[46-48] determined, in another series of Monte Carlo calculations, the transmitted and reflected flux due to monoenergetic neutron beams incident at various angles. The neutron energies were 0.5, 1, 2, 3, 5, and 14 MeV. The composition of the concrete is given in Table 6, and the calculated dose transmission factors are shown in Figs. 13 to 18. In order to use this curve for monoenergetic, monodirectional sources, one only has to know the dose value at the inner surface of the slab. Then the attenuation factor appropriate to the thickness, energy, and angle is read from the curve, and the incident dose multiplied by that factor should approximate the dose that has penetrated the slab. Sources with more complicated energy and angle distributions have to be replaced by histograms or groups of neutrons. Then for each energy-angle band, one may estimate the fraction of the transmitted dose due to this interval. The total dose is the sum over all energy and angle groups.

TABLE 6

CONCRETE COMPOSITIONS USED IN MONTE CARLO CALCULATIONS

Element	Nuclear Density ($10^{21}/cm^3$)				
	Clark, et al.*	Maerker and Muckenthaler*			Allen, et al.*
		a	b		
H	9.3	8.22	8.5	9.43	13.75
O	46.3	34.30	35.5	47.6	45.87
C	6.5	19.50	20.2		
Mg		1.80	1.86		
Al		0.538	0.556		1.743
Si	9.92	1.64	1.70	11.85	20.15
Ca	8.83	10.80	11.1	7.8	
Fe		0.296	0.193		
Na+K		0.045	0.057		
Density (g/cm^3)	2.43	2.75	2.3	2.35	2.26

a - All concretes are considered ordinary except this column.

b - The calculations described in Sec. IV assumed this composition.

* Clark: Ref. 43, Maerker: Ref. 44-45, Allen: Ref. 48.

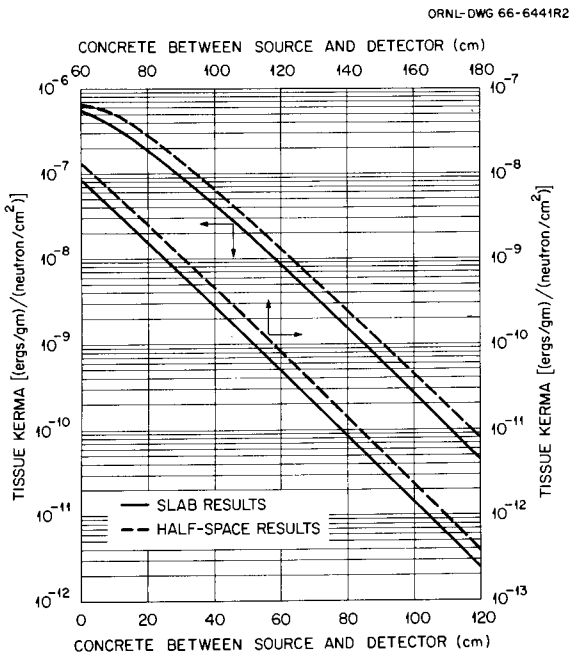

Fig. 3. Transmission of 14-MeV Normally Incident Neutrons in Ordinary Concrete (From Ref. 43).

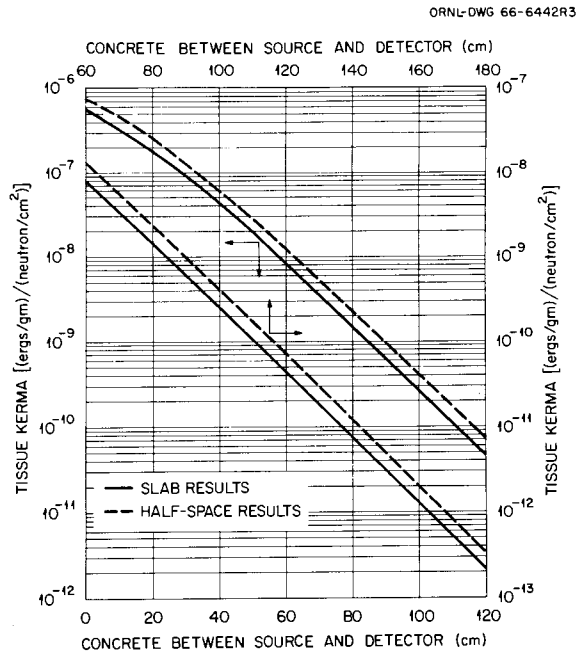

Fig. 4. Transmission of 10-MeV Normally Incident Neutrons in Ordinary Concrete (From Ref. 43).

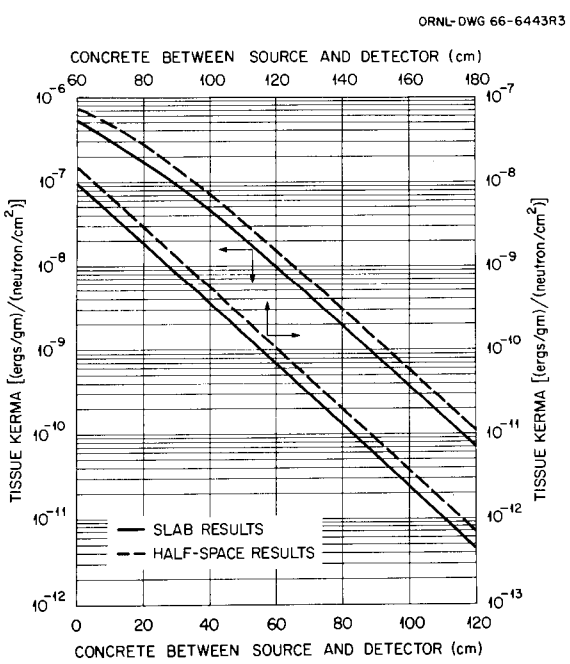

Fig. 5. Transmission of 12-MeV Normally Incident Neutrons in Ordinary Concrete (From Ref. 43).

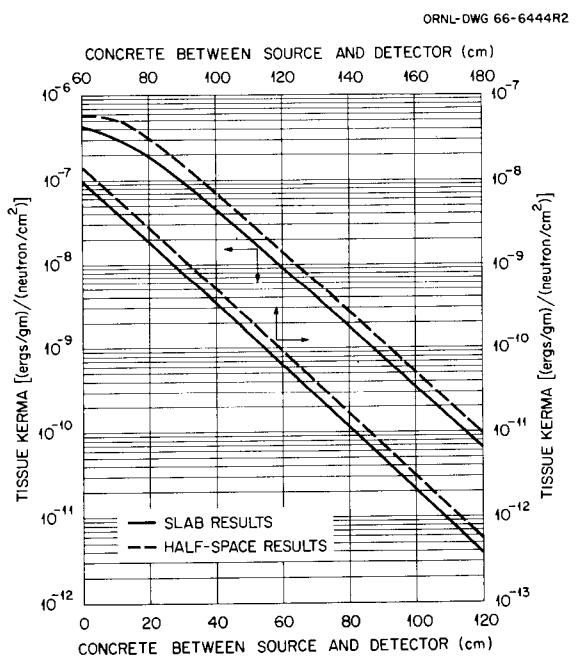

Fig. 6. Transmission of 8-MeV Normally Incident Neutrons in Ordinary Concrete (From Ref. 43).

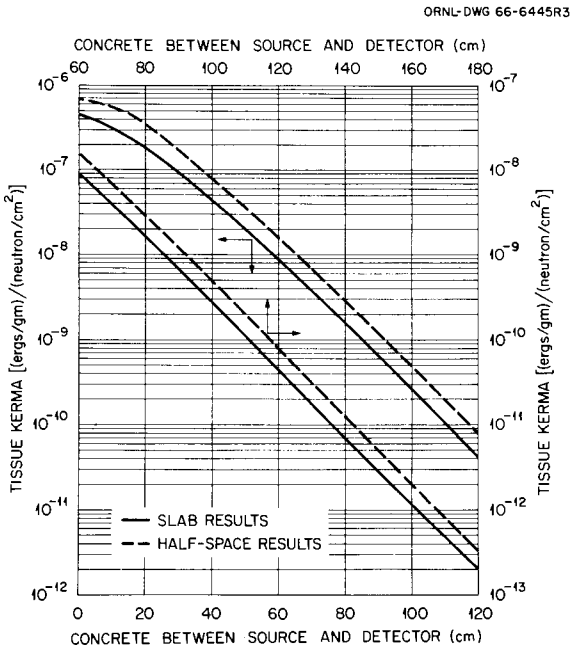

Fig. 7. Transmission of 6-MeV Normally Incident Neutrons in Ordinary Concrete (From Ref. 43).

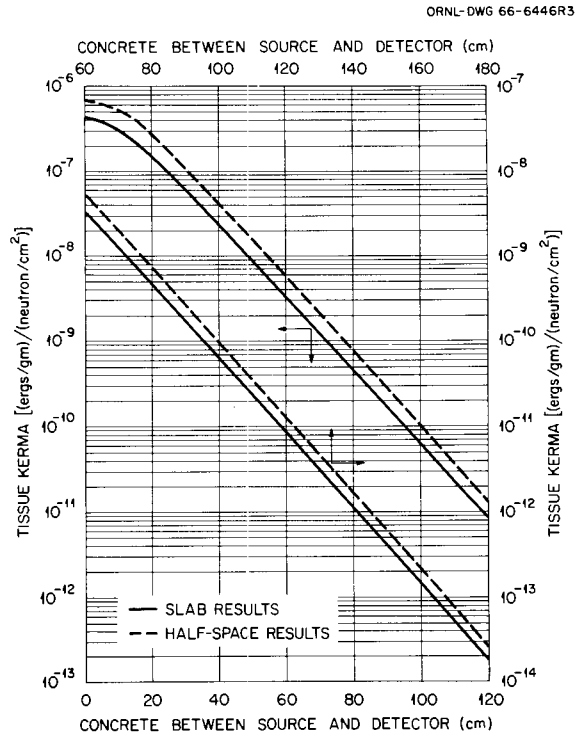

Fig. 8. Transmission of 3-MeV Normally Incident Neutrons in Ordinary Concrete (From Ref. 43).

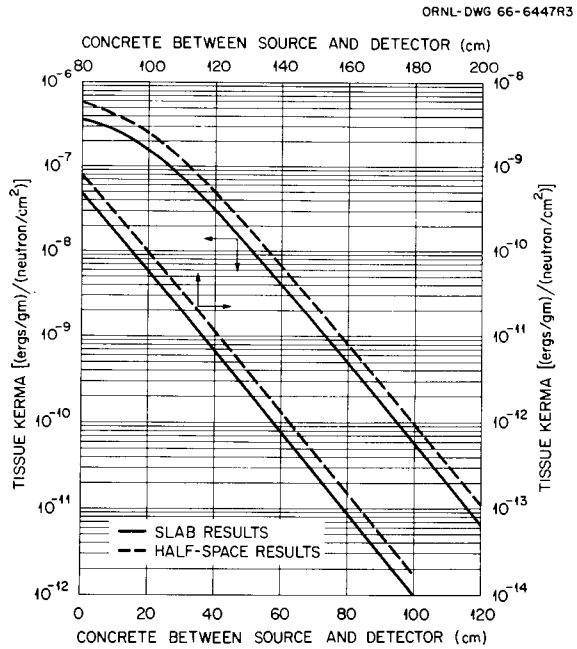

Fig. 9. Transmission of 4-MeV Normally Incident Neutrons in Ordinary Concrete (From Ref. 43).

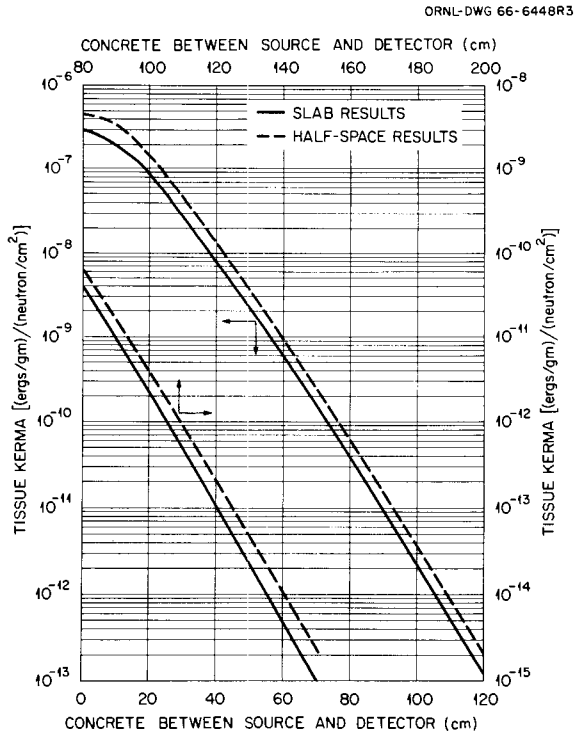

Fig. 10. Transmission of 2-MeV Normally Incident Neutrons in Ordinary Concrete (From Ref. 43).

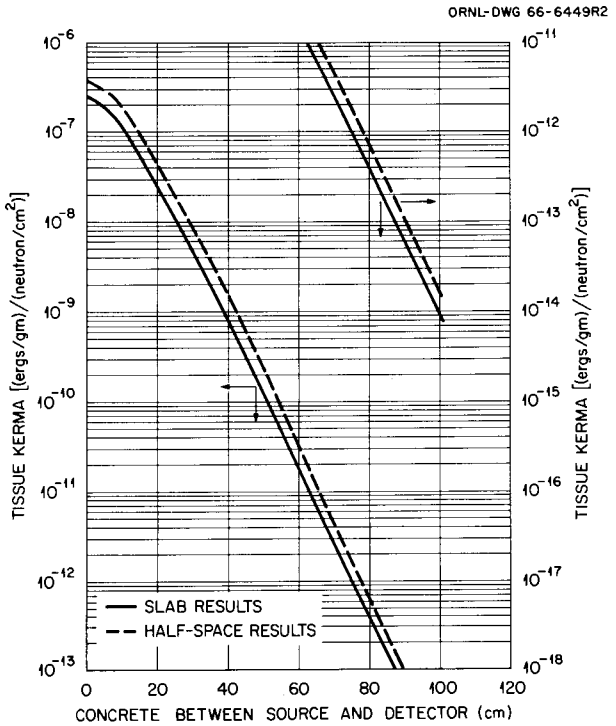

Fig. 11. Transmission of 1.3-MeV Normally Incident Neutrons in Ordinary Concrete (From Ref. 43).

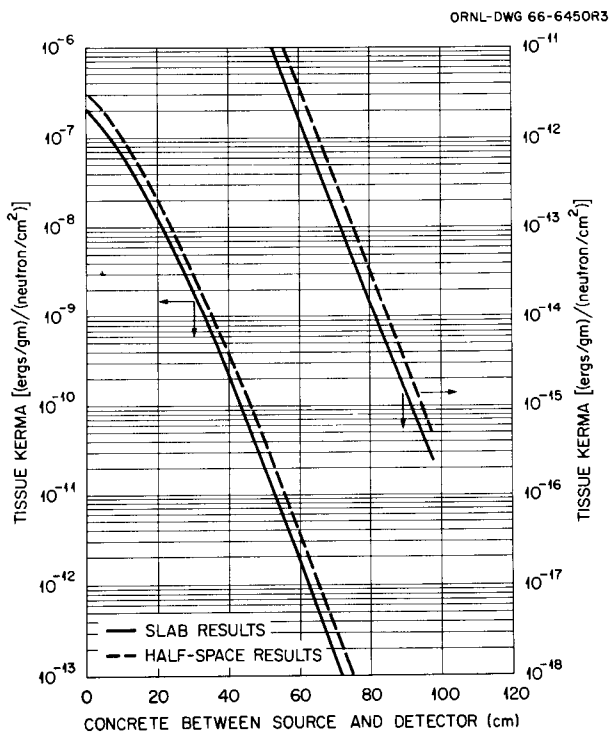

Fig. 12. Transmission of 0.7-MeV Normally Incident Neutrons in Ordinary Concrete (From Ref. 43).

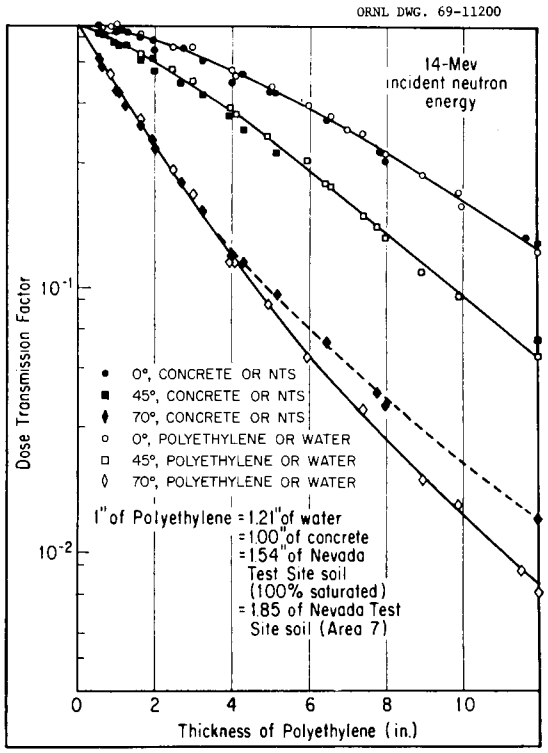

Fig. 13. Transmission of 14-MeV Neutrons Incident on Various Materials at Various Angles (From Ref. 48).

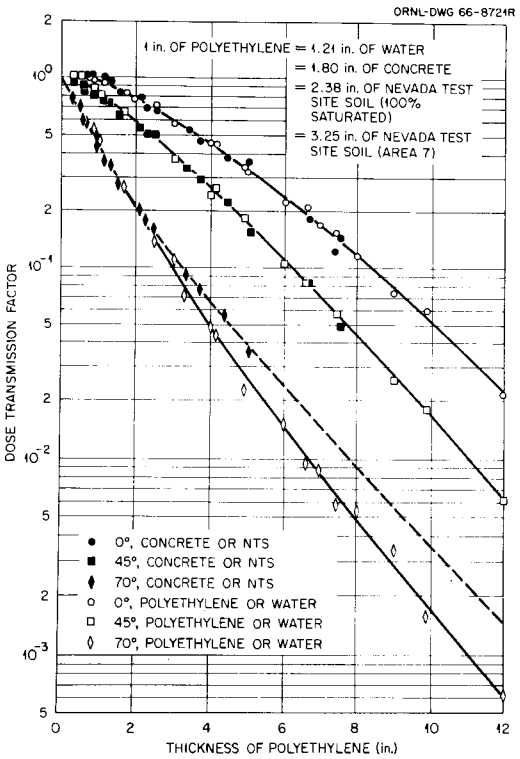

Fig. 14. Transmission of 5-MeV Neutrons Incident on Various Materials at Various Angles (From Ref. 48).

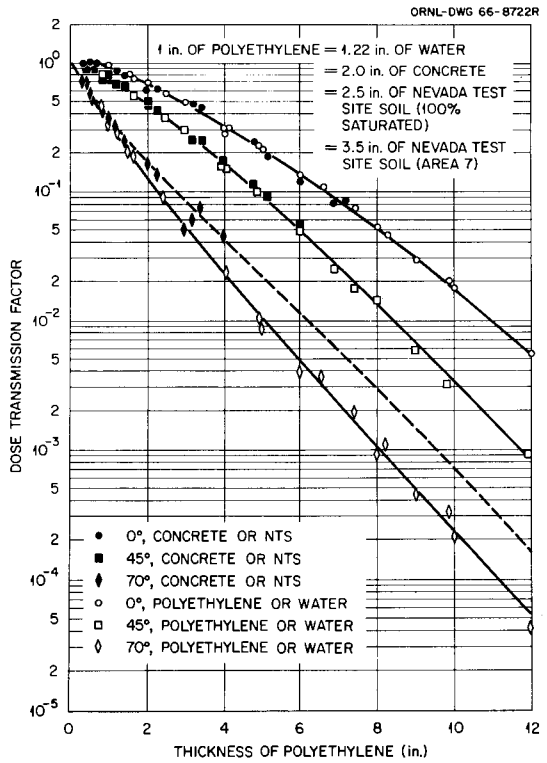

Fig. 15. Transmission of 3-MeV Neutrons Incident on Various Materials at Various Angles (From Ref. 48).

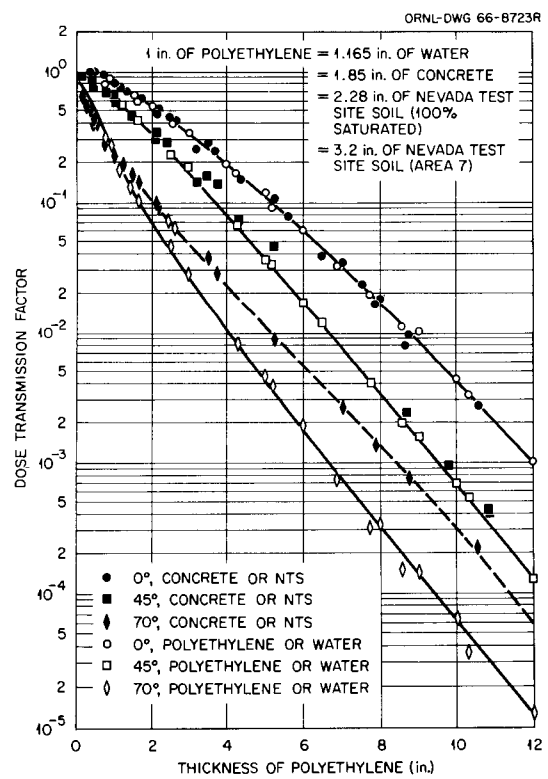

Fig. 16. Transmission of 2-MeV Neutrons Incident on Various Materials at Various Angles (From Ref. 48).

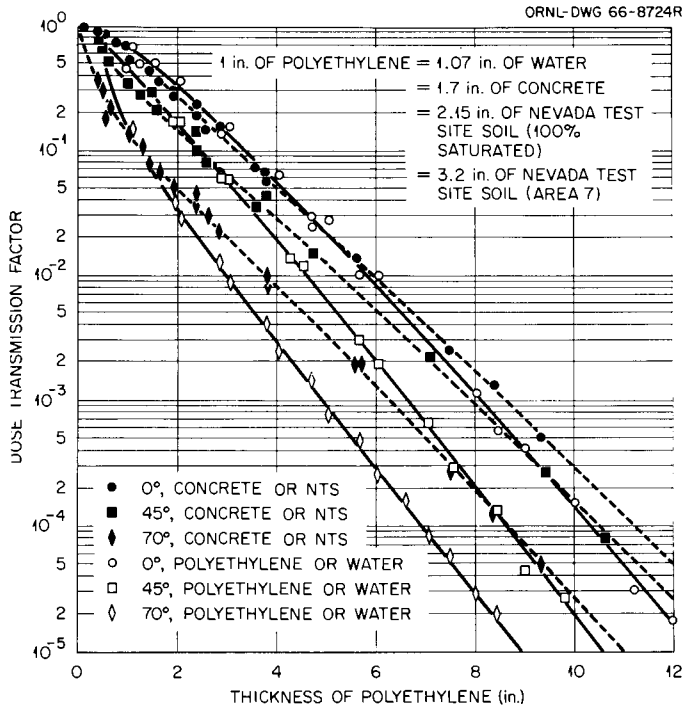

Fig. 17. Transmission of 1-MeV Neutrons Incident on Various Materials at Various Angles (From Ref. 48).

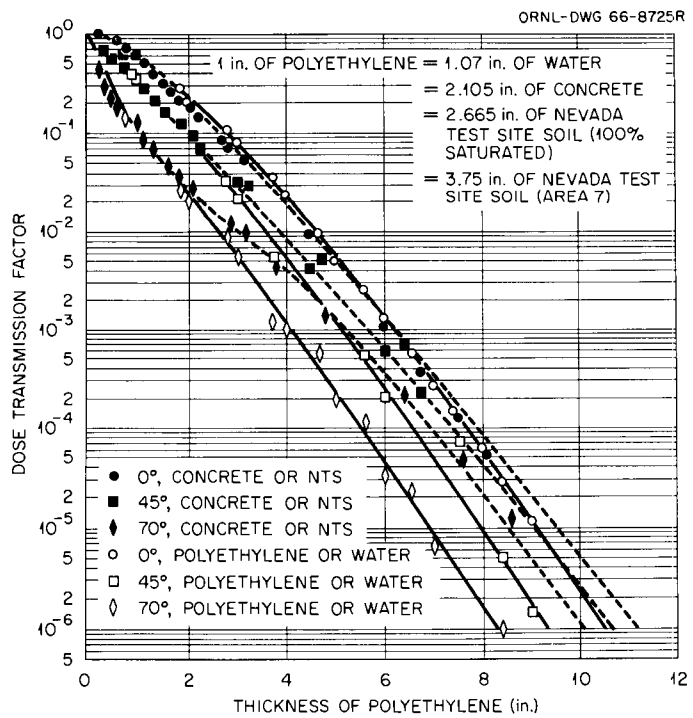

Fig. 18. Transmission of 0.5-MeV Neutrons Incident on Various Materials at Various Angles (From Ref. 48).

If one is interested in half-space results it is simpler to use Clark's data. Spielberg[49] suggested, as a possible procedure for the conversion of slab transmission results into half-space results, that the available values for a special concrete mixture might be multiplied by factors corresponding to ratios taken from Clark.

Although it is relatively easy to compare Broder's results for fast-neutron attenuation with those of others, this is not true for the thermal and epithermal buildup factors. Not only are there very few results reported, but also the group energies are different. This is true especially for the cutoff energy of the fast-neutron group. Broder used as the lowest value 1.5 MeV, whereas other people chose values between 0.2 and 1.5 MeV. Therefore it is important to know the neutron spectrum. Measurements of fast-neutron spectra are reported by Aalto et al,[41] Nilsson and Aalto,[42] Lim et al,[50] Yegorov,[51] and Vasil'ev et al.[38] Aalto also did calculations using different removal-diffusion computer codes and the moments method. His measured and calculated results agree within around 50%. In all the papers one trend seems to be evident: the hardening of the spectrum with distance in the shield in the case of fission sources. The minimum at 2.35 MeV in the cross section of oxygen produces, for deep penetration, high values in the spectrum, while a relative minimum in the spectrum occurs near 4.5 MeV.

Nilsson and Aalto[42] also measured and calculated neutron spectra in the epithermal and thermal energy regions. A 1/E spectrum reproduces their epithermal results satisfactorily. This is in agreement with data given by Broder[17] (see Fig. 23). In the thermal region only integrated results are available. All the computations of the spatial distribution

of neutrons have been based on the assumption of Maxwellian spectra for different mean temperatures (normally 293° K). This assumption certainly has to be investigated more carefully.

Mooney and Wells[32] performed S_{16}-P_2 calculations for concrete No. 3 in Table 6. In Section II-4 we shall discuss their work in more detail. At a thickness of 100 cm, they found a ratio of thermal-neutron dose to fast-neutron dose (energy greater than 0.2 MeV) of about 1. The epithermal dose is only one-third of the fast-neutron dose. Both Broder and Mooney and Wells used dose conversion factors based on work done by Snyder and Neufeld.[52] These factors include contributions due to secondary gamma rays in tissue slabs. Therefore they give low-energy neutrons an important role in total dose considerations.

3. Neutron Reflection - Albedos

To understand the use of the various albedos, or reflection coefficients, we will note the difference between flux and current. Consider a monodirectional flux, or a differential part of a distribution, incident on a surface. The incident flux $\varphi_o(E_o,\theta_o)$ is the number of neutrons crossing a unit area normal to the direction of flow (given by the polar angle θ_o measured from the normal) per unit time, energy, and solid angle. The differential incident current $J_o(E_o,\theta_o)$ is the number of neutrons crossing unit area on the surface per unit time, energy and solid angle. Thus

$$J_o(E_o,\theta_o) = \varphi_o(E_o,\theta_o) \cos \theta_o \ . \tag{26}$$

In using albedos to compute the dose-rate due to reflected neutrons, one needs the flux at the receiver point but the current is needed at the surface to integrate or count all neutrons as they leave the surface. Consequently albedos, as defined below, may be either flux or current dependent as required by their use.

As was mentioned earlier, Selph[13] covers the work in the area of neutron reflection by concrete quite adequately. For various subsequent calculational uses, he defines three different types of differential albedos, for which the particle flux has been weighted, respectively, by a dose-rate response function of energy as follows (variables corresponding to the incoming neutron are marked by a subscript o):

> $\alpha_{D1}(E_o,\theta_o,\theta,\varphi)$, Differential Current Reflected from a Surface (in Dose-Rate Units) per Unit Incident Flux (in Dose-Rate Units).

If the dose rate due to particles of energy E_o incident at angle θ_o to the surface normal is D_o, then the particle current (in dose-rate units) per steradian reflected in the direction θ,φ is given by $D_o\alpha_{D1}$. The reflected particle current in dose-rate units (or dose current) has no physical meaning but is merely a mathematical convenience. It is expressed mathematically by

$$D_J(\theta,\varphi) = \int K(E)\ J(E,\theta,\varphi)\ dE, \tag{27a}$$

where $J(E,\theta,\varphi) = \Phi(E,\theta,\varphi)\cos\theta$ is the emerging current. $\Phi(E,\theta,\varphi)$ is the reflected flux, and $K(E)$ is the flux-to-dose-rate conversion factor for particles of energy E. In these definitions the surface at which the current is measured is the material interface.

$\alpha_{D2}(E_o,\theta_o,\theta,\varphi)$, Differential Current Reflected from a Surface (in Dose-Rate Units) per Unit Incident Current (in Dose-Rate Units).

If the dose rate due to particles of energy E_o incident at angle θ_o is D_o, then the particle current (in dose-rate units) per unit solid angle reflected in the direction θ,φ is given by $D_o \cos\theta_o \, \alpha_{D2}$, where $D_o \cos\theta_o$ is the incident particle current in dose-rate units. This quantity differs from the traditional current albedo only in that the current is weighted by a dose-rate response function.

As indicated above, the advantage of the "current" albedos is that they may be integrated over a reflecting surface area to yield the dose-rate at given space points.

$\alpha_{D3}(E_o,\theta_o,\theta,\varphi)$, Differential Flux Reflected from a Surface (in Dose-Rate Units) per Unit Incident Flux (in Dose-Rate Units).

If the dose rate due to particles of energy E_o incident at angle θ_o is D_o, then the dose rate per steradian due to particles reflected in the direction θ,φ is $D_o\alpha_{D3}$. If the incident particle current per unit surface area is $J_o(E_o)$, then $D_o = K(E_o)J_o(E_o) \sec\theta_o$. If the reflected particle current per unit surface area is $J(E,\theta,\varphi)$, then the reflected differential dose rate is

$$D_f(\theta,\varphi) = \int K(E)\ J(E,\theta,\varphi) \sec\theta \ dE, \tag{27b}$$

where $D_f(\theta,\varphi)$ is the dose rate per unit solid angle due to particles reflected in the direction θ,φ.

The three types of albedos defined are related by

$$\alpha_{D1} = \alpha_{D2} \cos\theta_o = \alpha_{D3} \cos\theta \ . \tag{28}$$

Total dose-rate albedos are obtained by integrating different dose-rate albedos over the solid angle represented by θ and φ of the exit hemisphere. Maerker and Muckenthaler performed detailed Monte Carlo calculations to determine doubly differential values $\alpha_{D2}(E_o,\theta_o,E,\theta,\varphi)$.[44,45,53] The composition of their concretes are given in Table 6. The albedo results are available from RSIC.* Expressions and curves which fit both the experimental data and the Monte Carlo results may also be found in Ref. 13.

Another major contribution to the data on fast-neutron albedos is the Monte Carlo study made by Allen, Futterer, and Wright.[47] For mono-energetic neutrons (source energies 0.1, 0.25, 0.5, 1.0, 2.0, 3.5, 5.0, and 14 MeV) incident at 0, 30, 45, and 70 degrees from the normal to the slab they calculated multicollision dose albedos $\alpha_{D3}(E_o,\theta_o,\theta)$. Also, the integrated value $A_{D3}(E_o,\theta_o) = \int_{2\pi} \alpha_{D3}(E_o,\theta_o,\theta,\varphi)d\Omega$ and the energy spectrum of the reflected flux for each energy-angle combination are given.

French and Wells[54] analyzed these differential data. Their fit is a simple function of the incident and reflected polar angles only:

$$\alpha_{D1} = k(E_o) \cos^{2/3}\theta_o \cos\theta . \tag{29}$$

* The data are included with computer code package CCC-90 (AMC: A Monte Carlo Code Utilizing the Albedo Approach for Calculating Neutron and Secondary Gamma Ray Distributions in Rectangular Concrete Ducts).

The quantity $k(E_o)$ is a normalizing factor which includes the effect of incident energy and the composition of the reflecting concrete. Values of $k(E_o)$ are shown in Table 7, where we also compare total dose albedos given by Eq. (29) with those of Allen et al. and Maerker and Muckenthaler.

Spielberg,[49] who calculated dose albedos for an average soil, pointed out that the albedo values are strongly dependent on the flux-to-dose-rate conversion factors. Maerker and Muckenthaler used Henderson's factors,[55] while Allen and Futterer chose those of Snyder and Neufeld.[52] Following Spielberg's arguments, one would expect differences of the same order as those seen in Table 7.

Yo Taik Song,[56] in his analysis of the streaming of fast neutrons through concrete ducts, also describes the use of the albedo concept. In addition to his calculated results, which he compared with experiments, he also gave a short review of this subfield.

4. Secondary Gamma Radiation

Neutron capture, inelastic scattering, and charged-particle reactions produce secondary gamma radiation in concrete. Normally for shielding calculations, dose contributions from activation are not considered. The actual secondary gamma-ray dose due to each of the possible processes is not known very well; neither is the total dose. This is mainly because very few reliable gamma-ray production data have been available in the past. Also, results are sometimes restricted or classified.

At present the most widely used source of data on thermal-neutron capture gamma-ray spectra is the compilation of Troubetzkoy and Goldstein.[57]

TABLE 7

VALUES OF THE ALBEDC FACTOR $k(E_o)$ AND COMPARISON OF TOTAL DOSE ALBEDOS $A_{D_i}(E_o,\theta_o) = \int_{2\pi} \alpha_{D_i}(E_o,\theta_o,\theta,\phi)d\Omega$

FOR NORMALLY INCIDENT NEUTRONS

Energy [MeV]	$k(E_o)$	A_{D3} (French/** Wells)	A_{D3} (Allen/** Futterer)	A_{D2} (French/** Wells)	A_{D2} (Maerker/** Muckenthaler)	Energy-band (MeV)
0.1	0.0948	0.594	0.598	0.297		
0.25	0.1027	0.644	0.691	0.322		
0.5	0.1062	0.730	0.673	0.365		
0.7*	0.1190	0.750	0.762	0.385		
1.0	0.1323	0.830	0.895	0.415	0.325	0.75-1.5
1.3*	0.1260	0.790	0.833	0.400		
2.0	0.1164	0.732	0.684	0.366	0.28	1.5 - 3.0
3.0	0.1030	0.648	0.616	0.324		
4.0*	0.0908	0.570	0.565	0.292	0.335	3.0 - 4.0
5.0	0.0834	0.522	0.514	0.261	0.245	4.0 - 6.0
6.0*	0.0780	0.490	0.497	0.245		
8.0*	0.0710	0.440	0.452	0.220	0.210	6.0 - 8.0
10.0*	0.0637	0.404	0.408	0.202		
12.0*	0.0598	0.375	0.363	0.187		
14.0	0.0552	0.348	0.319	0.174		

* Values of k and A, except data of Maerker-Muckenthaler, obtained by linear interpolation.

**French - Ref. 54, Allen - Ref. 47, Maerker - Ref. 44.

Broder[17] recommends similar data. He reported gamma-ray yields per captured neutron for some of the concretes of Table 1. They are reprinted in Table 8. From these data Broder concludes that the most important capture gamma rays have an initial energy near 6 MeV.

He thus chooses to approximate Eq. (25) by a simpler expression which contains only exponentials. Since there are no general studies using his formula and because of the simplicity of the functions ψ_o and ψ_1, which will be discussed in Section III-3, we will not reproduce Broder's formula.

Broder does not take account of gamma radiation due to inelastic scattering of fast neutrons. The work of Karcher and Wilson,[58] who studied the shielding properties of ordinary concrete of type 01 [density 2.33 g/cm^3, water content 1.85 weight % (see Ref. 9)] seems to justify this neglect, at least for fission-energy sources. But the transport calculations of Straker[59] for air indicate that for much harder neutron source spectra, most of the neutrons are slowed down by inelastic scattering processes and that the resulting gamma radiation should not be neglected. It may be treated, however, in a way similar to that used for thermal-neutron capture radiation. The gamma-ray source would be distributed roughly in proportion to the fast-neutron flux. The inelastic scattering cross sections vary rapidly with neutron energy. Therefore one has to sum over different neutron energies and introduce some assumptions about the fast-neutron spectrum. Karcher and Wilson[58] used a 1/E spectrum, which overestimates the higher-energy groups in their case. They also allowed only one representative gamma-ray energy

TABLE 8

CAPTURE GAMMA-RAY YIELDS (n_i) FOR THE CONCRETES DESCRIBED IN TABLE 1

(From Ref. 17)

Density (kg/m^3)	Concrete Numbers	Photons per Capture Gamma-Ray Energies (MeV) 2	3	4	6	8
2300	1-2	0.310	0.310	1.170	0.412	0.216
	3-6	0.359	0.359	0.575	0.269	0.137
2600	1-3	0.118	0.162	0.298	0.210	0.404
	4-6	0.159	0.159	0.204	0.186	0.375
3200	1-6			0.212	0.208	0.440
3500	1-6	0.262	0.262	0.489	0.276	0.175
3600	1-6			0.282	0.213	0.443
4200	1-6			0.238	0.218	0.490
4600	1-6			0.238	0.219	0.503
5200	1-6			0.238	0.224	0.505

$\overline{E}$ for each neutron group. Thus they found source terms of the form

$$S_i(x,\overline{E}_i) = \Sigma^i_{in}\, \varphi_f(x)\, f_i\, \overline{E}_i \,, \tag{30}$$

where f_i is the fraction of the fast-neutron flux in group i, defined by

$$f_i = \int_{E_{i-1}}^{E_i} \frac{dE}{E} \Big/ \int_{0.2}^{14\ \mathrm{MeV}} \frac{dE}{E} \tag{31}$$

if one takes 0.2 MeV as the lower boundary of the fast-neutron flux.

The gamma-ray dose rate from inelastic reactions was obtained by weighting this source with Taylor-type buildup factors[21] and integrating over all source locations with the computer program GRACE.[60] Despite the very conservative assumptions, the contribution to the secondary gamma-ray dose rate was only about 25% for a neutron source that was a combination of fission and 14-MeV fusion neutrons. The importance of inelastic scattering gamma rays would be even less in other concrete because of the presence of more hydrogen.

Some calculations by Mooney and Wells[32] were done for the TSF concrete (Table 6). Two spectra were used, a pure fission spectrum and a mixture of 25% 14-MeV neutrons and 75% fission-spectrum neutrons. Between the source and the concrete slabs was 700 m of air, which affected the spectra impinging on the slabs. Figure 19 shows the fraction of the neutron flux above energy E for fast neutrons. Calculations were done with the computer program ANISN (S_n discrete ordinates) and O5R (Monte Carlo), and quite good agreement was obtained. Figures 20 and 21 show the results for the fast-neutron dose and the capture gamma-ray dose.

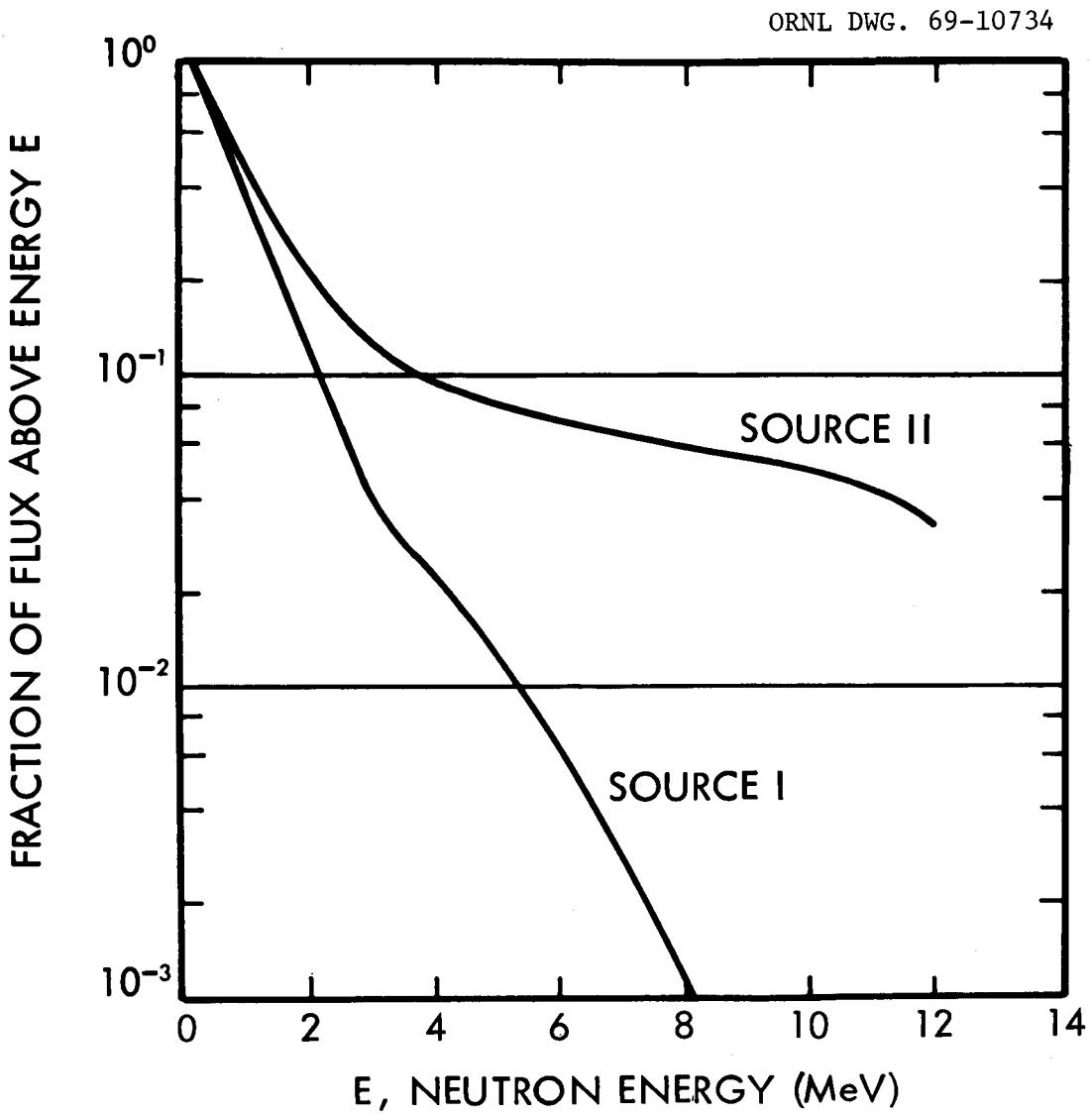

Fig. 19. Source Spectra Given as the Fraction of Neutrons Above Energy E of all Neutrons of Energy Greater than 0.2 MeV (From Ref. 32).

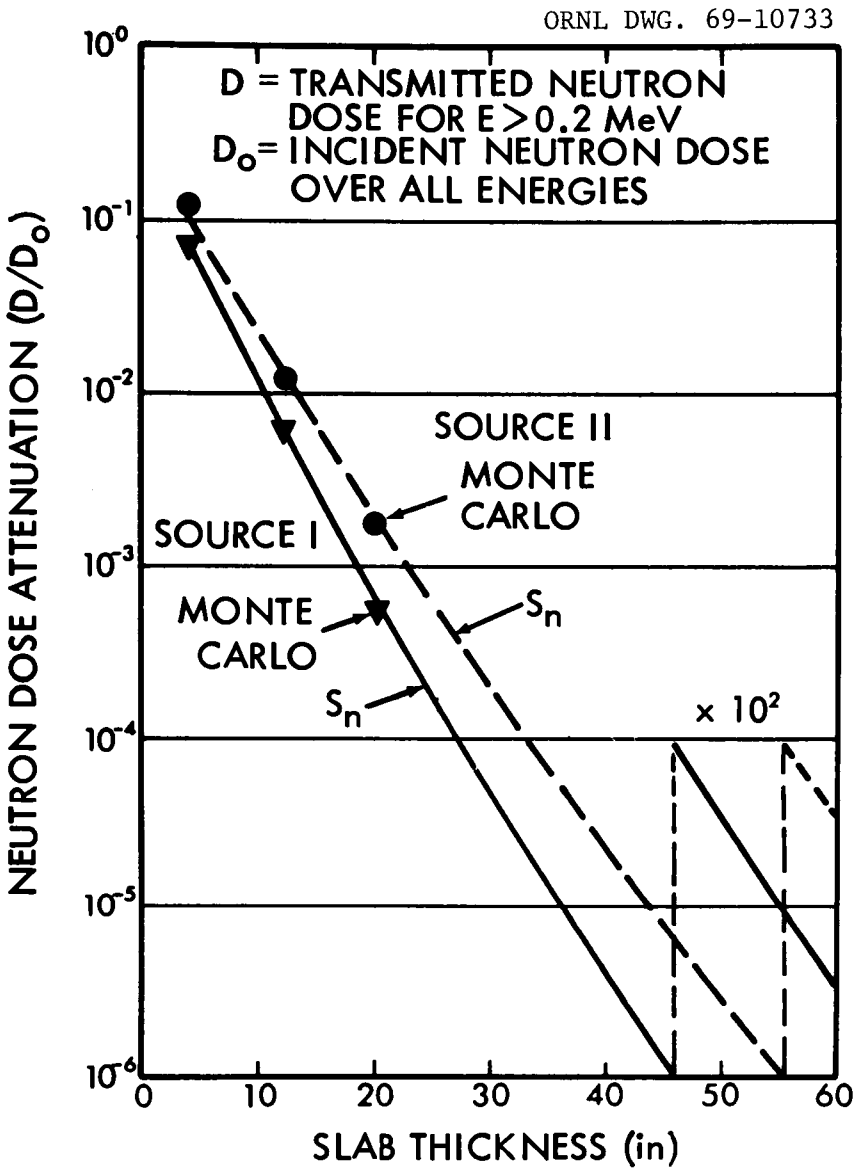

Fig. 20. Comparison of S_n and Monte Carlo Computed Neutron Dose Transmission Through Concrete for Sources I and II (From Ref. 32).

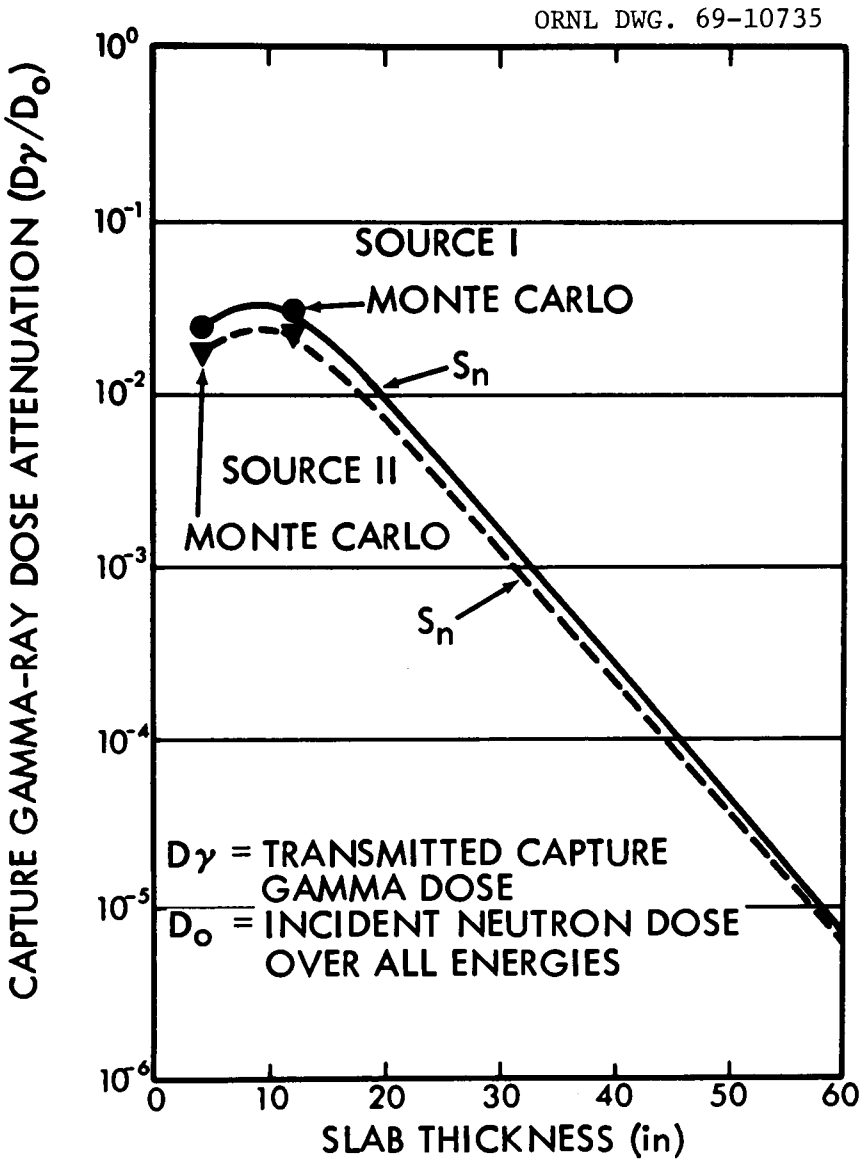

Fig. 21. Comparison of S_n and Monte Carlo Computed Capture Gamma-Ray Dose Transmission Through TSF Concrete for Sources I and II (From Ref. 32).

The neutron cross sections were basically those of the GAM library.[61] For the ANISN calculation they were reduced to 27 neutron groups and 23 gamma-ray groups. Even in the case of the very hard spectrum of Source II, no consideration was given to inelastic scattering. This was mainly because of the lack of data.

Very few results have been published for secondary gamma-ray albedos (gamma rays emerging per incident neutron). Here, too, only capture gamma rays have been considered. Both Budka's results[62] and those for the TSF concrete[45,53] are described by Selph.[13]

5. 14-MeV Neutrons

The so-called Source II used in the calculation of Mooney and Wells[32] (Fig. 19) contained a 25% contribution by 14-MeV neutrons. These neutrons are produced by the $^{3}H(d,n)^{4}He$ reaction, which not only occurs in connection with the thermonuclear weapons but also is a common neutron source for accelerators. Therefore, there are a number of papers in the literature which deal with the shielding properties of concrete against 14-MeV neutrons.

The results as given by Hacke[63] and Broerse[64,65] show considerable disagreement, which led to some discussion.[66] Hacke collected, measured, and compared transmission data. Some of his results are given in Fig. 22, from which one could choose e-folding, or relaxation, lengths varying from about 10 cm to more than 30 cm, which is quite unsatisfactory. Hacke's measurements, done "under unfavorable scattering conditions and with very poor geometry,"[63] resulted in a transmission factor of 10^{-4}

ORNL-DWG. 67-10851

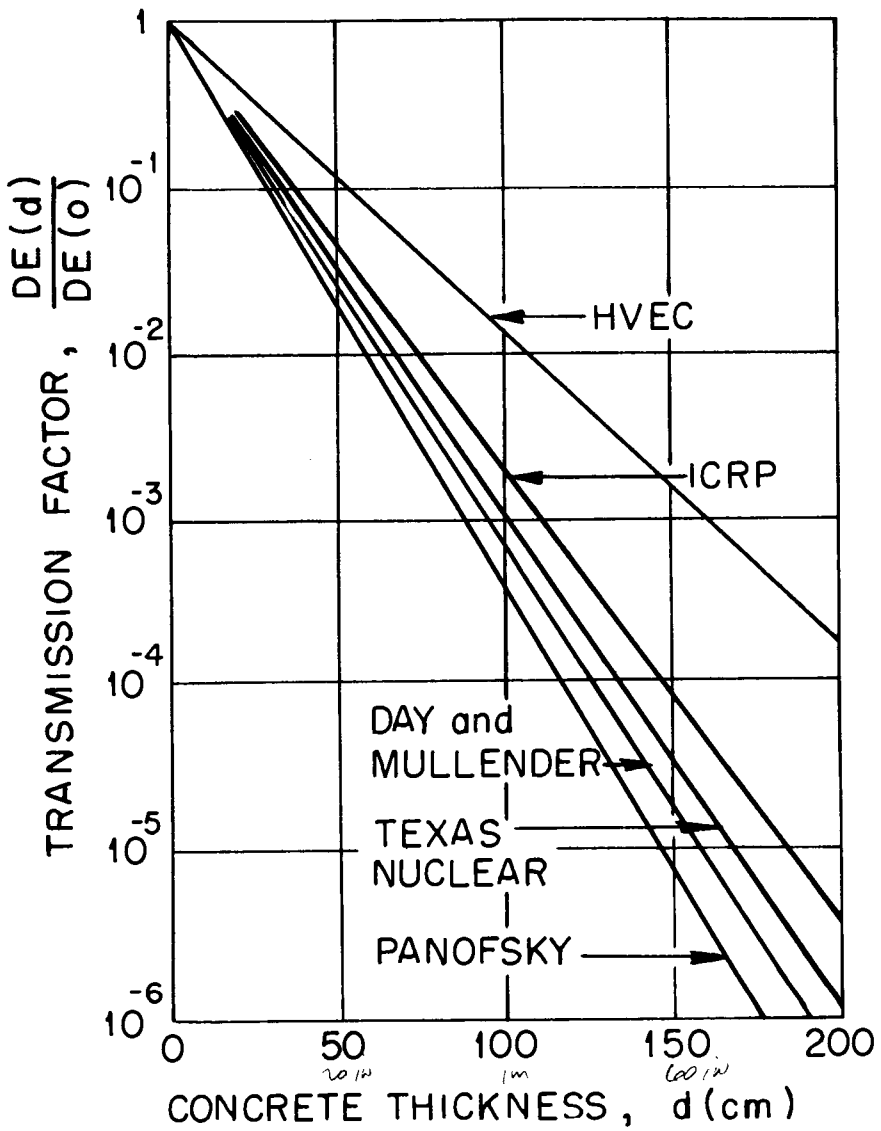

Fig. 22. Experimental Neutron Transmission as a Function of Ordinary Concrete Thickness for 14-MeV Neutrons, Mean Concrete Density 2.4 g/cm^3 (From Ref. 63, HVEC Ref. 68, ICRP Ref. 61, Day and Mullender Ref. 67, Texas Nuclear Ref. 70, Panofsky Ref. 71).

for 130 cm of concrete and a relaxation length of 15 cm. In comparison with Hacke's results, the conclusions of Broerse are very pessimistic. Broerse reported measurements for slabs up to 90 cm thick. The slabs were arranged perpendicular to the accelerator axis. For thin concrete slabs (up to 40 cm) he determined a relaxation length of 19.7 cm, while for the thicker ones he recommends a value of only 17.0 cm. Hacke's and Broerse's results as presented in Fig. 22 seem to disagree very much with those calculated by Clark (Fig. 3) and Allen and Futterer (Fig. 13). But these calculations also show a considerable buildup of the fast-neutron dose for 14-MeV sources. Therefore, instead of comparing relaxation lengths, as Hacke did, we compare calculated and measured transmission factors for the same concrete thicknesses. This is done in Table 9.

The agreement between the Monte Carlo results of Clark[43] and Allen and Futterer[47] is quite reasonable except at the greatest thickness (50- and 60-cm). But because Allen and Futterer could use only relatively simple importance sampling techniques and followed no more than 1000 case histories, we believe there is, for thick slabs, a serious possibility of underestimation.

Among Hacke's experimental values the one for the 130-cm slab is the only one in reasonable agreement with other data. His result, a factor of 2.7 higher than Clark's, might be explained by background effects. Values for greater slab thicknesses were measured under very poor geometrical conditions. His estimated error is about 50%. Surprisingly good agreement exists between Clark's calculations and the measurements of Day and Mullender[67] for the 60- and 71-cm-thick slabs.

TABLE 9

DOSE TRANSMISSION FACTORS FOR 14 MeV NEUTRONS IN CONCRETE

Slab Thickness [cm]	Clark **	Allen-Futterer **	Hacke**	Broerse**	Day and Mullender **
10	0.630	0.594		0.80	
30	0.168	0.155		0.26	
50	0.037	0.025			
60	1.55(-2*)	8.4(-3)		6.1(-2)	1.57(-2)
71	6.3(-3)			3.5(-2)	9.8(-3)
100	5.2(-4)			6.0(-3)	
130	3.7(-5)		1.1(-4)		2.16(-4)
150	6.5(-6)		∿3.0(-5)		

*Read 10^{-2}

**Clark: Ref. 43; Allen: Ref. 47; Hacke: Ref. 63; Broerse: Ref. 65; Day: Ref. 67

Broerse's results also seem to be much too high. Possible explanations may be poor geometries for his results up to 30 cm and background effects like wall scattering in the case of thick-slab measurements. This explanation may be supported by the fact that he actually reported 3 different values for the relaxation length λ:

(1) λ = 19.7 cm for concrete thicknesses from 15 to 30 cm (target-to-detector distance about 1 m, target-to-slab distance less than 40 cm).

(2) λ = 17 cm for concrete thicknesses from about 60 to 96 cm. (target-to-detector distance greater than 2.3 m, target-to-slab distance less than 2 m, detector outside accelerator building).

(3) λ = 15.2 cm for 30 cm of concrete behind 30 cm of paraffin and geometry as in the case of λ = 19.7.

Because of the unsatisfactory agreement among the various investigators, we have carried out further calculations as described below.

6. Special Concretes

There seem to be few limitations for those who want concretes with special qualities. In this section some special concretes which may be of more than local interest are discussed.

The main factors that influence the choice of a concrete for a particular application are its attenuation characteristics (including secondary gamma-ray production), its engineering properties (such as strength and method of placement), maintenance conditions (heat resistance or time behavior), and, of course, the cost of materials, material transportation, and concrete placement.

One way to reduce the cost is to use local aggregates. This is only possible in cases where a suitable aggregate such as crushed rock, sand, barite, limonite, or magnetite is at hand. Less common materials should not be overlooked; Northup,[72] for instance, recommends the use of high-density waste slag. He made some investigations with lead slag, but probably other slags could be used also. The resulting concrete had a density of 3.8 g/cm^3 and was at the time of the report about 30% cheaper than other comparable concretes. Another way of using local stones or ores was mentioned by Dubrovski et al.[73,74] and is described for nonnuclear applications by A. K. Shreiber et al.[75] The resulting concrete is known under the name "stone concrete" in English translations. It is prepared by driving large stones into a matrix of concrete already containing normal aggregate by means of powerful vibrators. Limestone, sandstone, or other porous materials that can absorb relatively large amounts of water are generally used for nuclear applications. The shielding properties of this concrete are slightly better than those of the same concrete without stone. This is mainly due to an increase in density.

Chromite and fireclay concretes are used in the Soviet Union for special heat-resistant materials. It was claimed[76,77] that these would be satisfactory for fluxes up to 10^{18} n/cm^2-sec, temperatures around 1000-1100°C, and temperature changes up to 900°C. At those high temperatures concrete does not retain much water. But nevertheless the shielding properties seem to be not too bad.[78] (Sometimes fireclay concrete is called "chamotte" in English translations.)

A method of increasing the hydrogen content of concrete is the use of polyester resin instead of some of the cement. Loginov[79] describes a

heavy plastic concrete. The polyester resin improved the mechanical properties and the corrosion resistance, enhanced the hardness, and accelerated the hardening. He also speaks of better attenuation properties, but no understandable numbers are cited.

As may be seen from Fig. 2 and even better from a comparison of Figs. 20 and 21 the total dose behind a concrete shield is often dominated by the secondary gamma rays. Therefore many people have looked for some way to minimize this radiation. This can be done by adding substances to the concrete that produce only low-energy secondary gamma rays and at the same time have very high neutron absorption cross sections. The most commonly used element that fulfills this requirement is boron-10. It is usually added in the form of colemanite, borocalcite, or boron frit.[80] Tests by Shirayama[81] showed that both colemanite and borocalcite impair the setting time and strength of the concrete. But the deleterious effects of colemanite were far greater in this experiment than those of borocalcite. For both materials the effects increased with the fineness of the boron-containing minerals. Test results mentioned by Bingham[82] indicate that up to 5% elemental boron in the form of boron frit can be added to concrete without adversely affecting the set or the structural properties of the concrete. He recommends the use of a 12-inch-thick layer of 2% borated concrete in front of the inner surface of a nonborated concrete shield. This would reduce the total dose rate at the inner surface by more than a factor of ten compared with using a 12-inch nonborated layer only. A reactor spectrum was the assumed source in the calculations.

Before 1965, there was not much research concerning boron-containing concretes in the Soviet Union. Komarovskii,[8] for instance, mainly relies

on American sources. The only Soviet paper dealing with this aspect of shielding that he mentions is that of Avayev et al.[83] This paper describes some measurements done for various types of concrete with densities from 2 to 4.65 g/cm^3 and 0.5 to 3.44% boron in the form of calcium borate. A Po-Be source was used, and the attenuation of fast and thermal neutrons was measured under broad beam geometry conditions. Komarovskii does not seem to trust the results very much. He only mentions that there was no substantial change in the attenuation properties for the whole Po-Be spectrum.

Since then, the group around Broder[17,84-86] has become interested in adding boron to concrete mixtures. In his book[17] Broder extends the investigation of different concretes (see Table 1) to those containing boron. He especially considers the relaxation length and spectra of intermediate-energy neutrons. Table 10 and Fig. 23 give some of his results.

Recommendations concerning boron content are given in Ref. 84 and 85. There borated chromite concretes are investigated for shielding and heat release properties. The most efficient mixtures contain between 15 and 30 kg/m^3 of boron.

Studies of various very light concretes (densities 1.8 and 2.2 g/cm^3) are described in Ref. 86. About 2% boron (which would mean 40 kg/m^3) gave the most efficient results.

French investigators also are developing borated concretes.[87,88] Interesting too is their idea of adding rare earths instead of boron. In References 87 and 88 such concretes are mentioned. Detailed studies are given in Ref. 88 for the mixture used for the Rapsodie reactor shield

TABLE 10

NEUTRON DOSE BUILDUP FACTORS FOR BORON CONTAINING CONCRETES
IN INTERMEDIATE ENERGY RANGE (E< 1.5 MeV)

(From Ref. 17)

Density of Concrete (kg/m^3)	B-Content (Weight Percent)				Average Composition of Concretes with same Density (Weight Percent)						Dose Buildup Factors				
	Number of Concrete										Number of Concrete				
	7	8	9	10	H	O	Al	Si	Ca	Fe	1*	7	8	9	10
2300	0.48	1.00	1.52	2.56	0.1	52.90	4.41	30.95	7.66	2.03	10.3	7.35	6.95	6.60	6.28
2300a	0.48	1.00	1.52	2.56	0.35	54.21	4.68	32.77	5.85	2.14	3.40**	3.20	3.13	3.09	3.06
3200	0.34	0.72	1.09	1.84	0.30	32.82	0.89	11.10	4.94	48.81	4.20	4.05	3.97	3.92	3.83
4200	0.26	0.55	0.83	1.40	0.23	15.57	1.13	4.89	1.24	66.27	7.40	7.20	7.08	6.92	6.89

* Concrete #1 same as in Table 1

** Same as #2 in Table 1

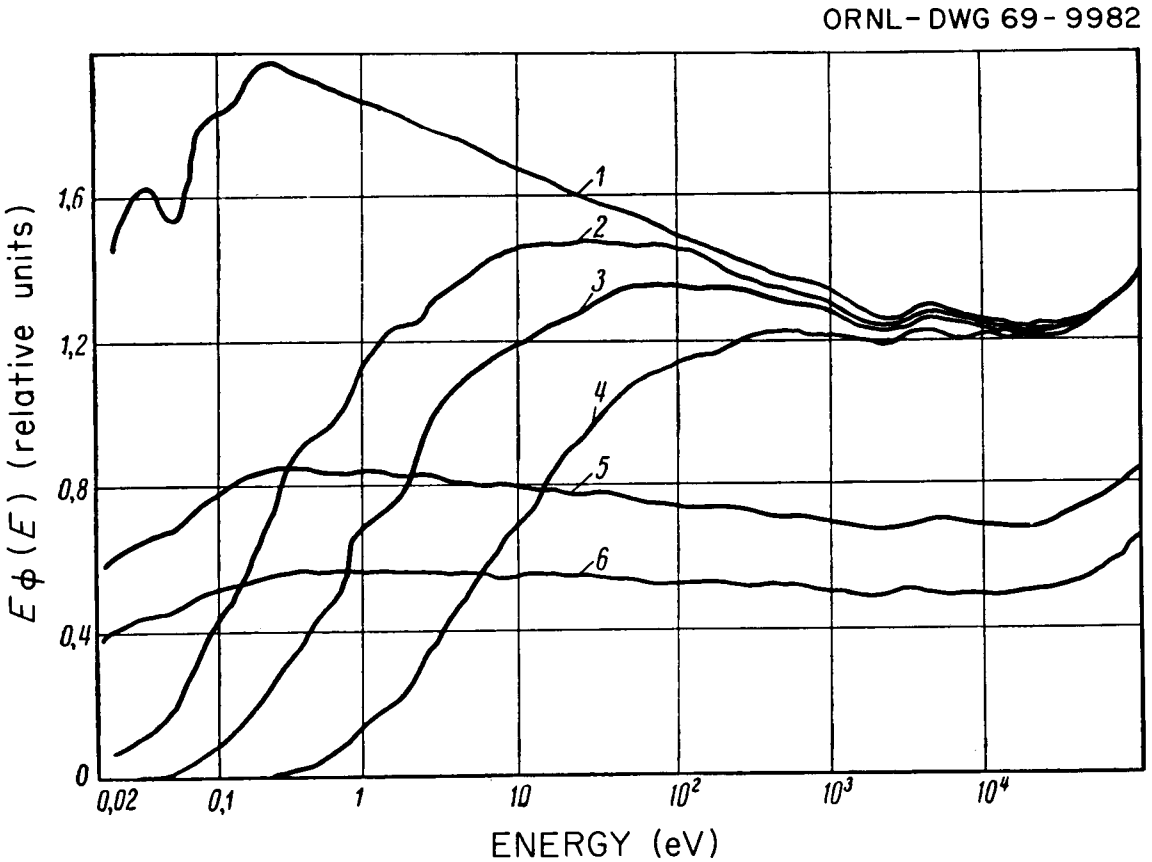

Fig. 23. Intermediate Neutron Spectra for Concretes, Density 2.3 g/cm³ (From Ref. 17) [1] 0.35% H, no B; [2] 0.35% H, 11 kg/m³ B; [3] 0.35% H, 23 kg/m³ B; [4] 0.35% H, 59 kg/m³ B; [5] 0.61% H, no B; [6] 0.84% H, no B.

to suppress activation of adjacent structures. Table 11 gives the elementary composition of the concrete. Because of the high thermal neutron absorption cross section of gadolinium (σ_a = 49,000 b), one expects the secondary gamma-ray spectrum of this concrete to be essentially the same as the one produced by pure gadolinium. We therefore include the capture gamma-ray yields for the most important gadolinium and samarium isotopes in Section III-4. There is one disadvantage: the price. For about 275 tons of concrete 17.25 tons of yttrium earths were needed. The cost was $1,130 per ton, compared with $110 for ordinary concrete.

This review should not be concluded without mentioning earth. Its chemical composition is similar to that of ordinary concrete. However, the density is lower by a factor of about two or three. Having this in mind, one may compare results for concrete with those found for soils. Spielberg,[49] for instance, did this. But one should regard this only as a first approximation, because the shielding properties of concrete are linear functions of the density only under very special conditions.

7. Conclusions

The greatest problem for all who do shielding calculations for concrete is the lack of reliable cross sections. Even for the work done for the Tower Shielding Facility concrete (Clark, Maerker, Wells) there was not enough information about secondary gamma-ray production available. But the situation has been changing rapidly as a result of work done by Drake,[89,90] Maerker and Muckenthaler,[91] Yost and Kremer,[92] and many others. We therefore felt that it would be worth while to collect this new

TABLE 11

ELEMENTARY OXIDE COMPOSITION OF SERCOTER CONCRETE*

(From Ref. 88)

Elements	Element Content (Weight percent)	Oxygen in the Oxide (Weight per cent)	Total (Weight per cent)
Si	4.32	9.88	14.2
Al	21.7	19.3	41
O	49.2		
Fe	4.75	1.86	6.61
Ca	4.64	1.86	6.50
Mg	8.55	4.45	13.00
Mn	0.25	0.07	0.32
Na	0.18	0.13	0.31
Ti	0.89	0.59	1.48
K	0.15	0.03	0.18
P	0.026	0.034	0.06
C	0.0054	0.0146	0.02
H	1.28	10.21	11.49
La	0.62	0.11	0.73
Nd	1.85	0.31	2.16
Pr	0.32	0.06	0.36
Sm	0.53	0.09	0.62
Y	0.43	0.11	0.54
Gd	0.28	0.04	0.32
Dy	0.19	0.03	0.22
Ce	0.14	0.02	0.16

* Density 2.78 g/cm^3

information and to combine it with older data to produce a cross-section library for concrete which would be made available by RSIC as DLC-9. This library will be described in the next chapter. We also give data for use in analytical formulas such as those proposed in Section II-1.

As was mentioned previously, we will present in Section IV results of new calculations using the cross section library mentioned above and described in the next section. The library is coupled, that is, contains both neutron and gamma-ray cross sections and so was used to calculate both neutron and secondary gamma-ray transmission. The ANISN discrete ordinates transport code was used for the calculations.

III. CROSS SECTIONS FOR CONCRETE

1. Removal Cross Sections

As we have seen in Sec. II-1 the removal cross section of a compound can be given by

$$\Sigma_r = \sum_j \rho_j (\Sigma_r/\rho)_j \ . \tag{3}$$

Values of $(\Sigma_r/\rho)_j$ for different elements are shown in Fig. 1 and given in Table A-1.

In the case of concrete the materials are normally in the form of oxides. We may distinguish three different groups:

1. H_2O. Because of the large removal cross section of hydrogen, Σ_r is strongly dependent upon the water content.
2. SiO_2, CaO, and other oxides of elements with atomic numbers between 10 and 20. Both cement and light aggregates consist of these oxides. Thus concretes contain at least a certain amount of them, and because the removal cross sections of elements like Si, Ca, Al, and Mg do not differ greatly, the contribution of these oxides is roughly constant.
3. Fe_2O_3 and oxides of the other main elements of the heavy aggregates. Their concentration normally determines the density of special concretes.

In view of these conditions, Broder was able to simplify and get removal cross sections which depend only upon the density and the water content of the concrete. The results are shown in Fig. 24. The curves of type 1 show Σ_r for varying water content at several densities. If both the density and the water content of the concrete are given, the corresponding value from curve 1 is an estimate of the removal cross section. Curve 2 is an example of how this would look for barite. The curves of type 3 show how Σ_r varies for a given concrete if the water content of the concrete is changed (the density will of course change also).

ORNL-DWG 69-9983

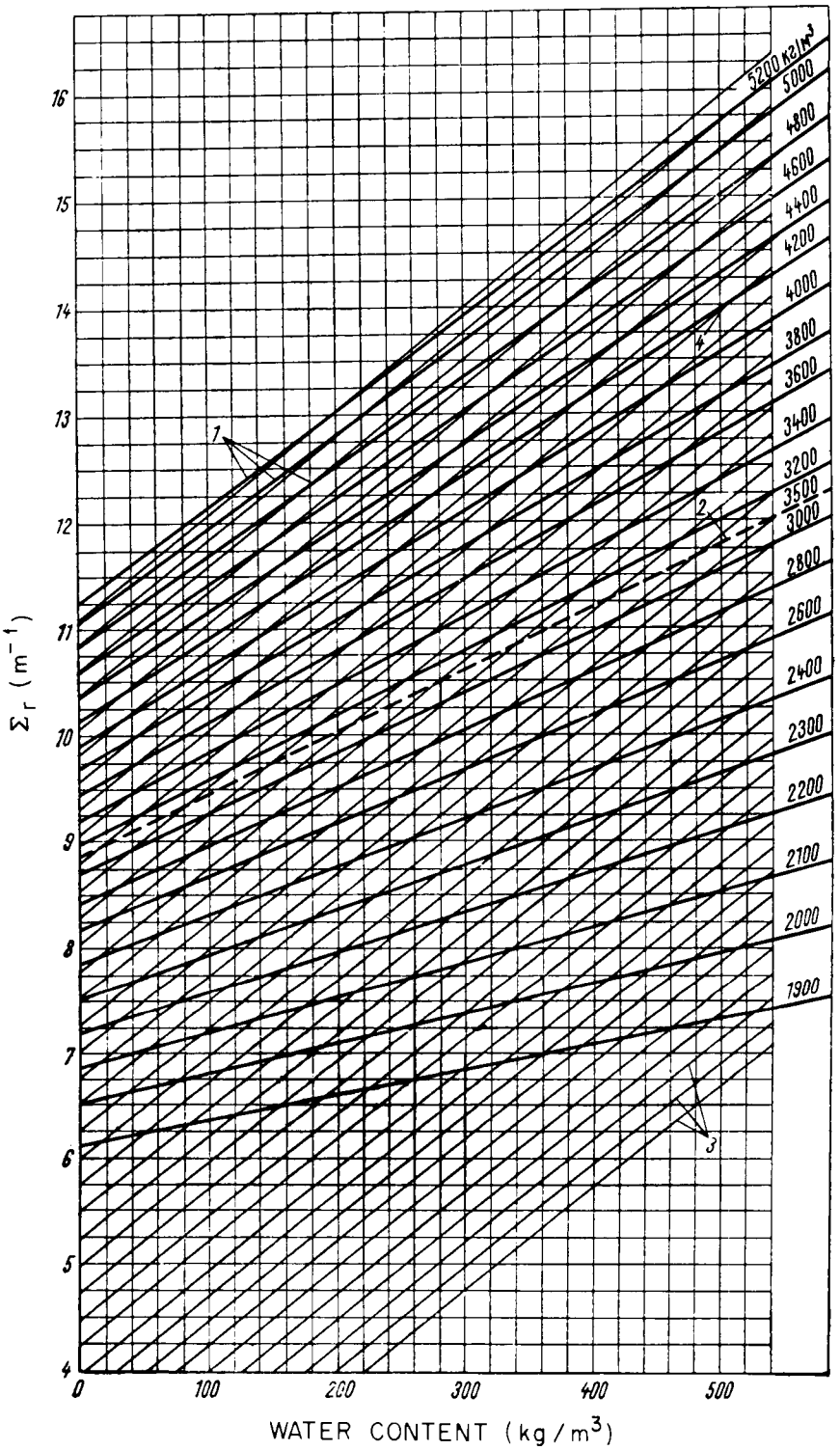

Fig. 24. Removal Cross Sections for Concrete as Functions of Density and Water Content (From Ref. 17) [1] Σ_r for Changing Water Content and Constant Density, [2] Same as [1] But For Barytes Concrete, [3] Σ_r for Changing Water Content and Constant Amount of Other Constituents.

(Hilsdorf[1] investigated possible mechanisms of water losses for hardened concretes.) Curves of type 3 are simply straight lines with the removal cross section of water as the slope

$$\Sigma_r\ (\rho_{H_2O}) = \left[\ \text{const} + \left(\frac{\Sigma_r}{\rho}\right)_{H_2O} \cdot \rho_{H_2O}\ \right]\ \text{cm}^{-1} \tag{32}$$

The slopes of curves 1 are dependent upon the density of the chosen concrete. Broder does not describe in any detail how he determined these curves, nor does he give their mathematical description. The data can be fitted by

$$\Sigma_r\ (\rho, \rho_{H_2O}) = \left[0.042 + f(\rho)\ (0.767 + \rho_{H_2O})\right]\ \text{cm}^{-1} \tag{33}$$

From values of Σ_r for constant ρ_{H_2O} one may further approximate:

$$f(\rho) = 0.0148 \cdot \sqrt{\rho^2 - 1.9^2} + 0.024. \tag{34}$$

Eqs. (33) and (34) combined still give a relatively unwieldy expression. Therefore we reproduced Broder's results by a simpler approach. A form suggested by Kunszt[93] seemed to be most suitable. With all the coefficients calculated we recommend

$$\Sigma_r = \left[0.0383 + 0.0159\ \rho + 0.0018\ w\right]\ \text{cm}^{-1} \tag{35}$$

where

ρ is the specific gravity of the concrete and w the water content in weight percent.

One can easily check that most of the removal cross sections in Table 4 agree with Eq. (35) within 10%. The Hanford experimental results[27-31] can also be described within about 10%. This is shown in Table 12. The concretes are listed with their numbers as used in

TABLE 12

RESULTS OF THE HANFORD MEASUREMENTS

(From Ref. 27 to 31)

ρ - density (g/cm^3)

w - water content (percent)

Σ_{rc} -removal cross section calculated by Eq. (35) (cm^{-1})

Σ_{rm} -removal cross section measured (cm^{-1})

Concrete from Table 4		'as cured'	100°C	200°C	320°C
I - 4	ρ	4.8	4.72	4.86	4.67
	w	2.8	1.8	0.93	0.75
	Σ_{rc}	0.122	0.117	0.118	0.114
	Σ_{rm}	0.128	0.121	0.117	0.114
L - 4	ρ	4.23	4.14	4.04	4.05
	w	6.0	3.9	1.56	1.78
	Σ_{rc}	0.116	0.109	0.103	0.104
	Σ_{rm}	0.120	0.112	0.097	0.093
L - 3	ρ	3.39	3.33	3.24	3.26
	w	6.1	4.31	1.67	2.5
	Σ_{rc}	0.109	0.099	0.092	0.094
	Σ_{rm}	0.105	0.092	0.082	0.083
L - 3 with different water content	ρ	3.29	3.27	3.25	3.21
	w	4.1	3.2	2.9	1.7
	Σ_{rc}	0.098	0.096	0.095	0.092
	Σ_{rm}	0.107	0.099	0.097	0.093
O - 6	ρ	2.33	2.26	2.24	2.23
	w	5.87	2.74	1.96	1.57
	Σ_{rc}	0.084	0.079	0.077	0.076
	Σ_{rm}	0.078	0.074	0.072	0.070

Table 5. The water content was changed by heating the concretes at 100°C, 200°C, and 320°C until equilibrium conditions were attained. The neutron attenuation measurements were done by activation of ^{35}S.

The greatest differences between measured and estimated results occur for water contents of less than 2%. Also, Eq. (35) is only a poor estimation for densities over 6 g/cm^3.

From these results we conclude that for the attenuation of fast neutrons, as well as for the attenuation of gamma rays, the density of the concrete is much more important than its water content. This is not true for intermediate and thermal neutrons, which are important as sources of secondary gamma rays.

These conclusions are in disagreement with measurements of Condat et al,[94] done for conditions which lead to Eq. (31). The dependence of Σ_r upon the water content which they found is roughly three times as strong as in Eq. (31).

2. Intermediate- and Thermal-Neutron Cross Sections

Table A-2 lists absorption and scattering cross sections for the most important elements in concrete. The information is taken from the ENDF/B library[95] (for the elements that were represented there in late 1968) and from BNL-325.[96] To use these cross sections in calculating neutron buildup factors one must multiply them by the atomic densities of the elements in the concrete and average them over the energy distribution of the flux. This leads to some difficulties for the thermal-neutron absorption cross sections. As one may see from Table A-2 the absorption cross sections are normally assumed to be proportional to

the reciprocal of the neutron velocity. If the neutrons follow a Maxwellian distribution with a mean energy of 0.0253 eV (20°C) one must multiply the tabulated cross sections by 0.8862 to obtain the effective absorption cross sections. Yet, as we mentioned earlier, there exists at present no information on the thermal-neutron spectrum in any concrete. Especially for concretes with low hydrogen content or strong absorbers the factor 0.8862 seems too high. In this case one would expect the mean neutron energy to be shifted to higher energies. Calculations done by N. M. Greene[97] for air and measurements of the thermal-neutron spectrum in poisoned water[98] show the same trend.

In deriving the expressions (12), (16a), and (16b) for the neutron buildup factors there were restricting conditions. We will now examine some of these conditions in more detail.

Normally one wants the main sources of the secondary gamma rays as far away from the outer shield surface as possible and prefers, therefore, the z-independent buildup factor for the thermal-neutron flux as given in Eq. (16a). Thus the following should hold:

$$3\Sigma_a\Sigma_s < \Sigma_r^2. \tag{36}$$

Comparing the elements in Tables A-1 and A-2 one easily finds that this may be achieved only by a few of those elements which have importance for concretes. Among them are all the strong absorbers, iron, and hydrogen.

Thus if a concrete is to be an efficient shielding material it has to contain a minimum amount of these elements. In both Eq. (12) and Eq. (16a) the exponential $\exp\left\{\tau\,\Sigma_r^2\right\}$ determines the magnitude of the

neutron buildup factor. The age τ was introduced as

$$\tau = \int_{E}^{E_o} \frac{1}{3\xi\, \Sigma_s \Sigma_{tr}} \frac{1}{E'} dE', \tag{6}$$

where we assumed an age 0 for the starting energy E_o.

The logarithmic decrement ξ is 1 for hydrogen and less than 1 for all other elements For mixtures one should use a value averaged over all the constituent elements with the scattering cross section as a weighting function. Therefore the average logarithmic decrement will be energy dependent but will always be smaller than one. Also, Σ_s and Σ_{tr} do not vary much with energy except near resonances. Thus for an approximate integration of Eq. (6) we may treat $1/(3\,\xi\Sigma_s\Sigma_{tr})$ as a constant, which means that

$$\tau \cong \frac{1}{3\xi\Sigma_s\Sigma_{tr}} \ln \left(\frac{E_o}{E}\right) . \tag{37}$$

Σ_{tr} is almost proportional to Σ_s, and therefore a small value of τ requires a relatively large value of Σ_s.

Table A-2 shows that hydrogen is the most suitable element. Because of its high value of ξ, it is valuable even in small quantities. This makes it very desirable to have some minimum hydrogen content in a concrete mix.

For Broder's concretes,[17] scattering and absorption cross sections are given in Figs. A-1 to A-3. He found that the scattering cross section is roughly proportional to the water content (Fig. A-1). The absorption cross section depends primarily upon the main absorber. Examples are given for boron (Fig. A-2) and iron (Fig. A-3). Again a linear

relation seems quite satisfactory.

For more accurate determinations of τ, we include Tables A-3 and A-4 and Figure A-4. In Table A-3 we give slowing-down parameters for the elements in Table A-2. They are taken from Ref. 99. In Table A-4, scattering cross sections are given for all elements of the library described in Section III-5. The intermediate energy range is divided into 11 groups. The group boundaries are those of the 22-group neutron cross-section set (see Section IV).

Finally estimates of the thermal-neutron ages of different concretes are given in Fig. A-4 (from Ref. 100) shows results for different American concretes as reported in Ref. 101. Included is a measured point by Lim. In Table A-5 some of Broder's results are reprinted from Ref. 17.

3. Gamma-Ray Attenuation Data

This report is primarily concerned with neutron attenuation, and the gamma-ray data we present are by no means complete. They are intended to help in calculating the attenuation of secondary gamma radiation. Three sorts of data sets are included:

A. Coefficient for Berger's gamma-ray buildup formula.

B. Values of the ψ_o and ψ_1 functions.

C. Total gamma-ray attenuation coefficients.

The following is a short description of the sources of the data.

A. Coefficient for Berger's Gamma-Ray Buildup Formula

In Section II-1 we chose for the gamma-ray buildup factor the following expression:

$$B_\gamma(E,\mu z) = 1 + C(E)\ \mu z \exp\left\{D(E)\ \mu z\right\}, \tag{20}$$

where μz = distance from source (in mean free paths). Trubey[22] determined the parameters C(E) and D(E) for four concretes by fitting moments-method results by a least-squares procedure. For this report, he determined new values based on later data. The results are given in Table A-6. The compositions of the concretes are taken from Ref. 9.

B. Values for the ψ_o and ψ_1 Functions

Trubey[22], who extended previous work of Claiborne[22b], found the following equations useful to represent the transmission of secondary gamma rays from a source which is exponential with depth*:

$$\underline{\psi}_o(\mu z,a) = \frac{1}{2a}\left[E_1\ (\mu z) - e^{-a\ \mu z}\left(E_1([1 - a]\mu z) + \ell n|1 - a|\right)\right], \tag{38}$$

and

$$\underline{\psi}_1\ (\mu z,a') = \frac{e^{-a'\mu z}}{2}\ \frac{1 - e^{-\mu z(1 - a')}}{1 - a'}, \tag{39}$$

where $a = \Sigma_r/\mu$

and $a' = a + D$.

The E_1 function is defined by

$$E_1(x) = \int_x^\infty \frac{e^{-y}}{y}\ dy\ . \tag{40a}$$

For negative arguments (a > 1) (40a) must be replaced by

$$E_1(-x) = -\ E_i(x) = +\ \int_{-x}^\infty \frac{e^{-y}}{y}\ dy. \tag{40b}$$

Graphs and further information are given by Blizard[12].

---

*See Sec. II-1B, p. 14.

Trubey[22] gives linear graphs of ψ_0 and ψ_1 which are useful for small values of μz. Since we were interested in thick shields, the maximum thickness was extended and the results were plotted on semilogarithmic graphs which are presented in Appendix A as Figs. A-5 to A-8. Extrapolations for thicker shields are easily carried out.

C. Gamma-Ray Attenuation Coefficients

In Table A-7 the total linear absorption coefficients are given for all the elements of Table A-2. They were taken from the OGRE gamma-ray cross-section package[102] and are listed at 0.5-MeV intervals. The table is included to give a complete set of all the data needed for calculations with the formulas in Sec. II-1.

4. Thermal-Neutron Capture Gamma-Ray Yields

As was mentioned earlier, Broder, like most other authors, used Troubetzkoy's gamma-ray production yields[57]. He calculated gamma-ray production cross-sections by multiplying those yields by the corresponding thermal-neutron capture cross-sections taken from Hughes and Schwartz.[96] Broder did not consider capture by other than thermal neutrons, gamma rays produced by inelastic scattering, or reactions in which charged particles are emitted. While this may be justified by the scarcity of available data, by the nature of the problems he was dealing with and by the simple assumptions he made, it hardly seems to be satisfactory for more present-day calcualtions. There is a growing demand for reliable gamma-ray production data and this demand is starting to be met. Fortunately we were able to incorporate some recent results both in this report and in our library, which will be described in the next section.

Table A-8 contains gamma-ray yields for most of the important elements found in concrete. They are given in units of photons per capture of 100 thermal neutrons. In the following we identify where the data were obtained or how they were calculated.

C. A. Bartholomew's compilation of thermal-neutron capture gamma-ray measurements[103] is a very valuable collection of data but most of the reported work was done without shielding in mind. Therefore, as a rule, only discrete gamma-ray energies are given, and the measurements are concentrated on a highly accurate determination of the energy of the radiation. Much less attention is given to intensity determination. Thus Bartholomew's data have to be used very cautiously. For light elements for which there is no strong continum contribution, we took most of the information given in Table A-8 from this compilation. Sometimes we could compare it with preliminary results of Maerker and Muckenthaler.[91*] For heavier elements we did calculations using, for instance, Yost's cascade model code DUCAL.[104]

HYDROGEN has a binding energy of 2.224 MeV, and the emitted gamma radiation has the same energy (Ref. 103).

BORON: The cross section for thermal-neutron capture is small compared with that for the (n,α) reaction. Assuming a branching ratio of 0.065[105] leads to the given yield of the 0.4778-MeV[103] gamma-ray line.

CARBON: The line energies are well known, but some doubt still exists as to how to evaluate the intensities. Our values follow the recommendation of Ref. 103.

NITROGEN shows two competing thermal-neutron reactions: capture and (n,p).

*A summary of their results is given in Table A-9.

The cross sections are 0.075 and 1.50 respectively. The (n,p) reaction does not contribute gamma rays if induced by thermal neutrons,[106] and therefore only capture gamma-ray yields are given. We took them from Ref. 107.

OXYGEN: Because of the low absorption cross section no reliable intensity information is available. Normally for shielding calculations the contribution of oxygen to the thermal-neutron capture gamma rays may safely be neglected (Ref. 108).

SODIUM: The yields are taken from Ref. 103. We mainly follow Greenwood's results; some of Barfield's information about low-energy gamma-rays is also included. We chose these data because the emitted gamma-ray energy best fits the binding energy of the captured neutrons.

MAGNESIUM: Here we used Spilling's data as reported in Ref. 109. The relative intensities were normalized to a binding energy of 8.37 MeV per capture in natural magnesium. We chose these data because they fit well in the level schemes of the magnesium isotopes. No continum contribution was taken into account.

ALUMINUM: Maerker's data[91] are given. They are experimental values and include both discrete and continum contributions. We extended his results at lower energies by including Orphan's results as given in Ref.103. Because Orphan's values correspond to only 59% of the binding energy, we normalized them.

SILICON: We give Lycklama yields[110] as reported in Ref. 103. Because the absorption cross sections of the silicon isotopes are not known well it is difficult to calculate the effective binding energy of the element.

Thus this simple check could not be applied in this case. Preliminary analytical results of Maerker[91] indicate that the intensity distribution in the energy bands of Table A-8 fits Muckenthaler's experimental yields approximately.

PHOSPHORUS: Rasmussen's data as reported in Ref.103 seem to contain the most detailed information. Unfortunately the released gamma-ray energy would be much higher than the neutron binding energy. Therefore, we renormalized the results. The data obtained show good agreement with those of Van Middelkoop.[111]

SULFUR: Venett's results are given with corrections from Van Middelkoop at energies below 2.0 MeV. Both sets of data are given in Ref. 103.

CHLORINE: The yields in Table A-8 are due to the $^{35}Cl\ (n,\gamma)\ ^{36}Cl$ reaction. They were taken from Drake's evaluation.[89]

POTASSIUM is one of the elements that will be experimentally investigated by Maerker and Muckenthaler. At present, the best we can do is to take Rasmussen's results from Ref. 103 and renormalize them to the total binding energy of the captured neutron. The results obtained are reported in Table A-8.

CALCIUM: Experimental results of Rasmussen et al. and Gruppelaar are available. But Rasmussen's results disagree completely with energy conservation. Therefore Gruppelaar's results[112] are reported here. We added values from Rasmussen[103] for energies greater than 6.5 MeV.

TITANIUM: Here too we combined two sets of measurements: those of Knowles et al. and of Groshev et al. (1.5-3.0 MeV). Both are reported in Ref. 103. To meet the binding energy test we had to multiply the results by 1.09.

CHROMIUM is the first element for which no experimental results were available. Calculations were done for the capture in ^{54}Cr, ^{52}Cr, and ^{56}Cr by Kremer[92] and are combined in Table A-8 for natural chromium. The product of natural abundance and thermal-neutron absorption cross section was used to weight contribution of each isotope.

MANGANESE: Very detailed measurements by Rasmussen et al. are reported in Ref. 103. In the case of manganese, Rasmussen's results pass the binding energy test satisfactorily. But from the experiments which this group did for other nuclei one may suspect this to be by chance only. Again we should like to stress that statements of this kind are not intended to disparage the measurements; the purpose of these authors was to produce data for nuclear physics studies. If the data are used for shielding, however, we should evaluate them with discrimination. We report Rasmussen's data as preliminary results and urge the reader to replace them as soon as he finds better data for the line intensities.

IRON is one of the rare cases where we could rely on data measured for shielding purposes. Maerker and Muckenthaler's results are presented as given in Ref. 91.

NICKEL: The results we report are those of Groshev et al. taken from Ref.103. For energies greater than 6 MeV we preferred the line intensities as measured by Huynh (in Ref. 103). The results still correspond to a released energy that is lower than the binding energy, but this may be mainly due to the lack of low-energy contributions.

COPPER was measured by Muchenthaler.[91] We give his results, and for energies below 1 MeV we add the results reported by Rasmussen (Ref. 103).

ZINC: The capture cross sections of the zinc isotopes are not known. Therefore it makes no sense to do complicated calculations. To get the data in Table A-4 we assumed that Rasmussen's measurements[103] would describe the contribution of the resolved line spectrum only. We then added a continuum contribution of the form

$$f(E) = a - bE, \tag{41}$$

where E is the energy in MeV and a and b are parameters. We determined a and b by the following conditions:

1. $f(E) = 0 \quad \text{for } E = 8 \text{ MeV}, \tag{42}$
2. $\int_0^{8\ \text{MeV}} E\ f(E)\ dE = 320 \text{ MeV}. \tag{43}$

The first condition means that we considered continuum contributions with energies up to 8 MeV. This is about the difference between the binding energy of ^{68}Zn and the energy region where not all the levels are known.

The second condition describes the energy release by continuum gamma rays. We assumed that the binding energy of 100 neutrons in natural zinc is 800 ± 100 MeV.[103] The energy contribution from the resolved gamma rays is about 465 MeV. The value 320 MeV is slightly less than the missing amount of energy.

BARIUM is difficult to calculate because the neutron numbers of its isotopes are magic or at least near magic. Data for ^{135}Ba, ^{137}Ba, and ^{138}Ba determine the capture yields of natural barium. Thus if one tries the same procedure that we used with zinc, one gets for the maximum energy of the continuum about 7.5 MeV (because the highest binding

energy is only 9.23 MeV), and the missing amount of released energy is about 420 MeV. With this assumption and Rasmussen's measured data we found the yields given in Table A-8 for barium.

SAMARIUM: Because of the huge capture cross section of ^{149}Sm, only this isotope has to be considered. In Table A-8 we give its gamma-ray yields as calculated by Kremer.[92]

GADOLINIUM: The isotopes ^{155}Gd and ^{157}Gd are by far the strongest neutron absorbers in gadolinium. We calculated capture gamma-ray yields for both of them using Yost's cascade model code DUCAL.[104] The results are given in Table A-8.

5. Data Library

A 122-energy-group library in the ANISN/DOT/DTF-IV format for coupled neutron-gamma-ray transport calculations was produced from the most recent energy-point data. The library contains cross sections for nine elements: H, C, N, O, Mg, Al, Si, Ca, and Fe. The sources for the point data were the following:

A. Neutron Data

For all elements but Ca, Si, and Fe we used the 1968 ENDF/B data.[95] The cross sections for Ca were taken from Drake.[89] Those for Si and Fe, especially in the thermal and epithermal energy range, were the relatively old values of the O5R library,[113] but the Fe data were updated with values from J. J. Schmidt's evaluation.[114] Two programs were used for the conversion of the point data into group data: modified versions of CSP by Yost and Greene,[115] and SUPERTOG by Wright *et al.*[116]

B. Gamma-Ray Interaction Data

All data are taken from the OGRE library.[117] The conversion into group data was done with the MUG code.[118]

C. Thermal-Neutron Capture Gamma Rays

The data are basically the same as those described in Sec. III-4. They were checked against experimental data from Maerker and Muckenthaler.[91]

D. Epithermal-Neutron Capture Gamma Rays

No specific data were found in the literature at the time this report was written. Because most of the elements are light ones, we took the same yields as for thermal-neutron capture. No special provision for energy conservation was introduced. This is because the thermal-neutron data themselves fulfill this law only within about 10% accuracy, and for neutron energies greater than 100 keV, the capture cross section normally is negligib

E. Gamma Rays from Other Reactions

Fortunately we were able to use recently collected and tested cross sections. Thus for H, N, O, and Al we could rely on available group data by Straker.[59] For Mg, Ca, and Si, Drake's evaluations[89,90] were the sources of our point data. The situation in the cases of Fe and C is less satisfying. The only data for production of gamma-rays by fast neutrons which we included were inelastic scattering gamma-ray yields measured by Kinney and Perey[119] for Fe in the energy range 1 to 7.6 MeV and the carbon data that are reported in Ref. 120.

For each element the different yields were combined with reaction cross sections and transformed into transfer matrices for use in the

transport code ANISN. This was done with the computer code POPOP-4 by Ford and Wallace.[121] The final fine-group library contains 104 neutron groups and 18 gamma-ray groups. Table 13 shows the upper boundaries of the neutron groups. The group structure was designed by Straker[59] to describe the oxygen cross-section valley at about 2.37 MeV. This is due to the fact that the library was intended for transport calculations in oxygen-containing materials. Relatively less attention was given to the boundaries of the gamma-ray groups since there is no resonance structure. The upper boundaries of the 18 gamma-ray groups may be found in Table 14.

TABLE 13

ENERGY GROUP STRUCTURE

(UPPER BOUNDARIES OF THE 104 NEUTRON GROUPS)

Group No.	Energy in eV	Group No.	Energy in eV	Group No.	Energy in eV
1	1.50000E 07*	36	6.72055E 05	71	1.58461E 03
2	1.34986E 07	37	6.08101E 05	72	1.23410E 03
3	1.22140E 07	38	5.50232E 05	73	9.61117E 02
4	1.10517E 07	39	4.97871E 05	74	7.48519E 02
5	1.00000E 07	40	4.50492E 05	75	5.82947E 02
6	9.04837E 06	41	4.07622E 05	76	4.53999E 02
7	8.18731E 06	42	3.68832E 05	77	3.53575E 02
8	7.40818E 06	43	3.33733E 05	78	2.75365E 02
9	7.00000E 06	44	3.01974E 05	79	2.14454E 02
10	6.70320E 06	45	2.73237E 05	80	1.67017E 02
11	6.36000E 06	46	2.47235E 05	81	1.30073E 02
12	6.06531E 06	47	2.23708E 05	82	1.01301E 02
13	5.48812E 06	48	2.02419E 05	83	7.88933E 01
14	4.96585E 06	49	1.83156E 05	84	6.14421E 01
15	4.75000E 06	50	1.65727E 05	85	4.78512E 01
16	4.49329E 06	51	1.49956E 05	86	3.72665E 01
17	4.06570E 06	52	1.35686E 05	87	2.90232E 01
18	3.67879E 06	53	1.22773E 05	88	2.26033E 01
19	3.32871E 06	54	1.11090E 05	89	1.76033E 01
20	3.01194E 06	55	8.65169E 04	90	1.37096E 01
21	2.72532E 06	56	6.73794E 04	91	1.06770E 01
22	2.46597E 06	57	5.24752E 04	92	8.31529E 00
23	2.35000E 06	58	4.08677E 04	93	6.47595E 00
24	2.23130E 06	59	3.18278E 04	94	5.04348E 00
25	2.01896E 06	60	2.47875E 04	95	3.92786E 00
26	1.82683E 06	61	1.93045E 04	96	3.05902E 00
27	1.65299E 06	62	1.50344E 04	97	2.38237E 00
28	1.49569E 06	63	1.17088E 04	98	1.85539E 00
29	1.35335E 06	64	9.11882E 03	99	1.44498E 00
30	1.22456E 06	65	7.10174E 03	100	1.12535E 00
31	1.10803E 06	66	5.53084E 03	101	8.76425E-01
32	1.00259E 06	67	4.30743E 03	102	6.82561E-01
33	9.07180E 05	68	3.35463E 03	103	5.31579E-01
34	8.20850E 05	69	2.61259E 03	104	4.14000E-01
35	7.42736E 05	70	2.03468E 03		to 1.00000E-04

*Read 10^{+7}

TABLE 14

GAMMA-RAY ENERGY GROUP STRUCTURE FLUENCE-TO-TISSUE DOSE CONVERSION FACTORS AND TOTAL CROSS SECTION FOR TSF CONCRETE

Group No.	Upper Energy (MeV)	Dose Factors[122] [rad/(γ/cm²)]	Total Cross Sections [cm⁻¹]
1	10.0	2.42 (-9)*	5.48 (-2)
2	8.0	2.07 (-9)	5.84 (-2)
3	6.5	1.76 (-9)	6.36 (-2)
4	5.0	1.495 (-9)	7.03 (-2)
5	4.0	1.27 (-9)	7.88 (-2)
6	3.0	1.08 (-9)	8.82 (-2)
7	2.5	9.45 (-10)	9.77 (-2)
8	2.0	8.33 (-10)	1.09 (-1)
9	1.66	7.22 (-10)	1.20 (-1)
10	1.33	6.25 (-10)	1.37 (-1)
11	1.0	5.05 (-10)	1.55 (-1)
12	0.8	4.25 (-10)	1.75 (-1)
13	0.6	3.25 (-10)	2.03 (-1)
14	0.4	2.41 (-10)	2.35 (-1)
15	0.3	1.75 (-10)	2.69 (-1)
16	0.2	1.16 (-10)	3.39 (-1)
17	0.1	7.64 (-11)	6.08 (-1)
18	0.05 to 0.02	1.22 (-10)	3.54

* Read 2.42×10^{-9}

TABLE 15

UPPER BOUNDARIES OF THE 22 NEUTRON ENERGY GROUP SETS
FLUENCE-TO-TISSUE DOSE EQUIVALENT FACTORS,
HEAT RELEASE FACTORS AND TOTAL CROSS SECTIONS FOR TSF CONCRETE

Group No.	Energy [MeV]	Tissue Dose Equivalent Factors [rem/(n/cm^2)]	Heat Release Factors [w·s/(n·cm)]	Total Cross Section** [cm^{-1}]
1	15.0	5.640 (-8)	3.654 (-14)	0.1150
2	12.2	4.580 (-8)	2.704 (-14)	0.1186
3	10.0	4.160 (-8)	1.900 (-14)	0.1119
4	8.19	4.105 (-8)	1.635 (-14)	0.1160
5	6.36	3.882 (-8)	1.328 (-14)	0.1255
6	4.97	3.720 (-8)	1.255 (-14)	0.1512
7	4.07	3.607 (-8)	1.343 (-14)	0.1992
8	3.01	3.509 (-8)	9.456 (-15)	0.1485
9	2.46	3.500 (-8)	7.319 (-15)	0.1158
10	2.35	3.549 (-8)	8.109 (-15)	0.1658
11	1.826	3.667 (-8)	7.246 (-15)	0.2101
12	1.108	3.143 (-8)	5.954 (-15)	0.2870
13	0.55	1.591 (-8)	3.403 (-15)	0.3796
14	0.111	3.548 (-9)	8.172 (-16)	0.4046
15	3.35 (-3)*	1.224 (-9)	3.651 (-17)	0.4388
16	5.83 (-4)	1.306 (-9)	6.547 (-18)	0.4430
17	1.01 (-4)	1.336 (-9)	1.641 (-18)	0.4451
18	2.9 (-5)	1.270 (-9)	1.146 (-18)	0.4458
19	1.067 (-5)	1.222 (-9)	1.470 (-18)	0.4466
20	3.059 (-6)	1.186 (-9)	2.347 (-18)	0.4475
21	1.125 (-6)	1.155 (-9)	3.770 (-18)	0.4485
22	4.14 (-7) (thermal)	1.040 (-9)	8.347 (-18)	0.6244

* read 3.35×10^{-3}

**These were used for the adjoint calculations which considered neutron transport only. The collapsed set used in neutron plus secondary gamma-ray calculations had values of 0.3788 and 0.4061 for groups 13 and 14, respectively. The different values arise because collapsing from 104 groups was done with a different weighting function (see Section IV-1).

IV. Concrete Slab Transmission Factors for Neutron and Gamma-Ray Dose Equivalent

1. Calculation of Transmission Factors

If we know $\phi(T;z_1,E,\mu)$, the fluence emerging from the right surface, z_1, of a slab of thickness T, due to a source incident on the opposite face, z_o, we can calculate a "detector reading," $D(z_1)$, by performing an integration as follows:

$$D(z_1) = \int_0^\infty dE \int_o^1 d\mu \; F(E) \; \phi(T;z_1,E,\mu) \tag{44}$$

where E refers to energy and μ is the direction cosine measured from the slab normal. In the above, F(E) is some reaction cross section or detector response function. The purpose of this section is to provide calculational results which will allow the determination of $D(z_1)$ for a variety of source descriptions and slab thicknesses without having to determine $\phi(T;z_1,E,\mu)$ for each case.

Hansen and Sandmeier[124] have outlined methods of utilizing adjoint transport calculations for obtaining solutions to certain classes of neutron source-detector problems. We apply these methods for the case of a concrete slab with infinite lateral dimensions and finite thickness. On the left boundary of the slab, z_o, we assume a source of particles (neutrons or gamma rays) such that $S(E,\mu)\, dE\, d\mu = \phi(T;z_o,E,\mu)\, \mu\, dE\, d\mu$ of them strike unit area of the slab surface. Particles entering through an area A induce interactions in the slab such that the total number of reactions, R, taking place in some volume, V, inside the slab is given by

$$R = \int_V dV \int_0^\infty dE \int_{-1}^1 d\mu \; \phi(T;z,E,\mu) \; F(E) \quad , \tag{45}$$

or, as shown by Hansen and Sandmeier, by

$$R = \int_A dA \int_0^\infty dE \int_0^1 d\mu \; \phi(T;z_o,E,\mu) \; \mu \; \phi^+(T;z_o,E,\mu) \quad , \tag{46}$$

for cases where only a surface source, $\phi(T;z_o,E,\mu)\ \mu$, is present. F(E) is the reaction cross section (or detector response) assumed in this case to be spatially independent in V, $\phi(T;z_o,E,\mu)$ represents the differential particle fluence incident on the surface and $\phi^+(T;z_o,E,\mu)$ the "source effectiveness distribution," as it is denoted in Ref. 124. The quantity $\phi^+(T;z,E,\mu)$ is that function which satisfies the adjoint transport equation with source term F(E) and the boundary condition that $\phi^+(T;z_o,E,\mu) = 0$ for $\mu<0$. Hence, the integration in Eq. (46) is for positive μ only. For the one-dimensional problem under consideration we may look at surface quantities on a per unit area basis in Eq. (46) and reduce spatial integration in Eq. (45) to the z variable. From Eq. (45), we see that R is essentially a "detector reading," D(z), integrated over a volume, V, which for slab geometry can be denoted as Δz. For a small Δz, we may approximate

$$R = \int_{\Delta z} D(z)dz \cong D(\bar{z})\Delta z,$$

where $D(\bar{z})$ is the detector reading evaluated at some position $\bar{z}$ in Δz. Now, if Δz is a very small interval near the right boundary, then $D(z_1)\Delta z$ should be very nearly equal to R which would result from an application of Eq. (46) in which $\phi^+(T;z_o,E,\mu)$ was the solution of the adjoint transport equation with source F(E) in Δz. Hence the quantity of interest $D(z_1)$, may be approximated as

$$D(z_1) \cong \frac{R}{\Delta z} = \frac{1}{\Delta z}\int_0^\infty dE \int_{-1}^{1} d\mu\ \phi(T;z_o,E,\mu)\ \mu\ \phi^+(T;z_o,E,\mu) \quad . \tag{47}$$

Thus, once $\phi^+(T;z_o,E,\mu)$ has been calculated for a given detector response F(E) and slab thickness T, it can be used in Eq. (47) to compute the desired detector reading, $D(z_1)$, for any arbitrary source, $S(E,\mu) = \phi(T;z_o,E,\mu)\ \mu$.

Eq. (47) may be approximated by a double summation over energy and angle as

$$D(z_1) \simeq \frac{1}{\Delta z} \sum_{E_i} \sum_{\mu_j} \Delta E_i \, w_j \;\; \phi(T;z_o,E_i,\mu_j) \; \mu_j \; \phi^+(T;z_o,E_i,\mu_j) \quad . \qquad (48)$$

In the above, subscripts i and j refer to the i-th energy group and j-th cosine interval, respectively. $\phi^+(T;z_o, E_i \; \mu_j)$ is the result of the discrete ordinates solution of the adjoint transport equation at position z_o, for the i-th energy group and j-th direction. w_j is the weight associated with the j-th cosine in a Gauss-Legendre approximation to integration over μ, and ΔE_i is the width of the i-th energy group. Thus $\phi(T;z_o,E_i,\mu_j) \; \mu_j \; \Delta E_i \; w_j$ is the total number of source particles incident on the slab per cm^2 in the i-th group and j-th cosine interval.

The discrete ordinates code ANISN[15] was used to compute $\phi^+(T;z_o,E_i,\mu_j)$. Calculations were performed for 22 neutron groups and 18 gamma-ray groups whose energy boundaries are given in Tables 15 and 14, respectively. Two sets of runs were performed for seven different slab thicknesses.

The first set used as the adjoint source, F(E), the Snyder-Neufeld[52] neutron fluence-to-dose equivalent conversion factors for the neutron groups and the Claiborne-Trubey[122] gamma-ray fluence-to-dose conversion factors for the gamma-ray groups. (It should be noted that both these response functions are based on the maximum total dose in a 30 cm slab of tissue.) The neutron and gamma-ray fluence-to-dose conversion factors are shown in Tables 15 and 14, respectively. If we now denote neutron group indices with subscript i and gamma-ray groups indices with subscript g, the results of the above calculations may be more clearly identified as $\phi_t^+(T;z_o,E_i,\mu_j)$ and $\phi_\gamma(T;z_o,E_g, \mu_j)$. The quantity $\phi_t^+(T;z_o,E_i,\mu_j)$ gives the volume integrated <u>total</u> dose in the rightmost interval of a slab of thickness T from both neutrons and secondary gamma rays due to one neutron incident on the left face in the i-th energy group and j-th cosine interval, and $\phi_\gamma^+(T;z_o,E_i,\mu_j)$ gives the volume integrated gamma-ray dose equivalent in the rightmost interval of a slab of thickness T due to one gamma-ray incident on the left face in the g-th gamma-

ray group and j-th cosine interval. The cross sections used for this set of calculations (neutron plus gamma-ray adjoint source) were produced by reducing the 122-group set described in Sec. III. Special routines were required in the ANISN code to implement the multigroup adjoint weighting techniques outlined by Mynatt and Engle[125]. The group structure was collapsed by weighting with results of an adjoint calculation for a 75 cm-thick TSF concrete slab with the above adjoint source. Resulting values of total cross section for gamma-ray and neutron groups are given in Tables 14 and 15, respectively.

The second set of calculations was run to determine, for the neutron groups, the dose equivalent due only to neutrons. This was accomplished by using as an adjoint source the Snyder-Neufeld dose equivalent conversion factors for the neutron groups and zeros for the gamma-ray groups. The result is identified as $\phi_n^+(T; z_0, E_i, \mu_j)$ which gives the neutron dose equivalent in the rightmost interval of a slab of thickness T due to one neutron incident on the left face in the i-th energy group and j-th cosine interval. Naturally, the results for all the gamma-ray groups are zero. The cross sections used were generated by reducing the 122 group set by weighting with results of an adjoint calculation for a 75-cm-thick concrete slab with the adjoint source specified above (neutron groups only). The resulting neutron group values for the total cross section of TSF concrete are shown in Table 15.

For either set of adjoint runs, F(E) represents the energy dependence of a distributed source which, in the ANISN code, is specified by means of a 17* input array. This distributed source was specified as zero in all except the rightmost spatial interval. P_5, S_{16} calculations were performed for TSF concrete slabs 15, 30, 50, 75, 100, 150, and 200 cm thick. For each slab, the size of the rightmost interval was set at 0.001 cm with a mesh interval size in most cases of approximately 1.5 cm being used throughout the rest of the slab. The 150- and 200-cm thick slabs were run with a mesh interval size of approximately 0.75 cm. The concrete composition is given in column 3 of Table 6, p. 26.

If we define

$$\tau(T;E_i,\mu_j) = \phi^+(T;z_o,E_i,\mu_j)/\Delta z \quad ,$$

then Eq. (48) for computing the transmitted dose may be expressed as

$$D(z_1) \cong \sum_{E_i} \sum_{\mu_j} \mu_j \; \phi(T;z_o,E_i,\mu_j) \; \Delta E_i \; w_j \; \tau(T;E_i,\mu_j) \quad , \tag{49}$$

in which $\tau(T;E_i,\mu_j)$ may be interpreted as a transmission factor giving the dose equivalent transmitted through a slab of thickness T due to one particle incident on the surface in the i-th energy group and j-th cosine interval. More specific identification is obtained by denoting the transmission factors as $\tau_t(T;E_i,\mu_j)$, $\tau_n(T;E_i,\mu_j)$, and $\tau_\gamma(T;E_g,\mu_j)$.

Tables B-1 through B-7 list the values of transmission factors for neutron sources, each table containing data for a given slab thickness. τ_t gives the total dose equivalent and τ_n the neutron dose equivalent only. The difference between the two is due to the contribution of secondary gamma rays. Tables B-8 through B-14 list the values of $\tau_\gamma(T;E_g,\mu_j)$. These give the gamma-ray dose equivalent due to primary gamma-ray sources.

Transmission probabilities may be determined from $P_T(E_i,\mu_j) = \mu_j \; \tau(T;E_i,\mu_j)/F(E_i)$ where $F(E_i)$ are the fluence to dose equivalent factors given in Tables 14 and 15 for gamma rays and neutrons groups, respectively. These probabilities are normalized to unity for zero slab thickness.

2. Use of the Transmission Factors

The transmission factors $\tau(T;E_i,\mu_j)$ listed in Tables B-1 through B-14 may be used to calculate the dose equivalent transmitted through a concrete of thickness T by applying Eq. (49). One first must determine the number of source particles which are in each energy and angular interval. For the energy variable this amounts to integrating $S(E,\mu)$ over each energy group of interest. The same applies also to the angular variable. As mentioned earlier, the energy group structure which was used in the calculations, and into which we must partition a source, is given in Tables 14 and 15. The cosines and cosine intervals widths (weights) for

which the $\tau(T;E_i,\mu_j)$ are specified are listed in Table 16. These correspond to Gauss-Legendre quadrature of order 16 to approximate the integration over the angular variable in the discrete ordinates equations. Hence $S(E,\mu)$ can merely be evaluated at μ_j and multiplied by the corresponding weight to represent the number in j-th cosine interval.

TABLE 16

COSINES AND COSINE INTERVAL WIDTHS FOR USE WITH THE TRANSMISSION FACTORS

Direction	Cosine*	Weight**
1	0.9894	0.0272
2	0.9446	0.0622
3	0.8656	0.0952
4	0.7554	0.1246
5	0.6179	0.1496
6	0.4580	0.1692
7	0.2816	0.1826
8	0.0950	0.1894

*The cosine of the angle between source particle direction and slab inner normal.

**These numbers are twice as large as those used in ANISN because that code requires the sum of weights over all cosines, positive and negative, to be unity.

An example of the use of the transmission factors is shown in Tables B-1 through B-14. The last column on the right of these tables is titled "Scalar adjoint." For a i-th source group, this value, $A(T;E_i)$ is the dose equivalent transmitted through the slab due to a plane isotropic source of particles in that group. The values are normalized to one particle per cm^2 entering the slab and were calculated from the sum

$$A(T;E_i) = \sum_{j=1}^{8} (1)\ w_j\ \tau(T;E_i,\mu_j) \quad ,$$

where we have assumed a plane isotropic source. To obtain the dose equivalent due to neutrons from a plane isotropic energy dependent neutron source, we would take

$$D(z_1) = \sum_{i=1}^{22} f(E_i)\ \Delta E_i\ A(T;E_i) = \sum_{i=1}^{22} \sum_{j=1}^{8} f(E_i)\ \Delta E_i\ w_j\ \tau_n(T;E_i,\mu_j) \quad , \tag{50}$$

where f(E) is the spectrum of the source neutrons. Some results will be given later for the case of a plane isotropic fission source.

In using the transmission factor tables, two areas of apparent inaccuracy should be noted. The first can be seen by a comparison of total and neutron dose equivalent for the 15 cm slab (Table B-1). For source groups between 0.5 and 5 MeV, it will be noted that in some cases, the neutron dose equals or exceeds the total dose for a given source group. This results, in all probability, from the use of the different cross sections for the two sets. In any case the two numbers agree within three significant figures and, for practical purposes, the difference between the two is negligible for this small slab thickness.

The other area of inaccuracy occurs for source gamma-ray groups for slab thicknesses 75 cm or greater for the two most grazing source angles, μ_7=0.2816 and μ_8=0.095. The table entries are, in some cases, negative numbers. The counterpart of this result is the occasional negative angular fluxes obtained by forward discrete ordinates calculations. For gamma-ray groups, values found in Tables B-11 through B-14 for these slab thicknesses are seen to decrease rather rapidly with decreasing μ and, in general, the

contribution for these directions is very small. It is possible to plot the transmission factors as a function of μ and estimate, by extrapolation, the values for the last two cosines.

3. Results Obtained Using the Transmission Factors and Comparisons with Various Other Calculations.

Figure 25 gives the ratio of tissue dose* due to secondary gamma-rays to tissue dose equivalent due to neutrons as a function of incident neutron energy for various TSF concrete slab thicknesses and nearly normal incidence. The values plotted are $r(T;E_i,\mu_1)$, the ratio of gamma-ray to neutron dose due to source neutrons in the i-th energy group and at nearly normal incidence. They are computed from

$$r(T;E_i,\mu_1) = [\tau_t(T;E_i,\mu_1) - \tau_n(T;E_i,\mu_1)]/[\tau_n(T;E_i,\mu_1)] \quad ,$$

where subscript t or n refers to total or neutron dose transmission factors, respectively. The transmission factors used are found in the first column of Tables B-1 through B-7. The pronounced dip in the ratio at 2.4 MeV is due to the valley in the oxygen cross section near that energy. The proportion of the total dose attributed to gamma rays increases with increasing slab thickness and decreasing source neutron energy. The gamma-ray dose exceeds the neutron dose equivalent for all combinations of slab thicknesses greater than 50 cm and neutron source energies less than 1 MeV. For the 200 cm slab, the gamma-ray dose exceeds the neutron dose equivalent for all source neutron energies. For the 15 cm slab, the total equals the neutron dose equivalent to within about 0.2% for source neutron energies between 1 and 4 MeV.

The variation with incident neutron energy of transmitted tissue dose equivalent due to neutrons for nearly normally incident, $\tau_n(T;E_i,\mu_1)$, and plane isotropic, $A_n(T,E_i)$, sources is shown in Figures 26 and 28, respectively. For neutron source energies above 0.1 MeV, the transmitted

*The quality factor for converting gamma-ray dose (rads) to gamma-ray dose equivalent (rems) is taken as unity.

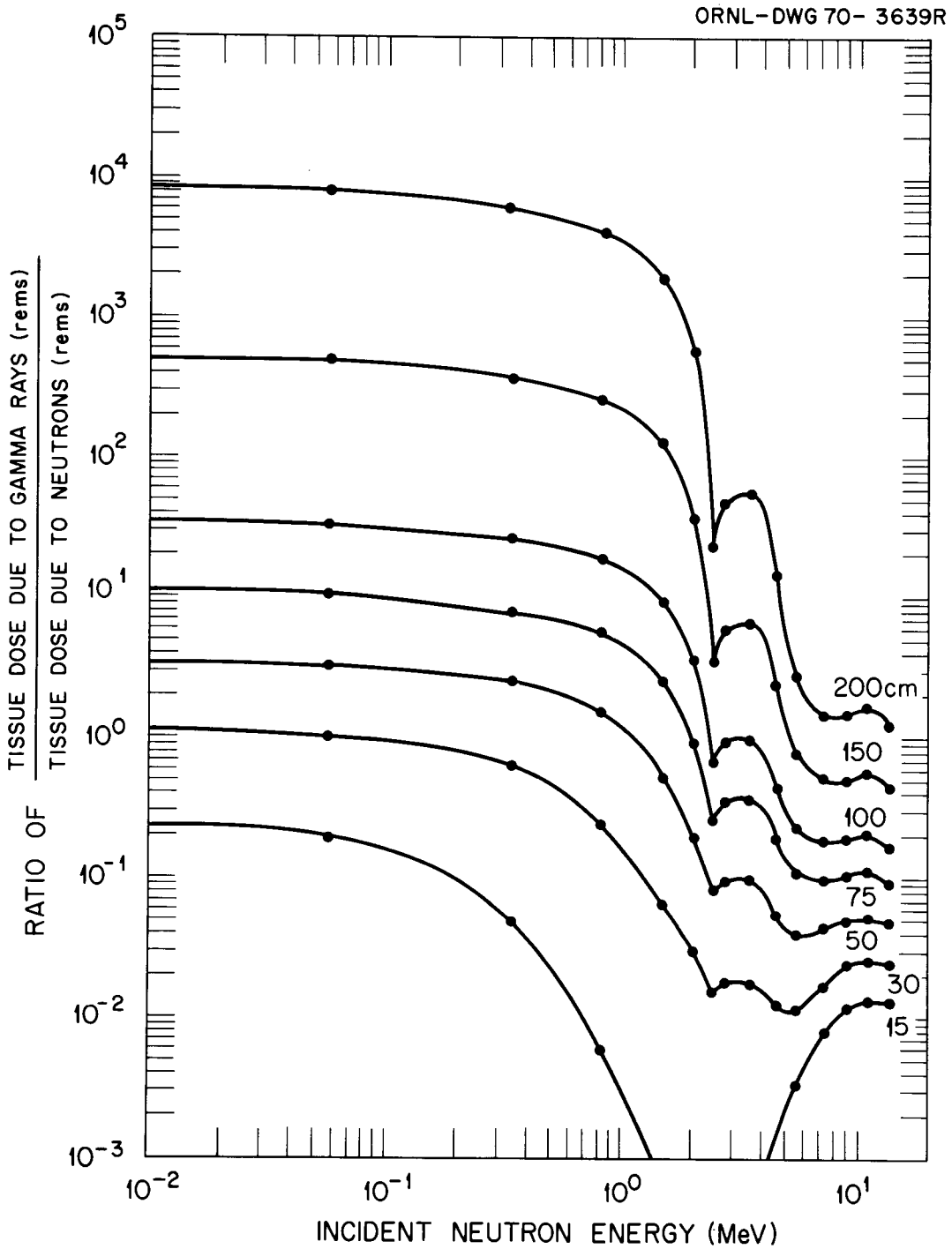

Fig. 25. Ratio of Tissue Dose (rems) Due to Secondary Gamma Rays to Tissue Dose (rems) Due to Neutrons as a Function of Incident Neutron Energy for Various Concrete Slab Thicknesses and Nearly Normal Incidence.

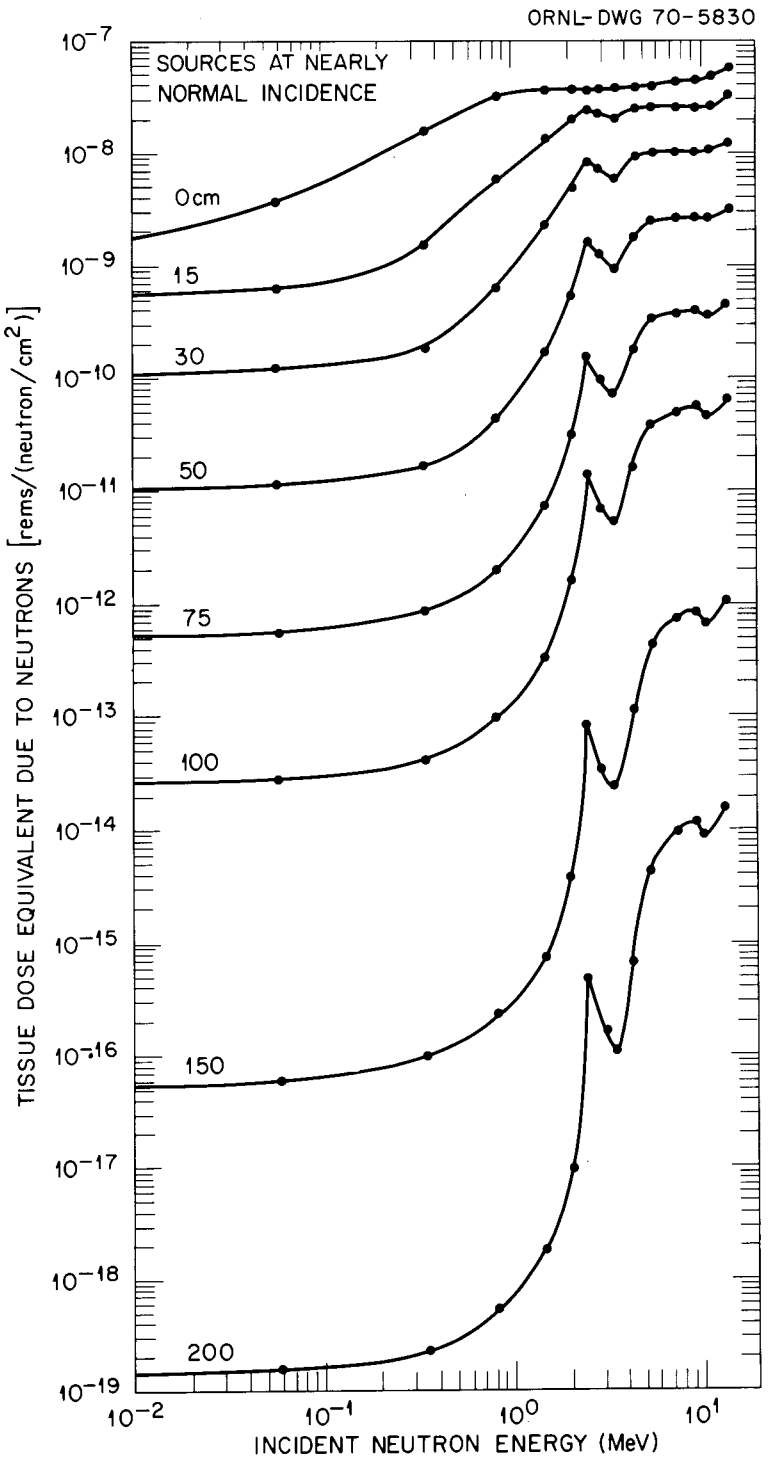

Fig. 26 . Tissue Dose Equivalent (rems) Due to Neutrons as a Function of Incident Neutron Energy for Various Concrete Slab Thicknesses and Nearly Normal Incidence (τ_n).

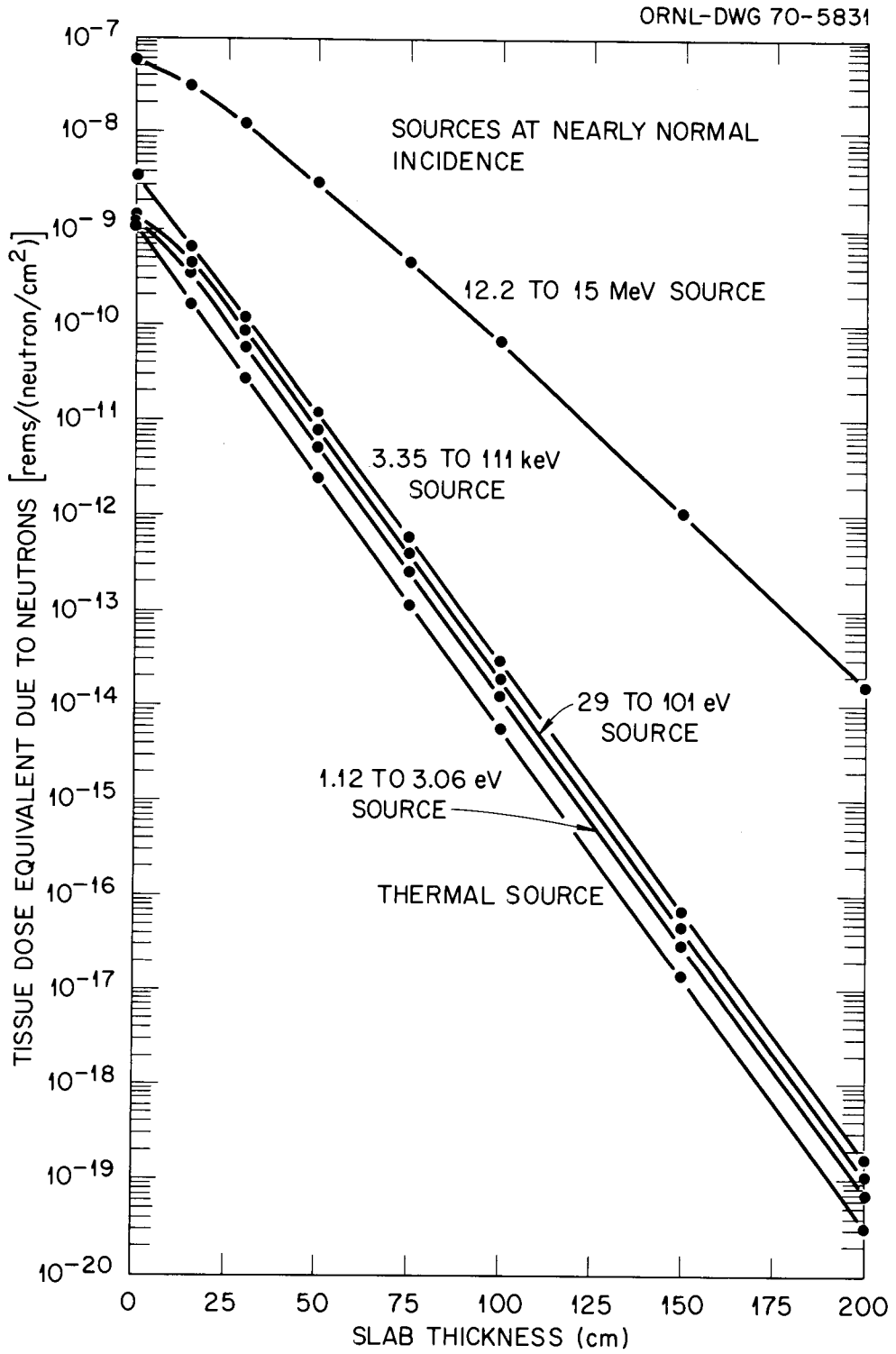

Fig. 27. Tissue Dose Equivalent (rems) Due to Neutrons as a Function of Concrete Slab Thickness for Neutron Sources at Nearly Normal Incidence (τ_n).

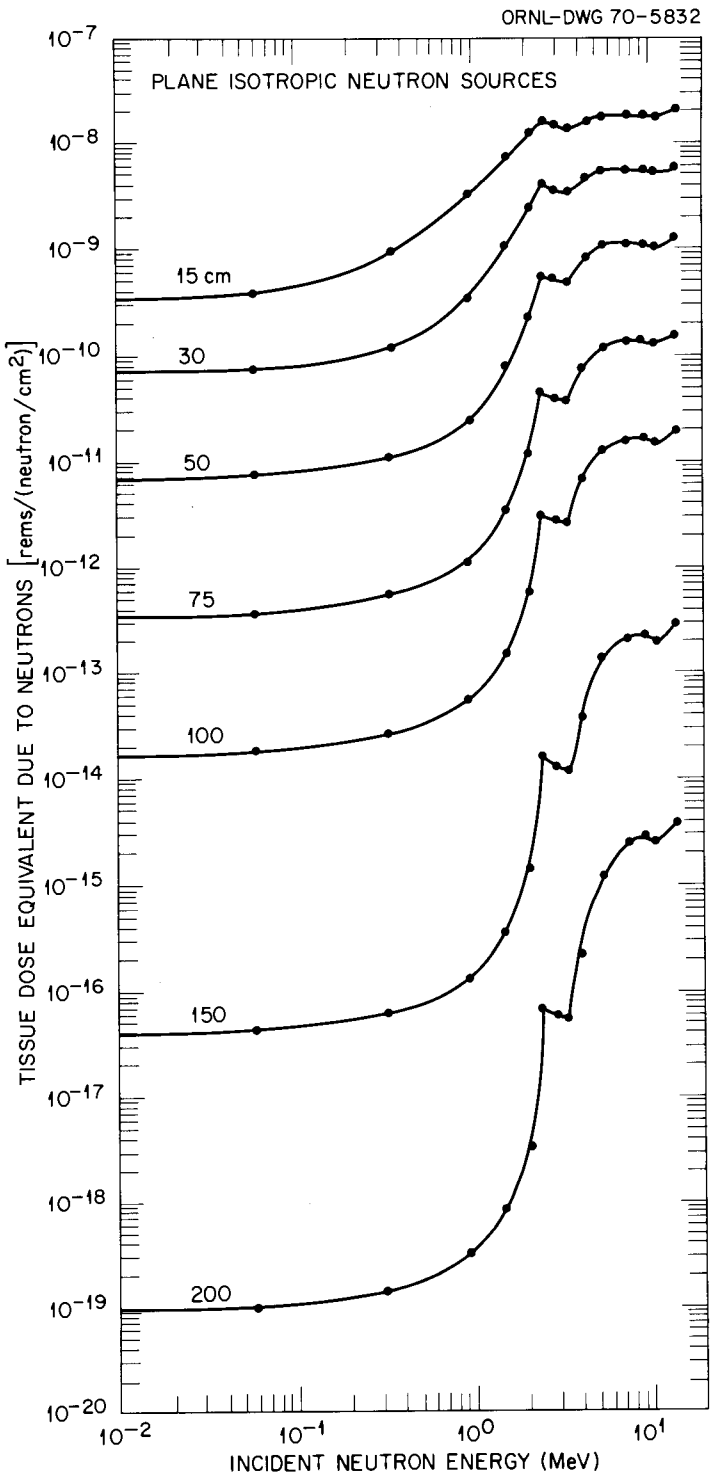

Fig. 28. Tissue Dose Equivalent (rems) Due to Neutrons as a Function of Incident Neutron Energy of Plane Isotropic Sources for Various Concrete Slab Thicknesses (A_n).

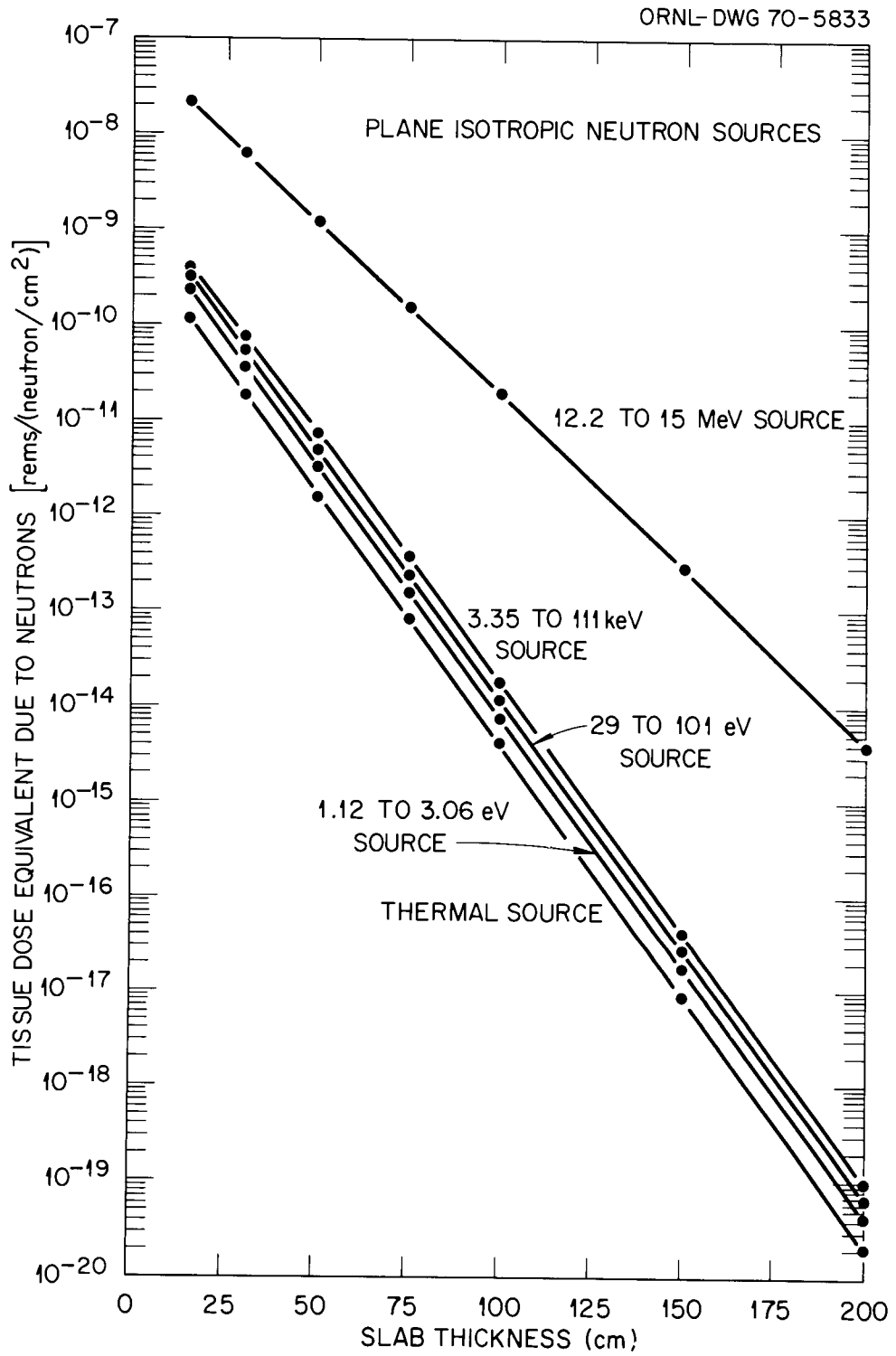

Fig. 29. Tissue Dose Equivalent (rems) Due to Neutrons as a Function of Concrete Slab Thickness for Plane Isotropic Neutron Sources (A_n).

tissue dose equivalent increases rather significantly with increasing energy and slab thickness. The valley in total cross section near 2.4 MeV causes the peak in the curves at that energy. Below 0.1 MeV the variation of transmitted tissue dose equivalent with neutron source energy is less pronounced. Figures 27 and 29 show $\tau_n(T;E_i,\mu_1)$ and $A_n(T;E_i)$, respectively, as a function of concrete slab thickness. The curves show this slow variation with source energy, especially between 29 eV and 111 keV.

In general, the $A_n(T;E_i)$ vary less rapidly with source energy than the $\tau_n(T;E_i,\mu_1)$. For example, the peaks in the curves near 2.4 MeV are not as high. Also, the $A_n(T;E_i)$ are smaller than the $\tau_n(T;E_i,\mu_1)$ for a given E_i and T.

Figure 30 shows the comparative attenuation of 12.2 to 15 MeV and fission sources as function of concrete slab thickness. The fraction of fission source neutrons in each group is shown in Table 17. We see that the gamma-ray component increases more rapidly for the fission source than for the higher energy 12.2 to 15 MeV source.

To test the reliability of the adjoint calculations, several 40 group forward, i.e., Eq. (44), calculations were performed using the ANISN code. These were for 12.2 to 15 MeV and fission sources at nearly normal incidence and the neutron and total doses equivalents were computed in the rightmost interval. The cross sections used in the forward calculations had been collapsed from the 122 group structure by weighting with fluxes computed in a 75 cm radius sphere. Two sets were used. One was for spherical geometry* with a nearly normally incident source in the 12.2 to 15 MeV group, and the other with a nearly normally incident fission source. The comparison of forward and adjoint results are shown in Table 18. For the fission source, the agreement is

*Later forward runs using 40 group cross sections collapsed in 75 cm slab geometry produced results that agree within 1% with the forward results in Table 18 for the 12.2 to 15 MeV source for 15, 75, 100, and 200 cm slabs.

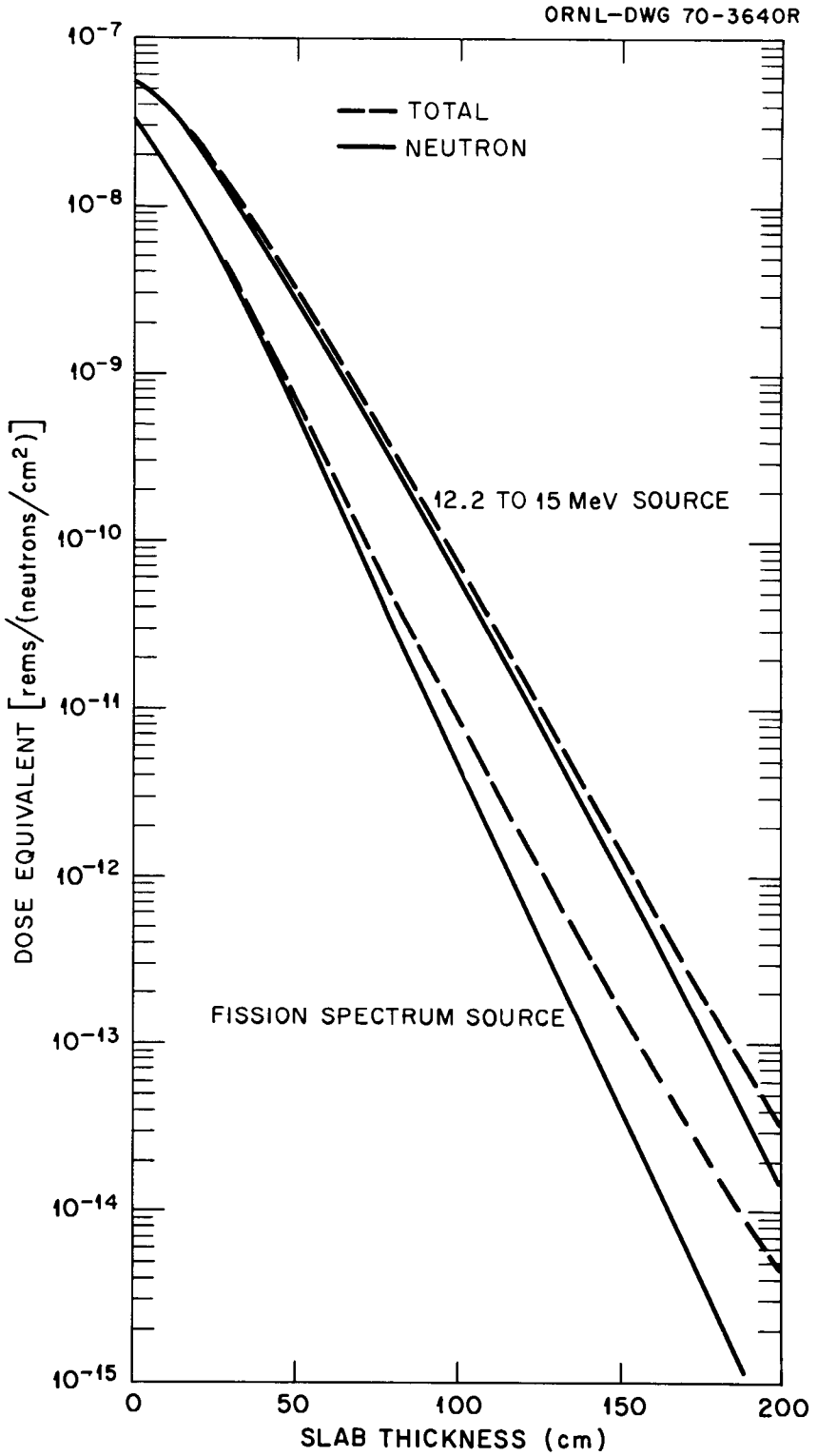

Fig. 30. Total and Neutron Dose Equivalent (rems) As a Function of Concrete Slab Thickness for 12.2 to 15 MeV and Fission Neutron Sources At Nearly Normal Incidence.

TABLE 17

FRACTION OF NEUTRONS IN EACH SOURCE GROUP FOR A FISSION SOURCE

Group	$f(E)\Delta E$
1	0.016(-2)
2	0.090(-2)
3	0.350(-2)
4	1.397(-2)
5	3.473(-2)
6	3.522(-2)
7	10.778(-2)
8	8.941(-2)
9	2.330(-2)
10	12.091(-2)
11	21.913(-2)
12	19.937(-2)
13	13.605(-2)
14	1.557(-2)
15 through 22	0.0

TABLE 18

COMPARISON OF FORWARD AND ADJOINT TRANSMISSION RESULTS FOR NEUTRONS AT NEARLY NORMAL INCIDENCE ON TSF CONCRETE SLABS

Source Energy	Slab Thickness (cm)	Neutron Dose Equivalent [rem/(n/cm^2)]		Total Dose Equivalent [rem/(n/cm^2)]	
		Forward	Adjoint	Forward	Adjoint
12.2 to 15 MeV	15	3.07(-8)*	3.06(-8)	3.08(-8)	3.10(-8)
	30	1.22(-8)	1.22(-8)	1.25(-8)	1.24(-8)
	75	4.67(-10)	4.59(-10)	5.08(-10)	5.01(-8)
	100	6.55(-11)	6.34(-11)	7.55(-11)	7.38(-11)
	150	1.11(-12)	1.04(-12)	1.55(-12)	1.49(-12)
	200	1.68(-14)	1.52(-14)	3.37(-14)	3.26(-14)
Fission Spectrum	30	3.55(-9)	3.53(-9)	3.67(-9)	3.66(-9)
	75	5.03(-11)	4.99(-11)	6.92(-11)	6.96(-11)
	100	4.60(-12)	4.59(-12)	8.21(-12)	8.31(-12)
	150	4.04(-14)	4.04(-14)	1.54(-13)	1.58(-13)

*read 3.07×10^{-8}

within 3% or less for both neutron and total dose for the four slabs considered. For the 12.2 to 15 MeV source, the neutron adjoint result is about 10% lower than the forward results for the 200 cm slab and about 6% lower for the 150 cm slab. For all other cases, the results agree within 4% or less. We feel that the comparatively close agreement between forward and adjoint results over the entire range of slab thicknesses is substantial verification that the adjoint method produces reliable results.

The fission source $f(E_i)\ \Delta E_i$ given in Table 17 and the transmission factors $\tau_n(T;E_i,\mu_j)$ were used in Eq. (50) to calculate the neutron dose equivalent transmitted through slabs of various thicknesses. This is compared to Moments Method results of Trubey and Emmett[34] in Fig. 31. Their results were doubled so that the comparison could be on the basis of 1 source neutron per cm^2 in the forward direction. Since the Moments Method results are for an infinite medium, we expect them to be higher than slab results due to increased scattering contributions at a given point. The attenuation characteristics are seen to be quite similar in the 200 to 400 g/cm^2 thickness region. The concrete composition used for the Moments Method calculation is given in Table 19.

To compare secondary gamma-ray results we refer to some recent Monte Carlo calculations by Spielberg[49], using the UNC-SAM-2 computer code. The results are given as a function of depth in a halfspace of soil with unit density and a water content of 10% by weight. The composition is given in Table 20 for the soil with density 1.0 g/cm^3 and for a similar soil with density 2.3 g/cm^3. Figures 32 and 33 show comparisons of secondary gamma-ray dose as a function of concrete or soil thickness for nearly normally incident neutron sources with energies near 14 and 8 MeV, respectively. For both source energies Spielberg's results are higher for distances near the interface in which the corresponding slab is thin. Thin slabs reduce the volume where gamma-ray production and scattering take place in comparison to the halfspace. In addition, the soil has a greater water content (10% as compared to 6%) which should shorten the distance for slowing neutrons down and thus increase the production of capture gamma rays near the surface. The attenuation beyond 150 cm appears to be quite similar for both soil and concrete.

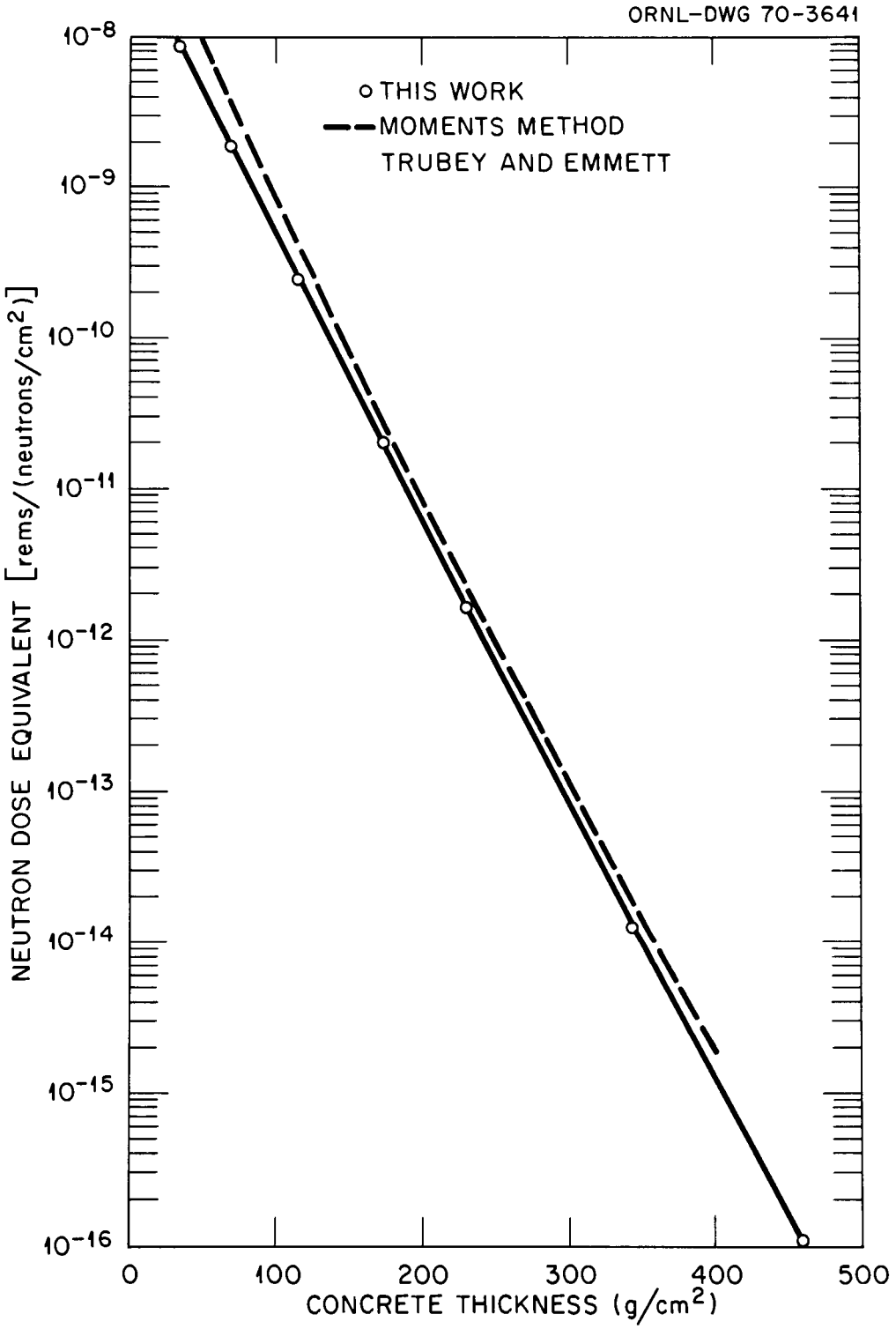

Fig. 31. Comparison of Adjoint Discrete Ordinates and Moments Method (Ref. 34) Calculations of Neutron Dose Equivalent (rems) from a Plane Isotropic Fission Source As a Function of Concrete Thickness, Source Normalized to One Neutron in Forward Direction.

TABLE 19

COMPOSITION ASSUMED FOR TRUBEY-EMMETT MOMENTS METHOD CALCULATION* AND FOR THIS WORK

Element	Nuclear Density ($10^{21}/cm^3$) Type 3	TSF
H	12.5	8.5
C	5.9	20.2
O	42.1	35.5
Si	10.3	1.7
Ca	8.7	11.3
Others	-	2.67
Density (g/cm^3)	2.31	2.3

*From Ref. 34

TABLE 20

SPIELBERG SOIL COMPOSITION*

Element	Nuclear Density ($10^{21}/cm^3$) Density: 1 g/cm^3	2.3 g/cm^3
H	6.63	15.3
O	20.20	46.4
Si	5.70	13.1
Al	1.75	4.01
Ca	0.52	1.20
Fe	0.52	1.20
K	0.38	0.87

*From Ref. 49

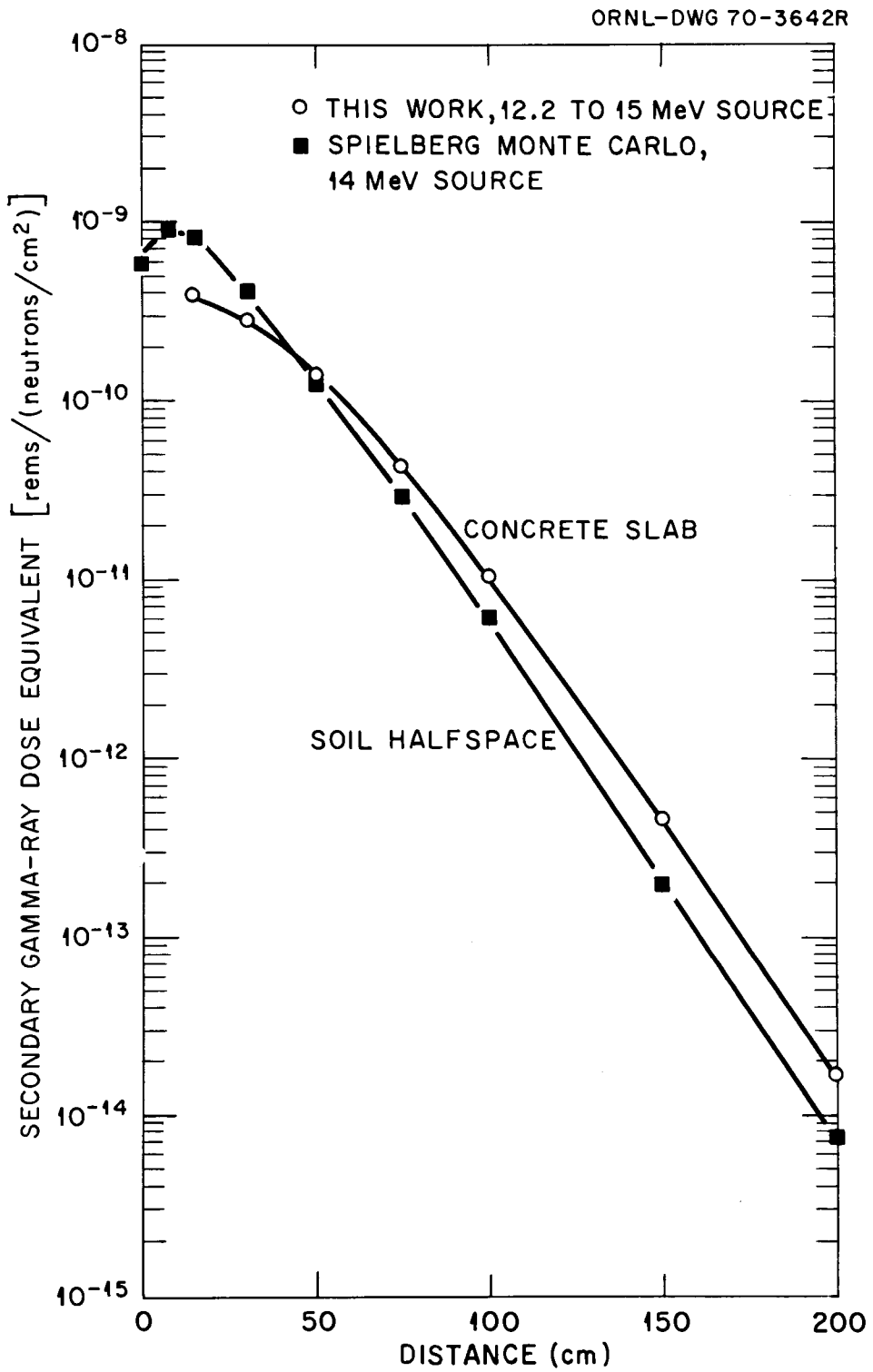

Fig. 32. Comparison of Adjoint Discrete Ordinates and Monte Carlo (Ref. 49) Calculations of Secondary Gamma-Ray Dose As a Function of Concrete or Soil Thickness for Neutron Sources Near 14 MeV and Normal Incidence.

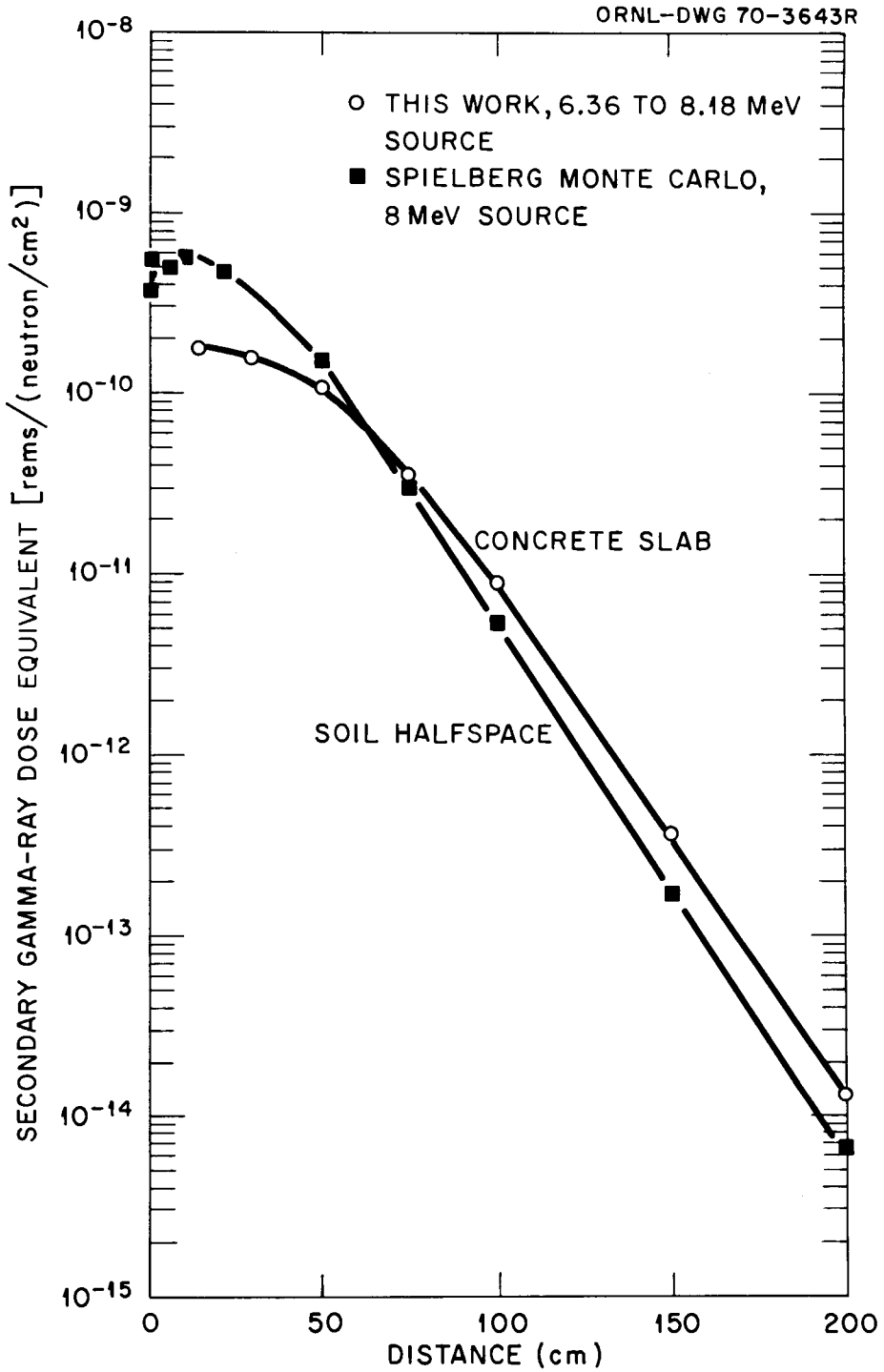

Fig. 33. Comparison of Adjoint Discrete Ordinates and Monte Carlo (Ref. 49) Calculations of Secondary Gamma-Ray Dose As a Function of Concrete or Soil Thickness for Neutron Sources Near 8 MeV and Normal Incidence.

Some comparisons of attenuation of primary gamma-ray sources were also made. Doggett and Bryan[126] recently published tables of calculated dose transmission factors for gamma rays incident on concrete barriers. The data reported is based on Monte Carlo calculations by Berger, Eisenhauer, and Morris. Figure 34 shows a comparison of the gamma-ray dose transmission probability, P_T, as a function of concrete slab thickness for gamma-ray source energy near 1.25 MeV and various incidence directions. The gamma-ray dose transmission probability for a gamma-ray source in the i-th energy group and j-th direction is given by

$$P_T\ (E_i,\mu_j) = \frac{\tau_\gamma(T;E_i,\mu_j)\ S(E_i,\mu_j)\ \Delta E_i\ w_j}{\phi(T;z_o,E_i,\mu_j)\ \Delta E_i\ w_j\ F(E_i)}$$

or (51)

$$P_T\ (E_i,\mu_j) = \frac{\mu_j\ \tau_\gamma(T;E_i,\mu_j)}{F(E_i)}$$

where μ_j is the incidence direction cosine, $F(E_i)$ is the gamma-ray fluence to dose conversion factor for the i-th energy group and $\tau_\gamma(T;E_i,\mu_j)$ is the transmission factor (Tables B-8 through B-14) for a slab of thickness T due to a gamma-ray source in the i-th energy group and j-th direction. In Fig. 34 we used data for the 1.00 to 1.33 MeV gamma-ray group, and values of μ_j = 0.9894, 0.458, and 0.095, and a value $F(E_i) = 6.25 \times 10^{-10}$ rads/(γ/cm^2). The Doggett and Bryan data plotted are for a source energy of 1.25 MeV and incidence direction cosines of μ = 1.0, 0.5, 0.4, and 0.1. The Doggett-Bryan data are for slab thicknesses from 0 to 70 g/cm^2 (about 4 mean-free-path-lengths) and the results of this study for slab thicknesses from 35 to 460 g/cm^2. Agreement is seen to be very good in the region of common thicknesses. Figure 35 shows more comparisons between this work and that of Doggett and Bryan. Again, the transmission probability, P_T, is shown as a function of concrete thickness. The Doggett-Bryan values are for normally incident gamma-rays of energy 0.66 and 10 MeV. They are compared with results of this study for μ = 0.9894 and energy groups 0.6 to 0.8 MeV and 8 to 10 MeV. Again, very reasonable agreement is noted.

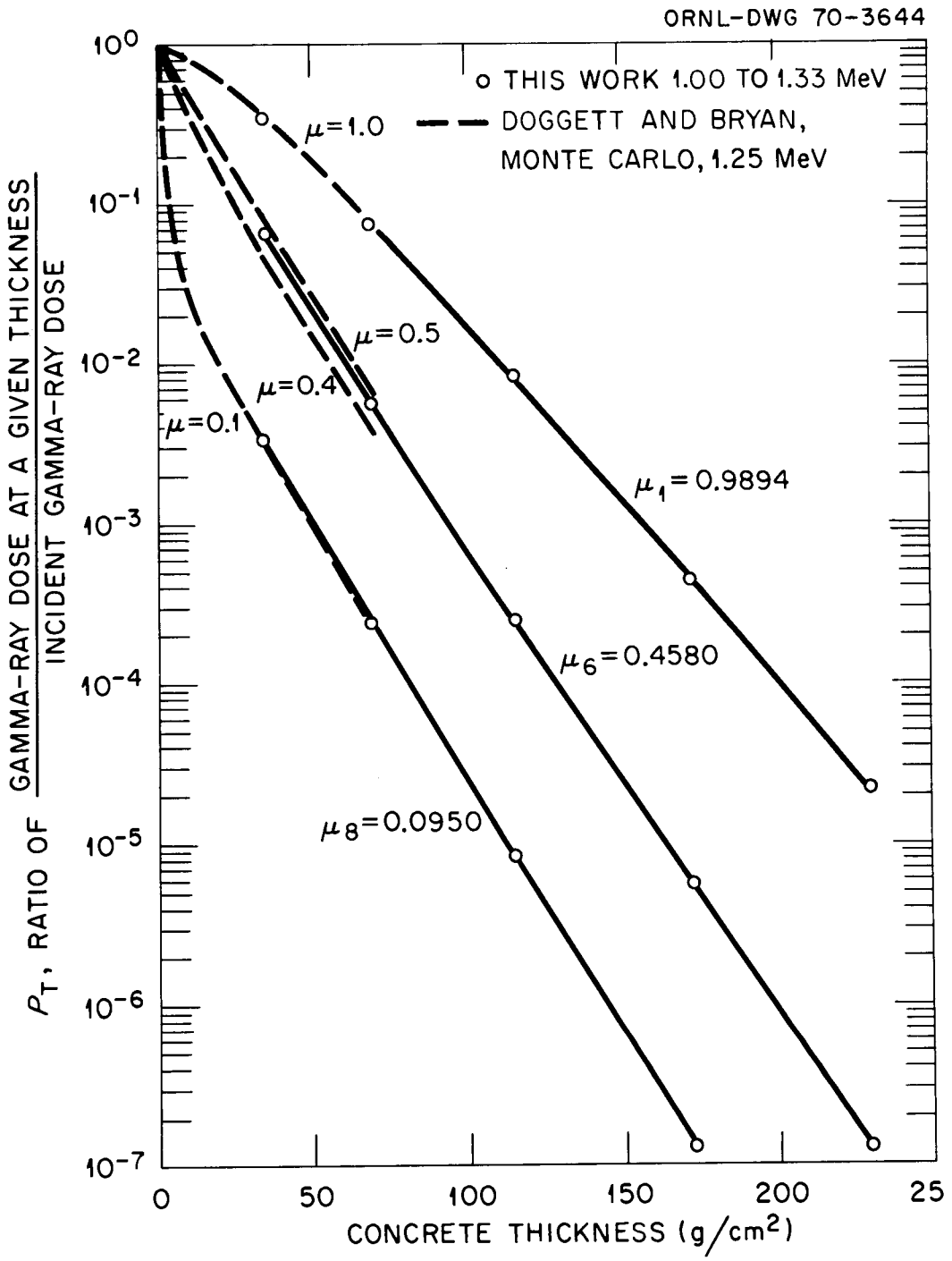

Fig. 34. Comparison of Monte Carlo (Ref. 126) and Adjoint Discrete Ordinates Calculations of Gamma-Ray Dose Transmission Probability As a Function of Concrete Slab Thickness for Gamma-Ray Source Energy Near 1.25 MeV and Various Angles of Incidence.

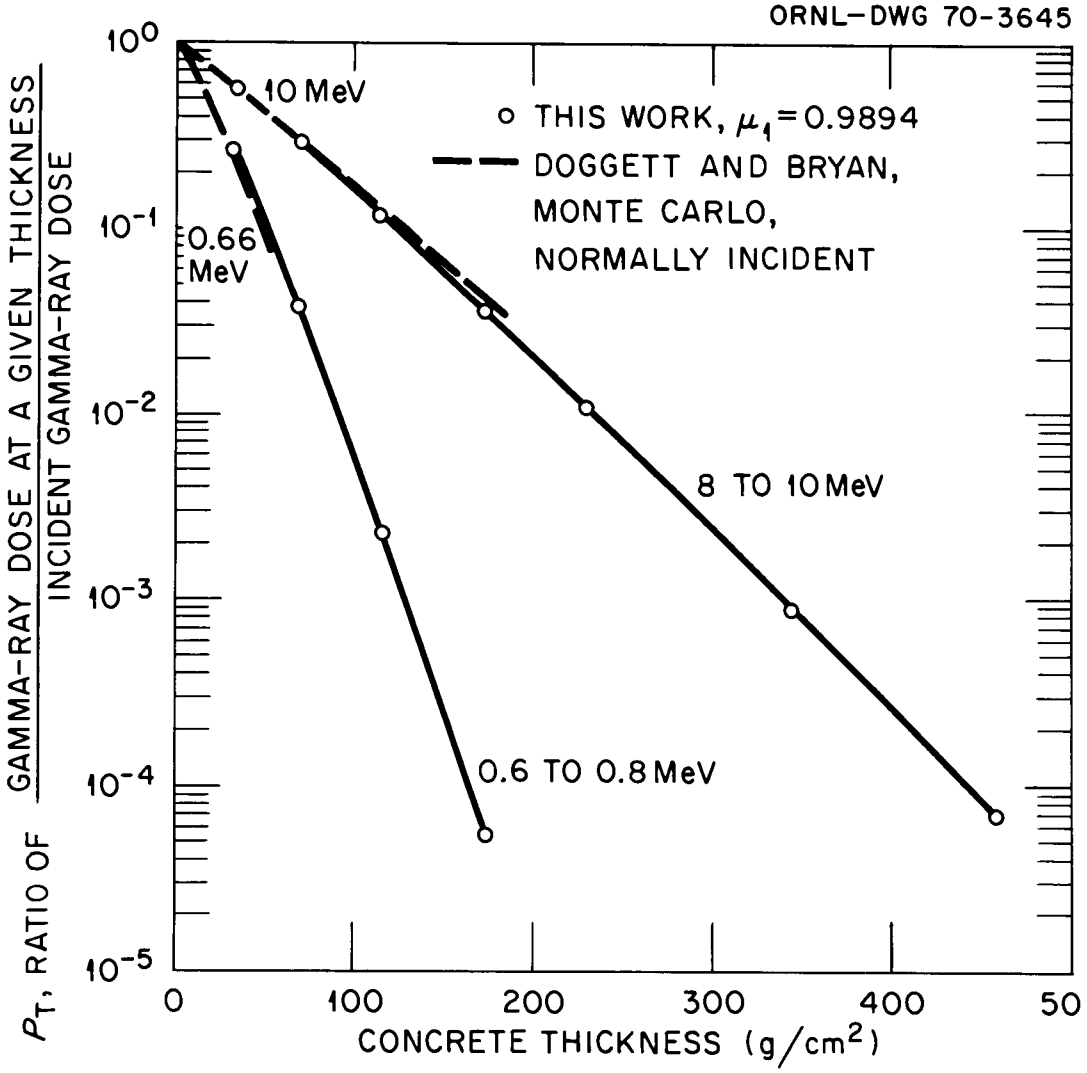

Fig. 35. Comparison of Monte Carlo (Ref. 126) and Adjoint Discrete Ordinates Calculations of Gamma-Ray Dose Transmission Probability As a Function of Concrete Slab Thickness for Nearly Normal Incident Gamma-Ray Sources with Energies Near 10 and 0.66 MeV.

References

1. H. Hilsdorf, "The Water Content of Hardened Concrete", Nucl. Radiation Shielding Studies Report No. 4, DASA 1875 (1967) [1616]*

2. A. M. Neville, Properties of Concrete, John Wiley and Sons, New York (1963).

3. W. H. Taylor, Concrete Technology and Practice, American Elsevier Publishing Co., New York (1965).

4. American Concrete Institute, P. O. Box 4754, Redford Station, Detroit, Michigan

5. Concrete for Radiation Shielding, Compilation No. 1, Second Edition, American Concrete Institute, (1962).

6. Harold S. Davis, "High Density Concrete for Shielding Atomic Energy Plants," ACI Journal, Vol. 27, No. 7, (1956) [723]

7. A. N. Komarovskii, Shielding Materials for Nuclear Reactors, Pergamon Press, (1961) [1072].

8. A. N. Komarvoskii, "Design of Nuclear Plants," AEC-tr-6722, (1968) (available from CFSTI, Springfield, Virginia) [1591 and 138 R].

9. R. L. Walker and M. Grotenhuis, A Summary of Shielding Constants for Concrete, ANL-6443, (1961), [68].

10. Transactions of the American Nuclear Society published twice each year before ANS meetings.

11. "Concrete in Radiation Shielding I and II," Trans. Am. Nucl. Soc. 8(1), 176 (1965).

12. Reactor Handbook, Second Edition, Vol. III, Part B: Shielding E. P. Blizard and L. S. Abbott, editors, Interscience Publishers, New York, (1962).

13. Wade E. Selph, "Neutron and Gamma-Ray Albedos," DASA-1892-2 reprinted as ORNL-RSIC-21, (1968) [1536].

14. "Radiation Shielding Analysis and Design Principles as Applied to Nuclear Defense Planning," William R. Kimel, Editor, TR-40 (1966) [1500].

* Numbers in squared brackets are the RSIC accession numbers. Abstracts are ordered by these numbers in the binder issued as ORNL-RSIC-6. If followed by R, they are Russian and abstracts may be found in ORNL-RSIC-23.

15. W. W. Engle, Jr., A Users Manual for ANISN, K-1693 (1967)

16. F. A. R. Schmidt, "Analytical Radiation Shielding Calculations for Concrete -- Formulas and Parameters," Nucl. Eng. Des., 10, 308 (1969).

17. D. L. Broder et al., Concrete in Shielding of Nuclear Installations, Moscow Atomizdat (1966). In Russian [41R].

18. D. L. Broder et al., "Effect of Water Content in Concrete on Thickness and Cost of Reactor Shielding," Sov. J. of At. Energy, 16, 26 (1964) [884 and 26 R].

19. B. T. Price, C. C. Horton, and K. T. Spinney, Radiation Shielding, Pergamon Press, (1957), [5].

20. L. K. Zoller, "Fast Neutron Removal Cross Sections," Nucleonics 22, 128 (1964).

21. P. N. Stevens and D. K. Trubey, "Methods of Calculating Neutron and Gamma Ray Attenuation," Chapter 3 of the Weapons Radiation Shielding Handbook edited by L. S. Abbott, H. C. Claiborne, C. E. Clifford DASA-1892-3, (1968).

22. D. K. Trubey, A Survey of Empirical Functions Used to Fit Gamma Ray Buildup Factors," ORNL-RSIC-10, (1966) [1052]

22b. H. C. Claiborne, "Analytical Solutions for Heat Generation Distributions in Regular Geometries," Engineering Compendium on Radiation Shielding, Vol. I, p. 441, Springer Verlag (1968).

23. M. J. Berger, "Proceedings of Shielding Symposium held at the Naval Radiological Defense Laboratory," USNRDL, Reviews and Lectures No. 29, p. 47 (1956).

24. L. N. Zaitsev et al.,"Concrete Shielding of Nuclear Reactors," Beton i Zhelezobeton, 1, 8 (1964) (in Russian).

25. H. Goldstein, Fundamental Aspects of Reactor Shielding, Addison-Wesley Publishing Co., (1959), [7]

26. A. Avery et al., "Methods of Calculation for Use in the Design for Power Reactors," AERE-R-321, 6, (1960), [103].

27. W. L. Bunch, "Attenuation Properties of High Density Portland Cement Concretes as a Function of Temperature," HW-54656 (1958), [236]

28. D. E. Wood, "The Effect of Temperature on the Neutron Attenuation of Magnetite Concrete," HW-58497, (1958).

29. E. G. Peterson, "Shielding Properties of Ferrophosphorus Concrete as a Function of Temperature," HW-64774, (1960) [178]

30. E. G. Peterson, "Shielding Properties of Ordinary Concrete as a Function of Temperature," HW-65572, (1960), [177].

31. E. G. Peterson, "Shielding Properties of Iron Serpentine Concrete," HW-73255, (1962).

32. L. G. Mooney and M. B. Wells, "Effects of Neutron Energy Spectrum in Air on the Neutron-Induced Dose in Concrete Underground Structures," RRA-M65, (1966), [1379].

33. D. K. Trubey, A Calculation of the Neutron Dose in Ordinary Concrete Due to Air-scattered Neutrons from a Point Fission Source, ORNL-TM-973, (1965), [864].

34. D. K. Trubey and M. B. Emmett, Some Calculations of the Fast Neutron Distribution in Ordinary Concrete from Point and Plane Isotropic Fission Sources, ORNL-RSIC-4, (1965), [888].

35. E. P. Blizard and J. M. Miller, Radiation Attenuation Characteristics of Structural Concrete, ORNL-2193, (1958), [180].

36. J. P. Nichols, Calculation of Concrete Shields for Fission Sources, ORNL-TM-1167, (1965), [986]

37. V. S. Dikarev et al., Atom. Ener., 1, 5, (1956).

38. G. A. Vasil'ev et al., "The Attenuation of Reactor Radiation by Means of Serpentine Concrete," Sov. J. Atomic Energy, 18, 151, (1965), [1335 and 59 R].

39. A. P. Veselkin et al., "Shielding Properties of Iron Serpentine Concrete," Sov. J. Atomic Energy, 20, 101, (1966), [1374 and 74 R].

40. E. Aalto, "A Comparison of Shielding Calculations with Absolute Measurements in Massive Shields," Nucl. Appl., 1, 359, (1965) [991].

41. E. Aalto et al., "Measured and Predicted Variations in Fast Neutron Spectrum in Massive Shields of Water and Concrete," Nucl. Str. Eng. 2, 233, (1965), [1037].

42. R. Nilsson and E. Aalto, "Test of Neutron Spectrum Calculations with the Help of Foil Measurements in a D_2O and in a H_2O Moderated Reactor and in Reactor Shields of Concrete and Iron," AE-155, (1964), [787].

43. F. H. Clark et al., Monte Carlo Calculations of the Penetration of Normally Incident Neutron Beams Through Concrete, ORNL-3926, (1967), [1245].

44. R. E. Maerker and F. J. Muckenthaler, "Calculation and Measurement of the Fast Neutron Differential Dose Albedo for Concrete," Nucl. Sci. Eng., 22, 455 (1965) [832].

45. R. E. Maerker and F. J. Muckenthaler, "Measurements and Single-velocity Calculations of Differential Angular Thermal-Neutron Albedos for Concrete," Nucl. Sci. Eng., 26, 339, (1966) [1199].

46. F. J. Allen, A. T. Futterer, and W. P. Wright, "Neutron Transmission versus Thickness for some Common Materials," BRL-1174, (1962) [530].

47. F. J. Allen, A. T. Futterer, and W. P. Wright, "Neutron Reflection and Flux versus Depth for Concrete," BRL-1189, (1963), [399].

48. F. J. Allen and A. T. Futterer, "Neutron Transmission Data," Nucleonics, 21, 120 (1963), [383].

49. D. Spielberg, "Shielding by Soil Against Neutrons and Secondary Gamma Rays," to be published in Engineering Compendium on Radiation Shielding, Vol. II, Shielding Materials and Design, Jaeger et al., Editors, Springer-Verlag (New York).

50. M. G. Lim et al., "Spectral Distribution of Fission Neutrons in Ordinary Concrete," Trans. Am. Nucl. Soc., 9 (1), 140 (1966).

51. Yu. A. Yegorov, "Deformation of Fast Neutron Spectrum in Concrete and Water," NASA-TT-F-411, p. 276 [1592].

52. W. S. Snyder and J. Neufeld, "Calculated Depth Dose Curves in Tissue for Broad Beams of Fast Neutrons," Brit. J. Radiol. 28, 342, (1955).

53. W. A. Coleman, R. E. Maerker, F. J. Muckenthaler, and P. N. Stevens, "Calculation of Doubly Differential Current Albedos for Epicadmium Neutrons Incident on Concrete and Comparison of the Reflected Subcadmium Component with Experiment," Nucl. Sci. Eng. 27, 411, (1967) [1268].

54. R. L. French and M. B. Wells, "An Angular Dependent Albedo for Fast Neutron Reflection Calculations," Nucl. Sci. Eng., 19, 441, (1964) [589].

55. B. J. Henderson, "Conversion of Neutron or Gamma Ray Flux to Absorbed Dose Rate," XDC-59-8-179, (1959) [32].

56. Yo Taik Song, "Fast Neutron Streaming through Concrete Ducts," USNCEL-TR-R-565, (1968) [1561].

57. E. Troubezkoy and H. Goldstein, A Compilation of Information on Gamma-Ray Spectra Resulting from Thermal Neutron Capture," ORNL-2904, (1961), [66].

58. R. H. Karcher and J. H. Wilson, "Structural and Shielding Considerations in the Design of Hardened Facilities," Holmes and Narver, Inc., Los Angeles, HN-183, (1965) [1125].

59. E. A. Straker, Time Dependent Neutron and Secondary Gamma Ray Transport in an Air-Over-Ground Geometry, ORNL-4289, Vol. II, (1968) and Trans. Am. Nucl. Soc., 11(1), 410 (1968).

60. D. S. Duncan and A. B. Speir, "GRACE I, An IBM 704-709 Program Designed for Computing Gamma Ray Attenuation and Heating in Reactor Shields," NAA-SR-3719, (1959), (Available from RSIC as CCC-26).

61. F. R. Mynatt, private communication.

62. A. J. Budka and T. J. Dolce, "Secondary Gamma Ray Transmission through Plane Slabs of Concrete," BRL R 1307, (1965) [1179].

63. J. Hacke, "Dosimetry and Shielding of a 14-MeV Generator," Int. J. of Appl. Radiation and Isotopes, 18, 33, (1967), English Translation ORNL-tr-1757, [1640].

64. J. J. Broerse and F. J. Werven, "Shielding Measurements for 3 and 15 MeV Neutrons," Health Physics 12, 83 (1966) [1085].

65. J. J. Broerse, "Penetration Parameters for 15-MeV Neutron Beams," Kerntechnik, 9, 446, (1967), [1652].

66. J. J. Broerse, "Shielding Properties of Concrete for D-T-Neutrons," Int. J. of Appl. Rad. and Isotopes, 19, 74, (1968)

67. L. R. Day, and M. L. Mullender, "Shielding Problems Associated with a Cockcroft Walton Accelerator," AWRE NR-1/63 (1963).

68. "Neutron Activation Analysis Data," Report TSI-600 of the High Voltage Engineering Corporation, Burlington, Mass.

69. "Recommendations of the International Commission on Radiological Protection," "ICRP Publication 4: Protection against Electromagnetic Radiation and Electrons, Neutrons, and Protons above 3 MeV," Pergamon Press, Oxford, (1964).

70. J. T. Prud'homme, Report No. 1149 of the Texas Nuclear Corp., Austin, Texas (1962).

71. "Conference on Shielding of High Energy Accelerators," TID-7545, p. 202, December (1957).

72. T. E. Northup, "High Density Slag Concrete," Nucl. Struct. Eng. 1, 347, (1965) [981].

73. V. B. Dubrovski et al., Energeticheskoe Stroitel' stov 46, 26-31, (1964) (in Russian)

74. V. B. Dubrovski et al., "Shielding Properties of Stone Aggregate Concrete," Sov. J. Atomic Energy, 22, 125, (1967), [1663 and 12 R].

75. A. K. Shrieber, L. I. Abramov, Yu. N. Malashkin, P. A. Vlasov, "Stone-Concrete," The Building Press (Stroiizdat) Moscow (1967).

76. V. B. Dubrovski et al., "The Use of Concrete for Shielding High Temperature Reactors," J. Nucl. Energy, Part A/B, 20, 1031 (1966), [1375 and 75 R].

77. V. B. Dubrovski and B. K. Pergamenshchik, "The Effect of Irradiation on Chamotte Concrete," Beton i zhelezobeton 1, 29, (1968).

78. D. L. Broder et al., "Shielding Properties of Fireproof Chromite and Magnesite Concretes," Sov. J. At. Energy 21, 959, (1966), [1433 and 97 R].

79. V. S. Loginov et al., "Heavy Plastic Concrete-Material for Radiation Shielding," Beton i zhelezobeton 4, 20, (1968).

80. J. D. Henrie, "Properties of Nuclear Shielding Concrete," ACI Journal 56, 37, (1959), See also: Ref. 4.

81. K. Shirayama, "Properties of Radiation Shielding Concrete," ACI Journal 60, 261, (1963) [672].

82. W. B. Bingham, Jr., "Low Activation Shielding Materials for Nuclear Reactor Environmental Test Chambers," Nucl. Struc. Eng. 2, 243 (1965) [1086].

83. V. V. Avayev et al., "Shielding Properties of Certain Types of Concretes," Translated in Problems in Reactor Shielding, Vol. 1, D. L. Broder et al, editors, NASA TT F-411 [1592].

84. D. L. Broder et al., "Shielding Properties of Borated Heat Resistant Chromite Concretes," Sov. J. Atomic Energy 22(2) 126, (1967) [1661 and 0 R].

85. V. B. Dubrovski et al., "Heat Release in Borated Concrete Shields," Sov. J. Atomic Energy, 22, 127, (1967), [1663 and 3 R].

86. D. L. Broder et al., "Investigation of the Shielding Properties of Concrete which Contains Boron," in Problems of Physics of Reactor Shielding II, D. L. Broder et al, editors, In Russian [125 R].

87. M. L. Condat et al., "Special Concretes for Protection in Reactors," CEA-23 12 (1963), RISLEY-TRANS-646, [1208].

88. W. Chwetzoff et al., "Development of the Shielding for the Rapsodie Reactor," Bul. Inf. Sci. Tech., No. 110, 3 (1966), translated as BNWL-TR-22 [1632].

89. M. K. Drake, "Neutron and Gamma Ray Production Cross Sections for Sodium, Magnesium, Chlorine, Potassium and Calcium," NDL-TR-89 I-VI (1967) [1606].

90. M. K. Drake, "Neutron and Gamma Ray Production Cross Sections for Silicon," GA-8628, (1968) [1821].

91. R. E. Maerker and F. J. Muckenthaler, "Gamma Ray Spectra Arising from Thermal Neutron Capture in Iron, Aluminum and Copper," Trans. Am. Nucl. Soc., 11(2), 701 (1968). See also ORNL-4382, (1969).

92. K. J. Yost and S. M. Kremer, "A Comparison of Measured and Calculated Neutron Capture Gamma Ray Spectra," Trans. Am. Nucl. Soc., 11(2) 703 (1968).

93. G. Kunszt, "High Water Content Shielding with Iron and Bauxite Aggregates," Nucl. Struct. Eng., 1, 118, (1965) [800].

94. M. Condat et al., "Study of Shielding and Shielding Concretes," Bul. Inf. Sci. Tech. No. 109, 21, (1966) Translated as ORNL-tr-2039.

95. H. C. Honeck, "ENDF/B -Specifications for an Evaluated Nuclear Data File for Reactor Applications," BNL-50066 (May 1966). Revised by S. Pearlstein, Brookhaven National Laboratory (July 1967). Version I, released 1968.

96. D. J. Hughes and R. B. Schwartz, "Neutron Cross Sections" Second Edition, (1958), BNL-325.

97. N. M. Greene, Private Communication.

98. "European American Committee on Reactor Physics Neutron Spectra" EACRP-L-62, Supplement 1, (1966).

99. H. Soodak, Reactor Handbook, Second Edition, Vol. III, Part A: Physics, Interscience Pub., New York (1962).

100. M. G. Lim, "Spectral Distribution of Fission Neutrons in Ordinary Concrete," Thesis, University of Virginia (1966).

101. "Reactor Physics Constants," ANL-5800 (1963).

102. S. K. Penny et al., OGRE, A Monte Carlo System for Gamma Ray Studies, Including an Example (OGRE-P1) for Transmission through Laminated Slabs, ORNL-3802, (1966). (available from RSIC as CCC-46/OGRE.).

103. G. A. Bartholomew et al., "Compendium of Thermal-Neutron-Capture Gamma Ray Measurements, Part 1, $Z \leq 46$," Nuclear Data A3, 367 (1967); "Part II, $Z = 47$ to $Z = 67$," Nuclear Data A5, 1 (1968); "Part III, $Z = 68$-94," Nuclear Data A5, 243 (1969).

104. K. J. Yost, DUCAL, a Code for the Calculation of Gamma Ray Production Cross Sections, ORNL-4165 (to be published).

105. D. C. Irving, Evaluation of Neutron Cross Sections for Boron 10, ORNL-TM-1872, (ENDF-109).

106. J. K. Dickens et al., "The $^{14}N(n,n'\gamma)$ Reaction for $5.8 \leq E_n \leq 8.6$ MeV," In Neutron Cross Sections and Technology. Proceedings of a Conference. NBS Special Publication 299, Vol. II, 811, (1968).

107. Health Physics Division Annual Progress Report for Period Ending July 31, 1966, ORNL-4007, pp. 183-186 (1966).

108. E. A. Straker, Private Communication.

109. P. Spilling et al., "Thermal Neutron Capture Gamma Rays for Natural Magnesium and Enriched Mg-25," Nucl. Phys. A, 102, 209, (1967).

110. H. Lycklama et al., "A Study of the Gamma Radiation Following Thermal Neutron Capture by Silicon," Can. J. Phys. 45, 1871, (1967).

111. G. van Middelkoop, "Gamma Rays from the $^{31}P(n,\gamma)^{32}P$ Reaction," Nucl. Phys. A 97, 209, (1967).

112. H. Gruppelaar and P. Spilling, "Thermal Neutron Capture Gamma Rays from Natural Calcium," Nucl. Phys. A 102, 226 (1967).

113. D. Irving, unpublished "O5R Memo No. 2," (1965).

114. J. J. Schmidt, "Neutron Cross Sections for Fast Reactor Materials, Part I: Evaluation," KFK 120 (1966).

115. K. J. Yost and N. M. Greene, Neutron Cross Section Averaging Code, ORNL-4130 (1967) (Available from RSIC as PSR-9/CSP.)

116. R. Q. Wright, J. L. Lucius, N. M. Greene, and C. W. Craven, Jr., SUPERTOG: A Program to Generate Fine Group Constants and P_n Scattering Matrices from ENDF/B, ORNL-TM-2679 (Sept. 1969). (Available from RSIC)

117. OGRE Photon Interaction Cross-Section Library [based on UCRL-50400, Vol. VI (1968)], Data available from RSIC as DLC-4.

118. J. R. Knight and F. R. Mynatt, "MUG, A Program for Generating Multigroup Photon Cross Section," Union Carbide Corp. Report CTC-17 (1970). (Code is available from RSIC as PSR-7/MUG.)

119. W. E. Kinney and F. G. Perey, Calculated Fe-56 Neutron Scattering and Gamma-Ray Production Cross Sections from 1.0 to 7.6 MeV, ORNL-4249 (1968).

120. J. Celnik and D. Spielberg, Gamma Spectral Data for Shielding and Heating Calculations, UNC-5140 (1965).

121. W. E. Ford, III, and David H. Wallace, POPOP4, A Code for Converting Gamma-Ray Spectra to Secondary Gamma-Ray Production Cross Sections, CTC-12 (May 1969). (Available from RSIC).

122. H. C. Claiborne and D. K. Trubey, "Gamma-Ray Dose Rates in a Slab Phantom," Trans. Am. Nucl. Soc. 12(1), 383 (1969), ORNL-TM-2574, and Nucl. Appl. Tech. 8, 5, 450 (1970).

123. J. J. Ritts, E. Solomito, and P. N. Stevens, "Calculations of Neutron Fluence-to-Kerma Factors for the Human Body," Nucl. Appl. Tech. 7 (1), 88-99 (July, 1969).

124. G. E. Hansen and H. A. Sandmeier, "Neutron Penetration Factors Obtained by Using Adjoint Transport Calculations," Nucl. Sci. Eng. 22, 315, (1965).

125. F. R. Mynatt and W. W. Engle, Jr., "Group Averaging of Cross Sections for Multigroup Adjoint Discrete Ordinates Calculations," Neutron Phys. Div. Ann. Progr. Rept. May 31, 1967, ORNL-4134, p. 78-80 (1967).

126. W. O. Doggett and F. A. Bryan, Jr., "Theoretical Dose Transmission and Reflection Probabilities for 0.2-10.0 MeV Photons Obliquely Incident on Finite Concrete Barriers," Nucl. Sci. Eng. 39, 92-104(1970).

APPENDIX A

MISCELLANEOUS DATA

TABLE A-1

FAST-NEUTRON REMOVAL CROSS SECTIONS[a]

Element	Atomic Number	ρ (g/cm^3)	Σ_r/ρ (Calc.) (cm^2/g)	Σ_r (cm^{-1})	Σ_r/ρ (Exp.) (cm^2/g)
Aluminum	13	2.699	0.0293	0.0792	0.0292 ± 0.0012
Antimony	51	6.691	0.0136	0.0907	
Argon	18		0.0244		
Arsenic	33	5.730	0.0173	0.0993	
Barium	56	3.500	0.0129	0.0450	
Beryllium	4	9.013	0.0678	0.1248	0.0717 ± 0.0043
Bismuth	83	9.747	0.0103	0.1003	0.010 ± 0.0010
Boron	5	3.330	0.0575	0.1914	0.0540 ± 0.0054
Bromine	35	3.120	0.0168	0.0523	
Cadmium	48	8.648	0.0140	0.1213	
Calcium	20	1.540	0.0230	0.0354	
Carbon	6	1.670	0.0502	0.0838	0.0407 ± 0.0024
Cerium	58	6.900	0.0126	0.0870	
Cesium	55	1.873	0.0130	0.0243	
Chlorine	17		0.0252		0.020 ± 0.014
Chromium	24	6.920	0.0208	0.1436	
Cobalt	27	8.900	0.0194	0.1728	
Copper	29	8.940	0.0186	0.1667	0.0194 ± 0.0011
Dysprosium	66	8.562	0.0117	0.1003	
Erbium	68	4.770	0.0115	0.0550	
Europium	63	5.166	0.0120	0.0621	
Fluorine	9		0.0361		0.0409 ± 0.0020
Gadolinium	64	7.868	0.0119	0.0938	
Gallium	31	5.903	0.0180	0.1060	
Germanium	32	5.460	0.0176	0.0963	
Gold	79	19.320	0.0106	0.2045	
Hafnium	72	13.300	0.0112	0.1484	
Helium	2		0.1135		
Holmium	67		0.0116		
Indium	49	7.280	0.0139	0.1009	
Iodine	53	4.930	0.0133	0.0654	
Iridium	77	22.420	0.0107	0.2408	
Iron	26	7.865	0.0198	0.1560	0.0214 ± 0.0009
Krypton	36		0.0165		
Lanthanum	57	6.150	0.0127	0.0783	
Lead	82	11.347	0.0104	0.1176	0.0103 ± 0.0009
Lithium	3	0.534	0.0840	0.0449	0.094 ± 0.007
Lutetium	71		0.0112		
Magnesium	12	1.741	0.0307	0.0535	
Manganese	25	7.420	0.0203	0.1505	
Mercury	80	13.546	0.0105	0.1424	
Molybdenum	42	10.200	0.0151	0.1543	
Neodymium	60	6.960	0.0124	0.0861	
Neon	10		0.0340		
Nickel	28	8.900	0.0190	0.1693	0.0190 ± 0.0010
Niobium	41	8.400	0.0153	0.1288	
Nitrogen	7		0.0448		
Osmium	76	22.480	0.0108	0.2432	
Oxygen	8		0.0405		0.031 ± 0.002
Palladium	46	12.160	0.0144	0.1747	
Phosphorus	15	1.820	0.0271	0.0493	
Platinum	78	21.370	0.0107	0.2279	
Potassium	19	6.475	0.0237	0.1533	
Praseodymium	59	6 500	0.0125	0.0812	
Radium	88	5.000	0.0100	0.0498	
Rhenium	75	20.530	0.0109	0.2238	
Rhodium	45	12.440	0.0145	0.1810	
Rubidium	37	1.532	0.0163	0.0249	
Ruthenium	44	12.060	0.0147	0.1777	
Samarium	62	7.750	0.0121	0.0941	
Scandium	21	3.020	0.0224	0.0676	
Selenium	34	4.800	0.0170	0.0818	
Silicon	14	2.420	0.0281	0.0681	
Silver	47	10.503	0.0142	0.1491	
Sodium	11	0.971	0.0322	0.0313	
Stronium	38	2.540	0.0160	0.0407	
Sulfur	16	2.070	0.0261	0.0540	
Tantalum	73	16.600	0.0111	0.1838	
Tellurium	52	6.240	0.0134	0.0837	
Terbium	65		0.0118		
Thallium	81	11.860	0.0104	0.1238	
Thorium	90	11.300	0.0098	0.1111	
Thulium	69		0.0114		
Tin	50	6.550	0.0137	0.0898	
Titanium	22	4.500	0.0218	0.0981	
Tungsten	74	19.300	0.0110	0.2120	0.0082 ± 0.0018
Uranium	92	18.700	0.0097	0.1816	0.0091 ± 0.0010
Vanadium	23	5.960	0.0213	0.1267	
Xenon	54		0.0131		
Ytterbium	70		0.0113		
Yttrium	39	3.800	0.0158	0.0599	
Zinc	30	7.140	0.0183	0.1306	
Zirconium	40	6.440	0.0156	0.1001	

[a]Table taken from L. K. Zoller, "Fast-Neutron-Removal Cross Sections," *Nucleonics* 22(8), 128–129 (1964).

TABLE A-2

THERMAL NEUTRON CROSS SECTIONS FOR SOME ELEMENTS OF IMPORTANCE IN CONCRETE

Element	σ_a[barn]	Comments	σ_s[barn]	Comments	Other Important Reactions
H	0.330	1/v	20.34	Constant up to 1 keV	
H_2O	0.66	1/v	70.5*	Exponentially decreasing with energy, above 1 eV sum of atomic cross sections	
B	0.1	1/v	2.00	Constant up to 1 keV	n,α σ = 3837 b 1/v up to 50 keV
C	0.0034	1/v	4.85	Constant up to 300 eV	
N	0.075	1/v	10.2	Constant up to 10 eV	n,p σ = 1.50 b slowly decreasing
O	<0.0002	O for shielding by concrete	3.76	Constant up to 10 keV	
Na	0.534	1/v up to 100 eV, First resonance at 35 keV	3.26	Constant up to 500 eV	
Mg	0.063	1/v up to 1 keV, First resonance in Mg 25 at 21 keV	3.34	σ_t = 3.4 b Constant up to 1 keV	
Al	0.235	1/v up to 100 ev, First resonance at 5.9 keV	1.41	Constant up to 5 keV	
Si	0.16	1/v up to 20 keV,	2.15	Constant up to 5 keV	
P	0.19	1/v	5.3	Constant up to 1 keV	
S	0.52	First resonance at 30 keV	1.1	Constant up to 10 keV	
Cl	33.2	1/v up to 200 eV, First resonance at 400 ev	16.0	Constant up to about 50 ev	n,p 1/v up to 200 ev $\sigma \approx 0.3$ b
K	2.10	1/v up to 1 keV	2.2	Slowly decreasing to 1 b at 1 keV	
Ca	0.44	1/v up to 10 keV	2.57	Constant up to 1.8 keV	
Ti	6.1	1/v up to 100 eV	4.13	Slightly increasing	

*Under assumption Σ_{tr} = 2.083 cm^{-1} (Ref. 101), isotropic scattering and Maxwell spectrum of flux with mean temperature 293°K.

TABLE A-2 (Cont'd)

Element	σ_a[barn]	Comments	σ_s[barn]	Comments	Other Important Reactions
V	5.06	1/v up to 100 eV	4.96	About 1 constant up to 100 eV	
Cr	3.1	1/v up to 20 eV		Rising to 4.3 b at 1.5 keV	
Mn	13.3	1/v up to 10 eV, First resonance 340 eV	2.3	Constant up to 10 eV	
Fe	2.55	1/v up to 50 eV	10.6	Constant up to 500 eV	
Ni	4.6	1/v up to 1 keV with a small resonance at 100 eV	17.5	Constant up to 1 keV	
Cu	3.8	1/v up to 100 keV	7.2	Constant up to 100 eV	
Zu	1.10	First resonance at 230 eV	3.6	Roughly constant up to 100 eV	
Ba	1.2	First resonance at 24 eV	8.1		
Sm	5820	From Sm 149 13.83% abundance and σ_a = 41000 b not 1/v	Sm 149 165	Strong energy dependence	
Gd	49000	From Gd 157 15.68% abundance and σ_a = 254000 b	180	~10 b at 1eV	

TABLE A-3

SLOWING-DOWN PARAMETERS FOR THE ELEMENTS OF TABLE A-2

(From Ref. 99)

Element	Atomic Weight	Density g/cm^2	Nuclear Density (10^{24}/cm^3)	ξ	$\bar{\omega}$
H	1.0080	0.00008[a]	0.000048	1.000	0.66137
B	10.82	2.3	0.12797	0.1756	0.06161
B^{10}	10.016				0.06656
C	12.010	2.22	0.11128	0.1589	0.05551
N	14.008	0.00116[a]	0.000050	0.1373	0.04759
O	16.000	0.00133	0.000050	0.1209	0.04167
Na	22.997	0.9712	0.02542	0.0852	0.02899
Mg	24.32	1.741	0.04310	0.0807	0.02741
Al	26.97	2.699	0.06024	0.0730	0.02472
Si	28.06	2.35	0.05042	0.0702	0.02376
P	30.98	1.83	0.03556	0.0637	0.02152
S	32.066	2.07	0.03886	0.0616	0.02079
Cl	35.457	0.0032 [a]	0.000054	0.0558	0.01880
K	39.096	0.87	0.01340	0.0507	0.01705
Ca	40.08	1.54	0.02313	0.0495	0.01663
Ti	47.90	4.5	0.05656	0.0415	0.01392
V	50.95	5.96	0.07042	0.0391	0.01308
Cr	52.01	6.92	0.08010	0.0383	0.01282
Mn	54.93	7.42	0.08132	0.0363	0.01214
Fe	55.85	7.87	0.08483	0.0357	0.01194
Ni	58.69	8.8	0.09026	0.0340	0.01136
Cu	63.54	8.89	0.08423	0.0314	0.01049
Zn	65.38	7.133	0.06568	0.0305	0.01020
Ba	137.36	3.5	0.01534	0.0146	0.00485
Sm	150.43	7.75	0.03101	0.0134	0.00443
Gd	156.9	7.95	0.03050	0.0128	0.00425

[a] As Gas

TABLE A-4

SCATTERING CROSS SECTIONS
IN INTERMEDIATE ENERGY RANGE FOR SOME ELEMENTS
OF IMPORTANCE IN CONCRETE

Energy Boundaries (MeV)	Lethargy Width of Group	Σ_s/ρ (cm^2/g) Elements							
		H	C	O	Mg	Al	Si	Ca	Fe
1.826- 1.108	0.5	3.513	2.136	2.634	2.950	3.150	2.718	2.81	2,682
1.108- 0.55	0.7	4.928	2.968	3.554	4.025	3.168	3.734	3.039	2.712
0.55 - 0.111	1.6	8.620	3.978	4.458	6.728	4.254	4.328	3.006	3.342
0.111 - $3.35(10^{-3})$	3.5	16.99	4.709	3.572	6.015	3.535	1.700	1.927	8.119
$3.35\ (10^{-3})$ - $5.83(10^{-4})$	1.75	19.94	4.841	3.656	3.500	1.410	2.214	2.565	7.712
$5.83\ (10^{-4})$ - $1.01(10^{-4})$	1.75	20.21	2.848	3.682	3.500	1.410	2.214	2.570	11.04
$1.01\ (10^{-4})$ - $2.9(10^{-5})$	1.25	20.34	4.849	3.705	3.500	1.410	2.300	2.570	11.40
$2.9\ (10^{-5})$ - $1.067(10^{-5})$	1.0	20.34	4.850	3.722	3.500	1.410	2.300	2.570	11.40
$1.067(10^{-5})$ - $3.059(10^{-6})$	1.25	20.34	4.850	3.739	3.478	1.410	2.300	2.570	11.40
$3.059(10^{-6})$ - $1.125(10^{-6})$	1.0	20.34	4.850	3.756	3.425	1.410	2.300	2.570	11.40
$1.125(10^{-6})$ - $4.14(10^{-7})$	1.0	20.34	4.850	3.765	3.410	1.410	2.300	2.570	11.40

TABLE A-5

THERMAL NEUTRON AGE FOR SOME OF BRODER'S CONCRETES

(From Ref. 17)

Density (kg/m^3)	H Content (kg/m^3)	Age (cm^2)
	2.30	541
	8.22	230
2300	14.30	139
	18.90	104
	25.60	81
	20.2	92
2600	33.3	58
	54.6	31
	9.6	162
3200	17.2	97
	27.2	63
	9.0	158
3600	17.6	88
	32.0	47
	9.65	175
	17.6	100
4200	31.0	56
	8.3	204
4600	15.2	120
	27.6	66
	7.8	224
5200	18.2	106
	27.0	67
	6.67	270
3500**	17.5	110
	28.0	67

** Barytes Concrete

TABLE A-6

COEFFICIENTS FOR BERGER BUILDUP FACTOR FUNCTION
FOR POINT ISOTROPIC SOURCE †

$$B(R) = 1 + CR \exp(DR)$$

Ordinary Concrete

	Exposure*			Tissue Kerma**		
E(MeV)	C	D	Max. Error	C	D	Max. Error
0.5	1.3029	0.08610	18%	1.3110	0.08073	12%
1.0	1.0914	0.54566	15%	1.0221	0.05160	9%
2.0	0.8126	0.01980	9%	0.7744	0.02456	5%
3.0	0.6731	0.00942	4%	0.6525	0.01258	3%
4.0	0.5953	0.00299	2%	0.5672	0.00753	2%
6.0	0.4915	-0.00159	3%	0.4718	0.00198	1%
8.0	0.4164	-0.00172	6%	0.4203	0.00096	1%
10.0	0.3585	-0.00005	9%	0.3716	0.00127	1%

	Energy Deposition*			Energy Deposition**		
E(MeV)	C	D	Max. Error	C	D	Max. Error
0.5	1.6280	0.09272	21%	1.6568	0.08538	13%
1.0	1.2367	0.04795	17%	1.1633	0.05325	10%
2.0	0.8850	0.01987	9%	0.8203	0.02465	5%
3.0	0.7171	0.00825	3%	0.6702	0.01221	3%
4.0	0.6154	0.00199	1%	0.5672	0.00753	2%
6.0	0.4882	-0.00205	3%	0.4583	0.00168	1%
8.0	0.4049	-0.00208	6%	0.3985	0.00084	1%
10.0	0.3435	-0.00041	9%	0.3609	0.00083	1%

*Constants based on A. B. Chilton, Nucl. Eng. Des. 6, 205-212 (1967).

**Constants based on F. H. Clark and D. K. Trubey, Nucl. Appl. 4, 37-41 (1968).

†Determined by D. K. Trubey (Nucl. Appl. Tech. [1970])

TABLE A-6 (cont'd)

COEFFICIENTS FOR BERGER BUILDUP FACTOR FUNCTION

FOR POINT ISOTROPIC SOURCE

$B(R) = 1 + CR \exp(DR)$

Magnetite Concrete

	Tissue Kerma**			Energy Deposition**		
E(MeV)	C	D	Max. Error	C	D	Max. Error
0.5	1.0971	0.06458	8%	1.6607	0.06696	8%
1.0	0.9281	0.04768	8%	1.1664	0.04877	8%
2.0	0.7318	0.02620	5%	0.8170	0.02591	5%
3.0	0.6154	0.01836	4%	0.6386	0.01747	3%
4.0	0.5308	0.01513	3%	0.5263	0.01428	3%
6.0	0.4345	0.01118	2%	0.4224	0.00705	3%
8.0	0.3752	0.01199	2%	0.3390	0.01010	2%
10.0	0.3245	0.01624	2%	0.3006	0.00999	2%

Barytes Concrete

	Tissue Kerma**			Energy Deposition**		
E(MeV)	C	D	Max. Error	C	D	Max. Error
0.5	0.7002	0.01624	1%	1.3542	0.01056	4%
1.0	0.7237	0.03007	4%	1.11017	0.02792	3%
2.0	0.6270	0.02373	4%	0.7672	0.02229	3%
3.0	0.5367	0.02158	4%	0.5806	0.01995	3%
4.0	0.4645	0.02122	3%	0.4689	0.01948	2%
6.0	0.3727	0.02233	3%	0.3408	0.02045	2%
8.0	0.3172	0.02588	2%	0.2787	0.02251	2%
10.0	0.2667	0.02878	2%	0.2420	0.02368	1%

TABLE A-6 (cont'd)

FERROPHOSPHOROUS CONCRETE EXPOSURE BUILDUP*

	7 MFP FIT			20 MFP FIT		
E(MeV)	C	D	Max. Error	C	D	Max. Error
0.5	0.9059	0.1283	8%	1.1098	0.0704	15%
1.	0.8467	0.0921	5%	0.9892	0.0481	10%
2.	0.7327	0.0397	2%	0.7703	0.0256	3%
3.	0.6331	0.0164	1%	0.6373	0.0152	2%
4.	0.4879	0.0237	2%	0.4966	0.0186	2%
6.	0.4346	0.0011	2%	0.4118	0.0167	3%
8.	0.3390	0.0043	2%	0.3207	0.0196	4%
10.	0.2563	0.0165	1%	0.2456	0.0287	3%

*Constants taken from Ref. 22.

TABLE A-7

GAMMA-RAY TOTAL LINEAR ATTENUATION COEFFICIENTS PER UNIT MASS (cm^2/g)

E(MEV)	HYDROGEN	BORON	CARBON	NITROGEN	OXYGEN	SODIUM	MAGNESIUM	ALUMINUM	SILICON	PHOS PHORUS
0.500	1.729E-01	8.284E-02	8.707E-02	8.711E-02	8.716E-02	8.347E-02	8.606E-02	8.412E-02	8.704E-02	8.462E-02
1.000	1.263E-01	6.051E-02	6.360E-02	6.363E-02	6.366E-02	6.093E-02	6.283E-02	6.137E-02	6.348E-02	6.169E-02
1.500	1.025E-01	4.916E-02	5.168E-02	5.171E-02	5.175E-02	4.957E-02	5.113E-02	4.995E-02	5.168E-02	5.023E-02
2.000	8.765E-02	4.219E-02	4.440E-02	4.447E-02	4.455E-02	4.279E-02	4.418E-02	4.321E-02	4.475E-02	4.353E-02
2.500	7.703E-02	3.733E-02	3.935E-02	3.948E-02	3.962E-02	3.824E-02	3.954E-02	3.873E-02	4.017E-02	3.915E-02
3.000	6.907E-02	3.367E-02	3.554E-02	3.571E-02	3.589E-02	3.479E-02	3.603E-02	3.534E-02	3.670E-02	3.582E-02
3.500	6.271E-02	3.082E-02	3.260E-02	3.281E-02	3.304E-02	3.220E-02	3.341E-02	3.283E-02	3.416E-02	3.339E-02
4.000	5.798E-02	2.868E-02	3.038E-02	3.063E-02	3.089E-02	3.024E-02	3.142E-02	3.092E-02	3.223E-02	3.154E-02
4.500	5.401E-02	2.698E-02	2.865E-02	2.895E-02	2.925E-02	2.882E-02	3.001E-02	2.959E-02	3.089E-02	3.030E-02
5.000	5.048E-02	2.545E-02	2.708E-02	2.743E-02	2.777E-02	2.754E-02	2.873E-02	2.837E-02	2.967E-02	2.917E-02
5.500	4.742E-02	2.412E-02	2.572E-02	2.610E-02	2.648E-02	2.639E-02	2.759E-02	2.729E-02	2.859E-02	2.814E-02
6.000	4.479E-02	2.297E-02	2.454E-02	2.495E-02	2.536E-02	2.539E-02	2.658E-02	2.634E-02	2.764E-02	2.725E-02
6.500	4.251E-02	2.204E-02	2.359E-02	2.404E-02	2.449E-02	2.467E-02	2.587E-02	2.568E-02	2.699E-02	2.665E-02
7.000	4.051E-02	2.120E-02	2.275E-02	2.323E-02	2.371E-02	2.402E-02	2.523E-02	2.509E-02	2.641E-02	2.611E-02
7.500	3.894E-02	2.055E-02	2.209E-02	2.259E-02	2.310E-02	2.350E-02	2.472E-02	2.461E-02	2.594E-02	2.568E-02
8.000	3.733E-02	1.986E-02	2.140E-02	2.192E-02	2.246E-02	2.296E-02	2.418E-02	2.411E-02	2.545E-02	2.522E-02
8.500	3.575E-02	1.926E-02	2.081E-02	2.137E-02	2.194E-02	2.258E-02	2.383E-02	2.380E-02	2.516E-02	2.498E-02
9.000	3.479E-02	1.890E-02	2.045E-02	2.104E-02	2.163E-02	2.235E-02	2.361E-02	2.361E-02	2.499E-02	2.483E-02
9.500	3.360E-02	1.844E-02	2.000E-02	2.062E-02	2.124E-02	2.206E-02	2.335E-02	2.337E-02	2.477E-02	2.464E-02
10.000	3.252E-02	1.802E-02	1.958E-02	2.023E-02	2.087E-02	2.178E-02	2.309E-02	2.314E-02	2.456E-02	2.447E-02

TABLE A-7 (Continued)

E(MEV)	SULPHUR	CHLORINE	POTASSIUM	CALCIUM	TITANIUM	VANADIUM	CHROMIUM	MANGANESE	IRON	NICKEL
0.500	8.726E-02	8.392E-02	8.525E-02	8.765E-02	8.095E-02	7.973E-02	8.166E-02	8.072E-02	8.285E-02	8.523E-02
1.000	6.357E-02	6.109E-02	6.195E-02	6.361E-02	5.861E-02	5.769E-02	5.889E-02	5.810E-02	5.952E-02	6.103E-02
1.500	5.178E-02	4.977E-02	5.049E-02	5.186E-02	4.780E-02	4.699E-02	4.805E-02	4.741E-02	4.856E-02	4.981E-02
2.000	4.492E-02	4.322E-02	4.392E-02	4.516E-02	4.169E-02	4.103E-02	4.199E-02	4.148E-02	4.252E-02	4.368E-02
2.500	4.045E-02	3.898E-02	3.974E-02	4.092E-02	3.790E-02	3.735E-02	3.829E-02	3.787E-02	3.887E-02	4.006E-02
3.000	3.706E-02	3.576E-02	3.657E-02	3.770E-02	3.500E-02	3.455E-02	3.546E-02	3.512E-02	3.610E-02	3.729E-02
3.500	3.461E-02	3.345E-02	3.432E-02	3.544E-02	3.301E-02	3.262E-02	3.353E-02	3.326E-02	3.423E-02	3.546E-02
4.000	3.274E-02	3.169E-02	3.259E-02	3.370E-02	3.146E-02	3.113E-02	3.204E-02	3.181E-02	3.278E-02	3.404E-02
4.500	3.150E-02	3.055E-02	3.153E-02	3.266E-02	3.059E-02	3.031E-02	3.124E-02	3.107E-02	3.205E-02	3.339E-02
5.000	3.037E-02	2.950E-02	3.056E-02	3.170E-02	2.979E-02	2.956E-02	3.051E-02	3.039E-02	3.138E-02	3.278E-02
5.500	2.936E-02	2.855E-02	2.966E-02	3.082E-02	2.903E-02	2.885E-02	2.981E-02	2.972E-02	3.074E-02	3.217E-02
6.000	2.846E-02	2.772E-02	2.887E-02	3.003E-02	2.836E-02	2.821E-02	2.919E-02	2.913E-02	3.016E-02	3.162E-02
6.500	2.789E-02	2.720E-02	2.841E-02	2.959E-02	2.802E-02	2.791E-02	2.892E-02	2.888E-02	2.995E-02	3.146E-02
7.000	2.736E-02	2.673E-02	2.799E-02	2.919E-02	2.770E-02	2.763E-02	2.866E-02	2.865E-02	2.975E-02	3.131E-02
7.500	2.694E-02	2.635E-02	2.765E-02	2.887E-02	2.745E-02	2.741E-02	2.845E-02	2.846E-02	2.959E-02	3.119E-02
8.000	2.650E-02	2.595E-02	2.729E-02	2.853E-02	2.718E-02	2.717E-02	2.823E-02	2.826E-02	2.942E-02	3.107E-02
8.500	2.628E-02	2.578E-02	2.718E-02	2.845E-02	2.717E-02	2.718E-02	2.829E-02	2.838E-02	2.954E-02	3.128E-02
9.000	2.615E-02	2.567E-02	2.712E-02	2.841E-02	2.718E-02	2.719E-02	2.832E-02	2.846E-02	2.962E-02	3.142E-02
9.500	2.599E-02	2.554E-02	2.704E-02	2.835E-02	2.718E-02	2.721E-02	2.837E-02	2.856E-02	2.973E-02	3.160E-02
10.000	2.583E-02	2.542E-02	2.696E-02	2.830E-02	2.718E-02	2.722E-02	2.841E-02	2.866E-02	2.983E-02	3.177E-02

TABLE A-7 (Continued)

E(MEV)	COPPER	ZINC	BARIUM	SAMARIUM	GADOLINIUM
0.500	8.197E-02	8.279E-02	9.465E-02	1.055E-01	1.077E-01
1.000	5.847E-02	5.884E-02	5.706E-02	5.887E-02	5.829E-02
1.500	4.771E-02	4.801E-02	4.542E-02	4.665E-02	4.617E-02
2.000	4.189E-02	4.215E-02	4.039E-02	4.162E-02	4.128E-02
2.500	3.846E-02	3.879E-02	3.823E-02	3.963E-02	3.938E-02
3.000	3.585E-02	3.620E-02	3.661E-02	3.813E-02	3.796E-02
3.500	3.414E-02	3.452E-02	3.586E-02	3.753E-02	3.745E-02
4.000	3.281E-02	3.322E-02	3.527E-02	3.705E-02	3.703E-02
4.500	3.222E-02	3.267E-02	3.557E-02	3.750E-02	3.751E-02
5.000	3.168E-02	3.216E-02	3.588E-02	3.796E-02	3.799E-02
5.500	3.115E-02	3.162E-02	3.592E-02	3.810E-02	3.816E-02
6.000	3.067E-02	3.113E-02	3.595E-02	3.822E-02	3.831E-02
6.500	3.054E-02	3.105E-02	3.637E-02	3.874E-02	3.885E-02
7.000	3.042E-02	3.097E-02	3.676E-02	3.923E-02	3.936E-02
7.500	3.033E-02	3.091E-02	3.709E-02	3.963E-02	3.978E-02
8.000	3.022E-02	3.085E-02	3.744E-02	4.007E-02	4.023E-02
8.500	3.042E-02	3.107E-02	3.817E-02	4.090E-02	4.109E-02
9.000	3.056E-02	3.122E-02	3.865E-02	4.144E-02	4.164E-02
9.500	3.073E-02	3.141E-02	3.927E-02	4.214E-02	4.236E-02
10.000	3.089E-02	3.159E-02	3.986E-02	4.281E-02	4.305E-02

TABLE A-8

GAMMA RAY SPECTRA FROM THERMAL NEUTRON CAPTURE

(PHOTONS PER 100 CAPTURES)

UPPER ENERGY (MeV)

Element	0.5	1.0	1.5	2.0	2.5	3.0	3.5	4.0	4.5	5.0	5.5	6.0	6.5	7.0	7.5	8.0	8.5	10	Main Ref.
H	-	-	-	-	100	-	-	-	-	-	-	-	-	-	-	-	-	-	103
B	93.5	-	-	-	-	-	-	-	-	-	-	-	-	-	-	-	-	-	103/105
C	-	-	31	-	-	-	-	31	-	69	-	-	-	-	-	-	-	-	103
N	-	-	-	-	-	-	5	32	16	-	57	32	17	-	9.8	-	4.0	12.7	107
O	-	-	-	-	-	-	-	-	-	-	-	-	-	-	-	-	-	-	108
Na	70	40.6	15	9.9	20.4	43.2	18.3	37.0	5.2	2.4	1.1	4.9	20.5	-	-	-	-	-	103
Mg	9	120	22.5	36.6	12.3	47.0	29.2	64.0	18.6	5.2	3.7	1.5	2.2	1.4	0.25	-	4.5	1.0	109
Al	25	13.1	18.6	10.4[a]	10.6	20.5	15.9	14.3	16.1	17.6	6.8	2.8	6.0	2.2	0.7	32.4	-	-	91
Si	-	-	20	-	24.4	3.0	-	70.9	-	61.0	4.5	-	15.2	1.5	10.0	-	2.7	-	110
P	45.3	24.6	26.4	25.6	36.0	14.0	17.7	34.7	10.0	15.8	7.0	5.6	3.4	14.0	6.85	1.99	-	-	103
S	-	59.2	1.3	2.0	47.4	19.2	27.1	3.2	4.7	12.9	60.3	2.5	-	0.7	1.6	3.8	-	2.3	103
Cl	-	55.4	29.4	33.0	2.2	13.0	6.3	9.0	2.1	8.9	1.6	12.0	29.9	18.0	14.0	9.0	-	3.0	89
K	3.5	51.5	19.8	28.4	38.7	20.2	15.4	22.6	19.3	5.3	18.8	17.7	0.63	3.1	0.20	6.0	-	-	103
Ca	7.5	16.8	7.5	90.0	32.0	9.5	1.8	11.4	17.1	6.5	0.7	10.5	43.7	2.0	1.35	-	-	-	112
Ti	36.5	1.6	96.0	25.7	3.6	6.5	3.9	4.3	0.65	10.6	0.4	0.8	31.8	51.8	1.1	0.20	-	-	103
Cr	26.1	5.4	13.9	5.3	18.6	6.3	8.1	4.4	3.6	2.1	8.7	5.2	12.9	4.3	15.7	8.9	11.9	25.0	92
Mn	15.0	16.4	1.3	44.2	33.8	6.5	8.0	5.3	4.0	10.7	17.3	9.7	3.1	6.1	32.7	-	-	-	103
Fe	17.0	13.5	5.0	15.0	3.9	6.0	9.2	3.5	7.2	3.3	1.0	10.0	10.0	0.5	5.5	50.6	0.8	3.3	91

[a]Does not include the ~ 100 1.78 MeV gamma rays following β decay of Al^{28}

TABLE A-8 (Cont'd)

Element	UPPER ENERGY (MeV) 0.5	1.0	1.5	2.0	2.5	3.0	3.5	4.0	4.5	5.0	5.5	6.0	6.5	7.0	7.5	8.0	8.5	10	Main Ref.
Ni	-	-	3.1	1.4	1.8	3.4	1.9	1.1	1.31	0.89	1.6	4.3	2.3	12.4	1.1	12.5	4.0	48.3	103
Cu	79.7	20.2	18.2	11.6	6.9	8.9	8.8	8.0	10.5	4.4	8.9	2.1	5.0	9.6	14.7	41.6	-	-	91
Zn	14.5	13.5	43.5	28.8	18.1	14.8	13.6	10.8	10.5	10.1	11.8	8.8	6.4	12.8	6.0	12.2	0.83	1.2	-
Ba	29.7	49.0	37.2	32.8	26.8	25.0	18.1	20.5	30.0	14.8	10.8	12.0	5.2	2.8	1.2	0.1	0.22	0.4	-
Sm^{149}	5.5	48.0	47.7	52.2	34.6	20.2	14.8	14.0	28.5	23.0	10.3	5.1	1.9	0.6	0.5	-	-	-	92
Gd^{155}	70.0	21.9	53.9	52.0	20.6	24.4	17.8	16.3	18.6	16.7	11.9	12.5	8.3	7.7	1.5	-	0.1	-	104
Gd^{157}	112.2	42.8	46.2	56.5	26.7	17.0	12.9	14.3	13.0	20.5	13.7	13.9	9.7	1.3	-	0.8	-	-	104

TABLE A-9. GAMMA-RAY SPECTRA FROM THERMAL-NEUTRON CAPTURE*

Energy (MeV)	Silicon	Calcium	Potassium	Sodium	Barium	Iron	Aluminum
	Photons/100 Captures						
1-1.5	15.3	20.9	35.0	14.8	63.4	5.0	18.6
1.5-2	0	79.6	25.6	11.9	34.6	15.0	10.4[a]
2-2.5	23.0	41.5	37.2	26.9	34.3	3.9	13.1
2.5-3	4.6	14.3	23.5	47.6	24.3	6.0	20.5
3-3.5	5.4	7.9	16.7	14.2	17.6	9.2	15.9
3.5-4	76.6	13.5	23.2	34.0	16.0	3.5	14.3
4-4.5	0.8	19.4	20.2	6.4	28.1	7.2	16.1
4.5-5	70.3	6.6	7.7	2.65	12.6	3.3	17.6
5-5.5	6.4	2.5	16.2	2.2	7.6	1.0	6.8
5.5-6	0.2	12.1	17.3	5.9	9.5	9.9	2.8
6-6.5	12.2	40.0	0.95	21.5	4.0	10.1	6.0
6.5-7	0.8	0	2.15	0	1.0	0.5	2.2
7-7.5	9.7	0	0.45	0	1.0	5.5	0.7
7.5-8	0	0	5.65	0	1.0	50.6	32.4
8-8.5	2.2	0	0	0	0.3	0.3	0
8.5-9	0	0	0	0	0.2	0.5	0
9-9.5	0	0	0	0	0.45	3.3	0
$\%\overline{BE}$[#]	104	100	96	89	91	95	95

$\overline{BE}$ = total amount of energy available to the photon from capture in the naturally occurring element.
[#]Does not include small contribution below 1 MeV to binding energy previously determined by others.
[a]Does not include the ~100 1.78-MeV gamma rays following β-decay of 28-Al.

TABLE A-9. (continued)

Energy (MeV)	Copper	Titanium	Zinc	Chlorine	Nickle	Sulfur	Stainless Steel
	Photons/100 captures						
1-1.5	11.3	83.8	52.1	45.2	6.3	1.7	14.5
1.5-2	11.6	25.7	30.5	45.4	2.2	3.1	9.7
2-2.5	6.4	3.6	25.4	14.3	2.2	43.9	6.1
2.5-3	9.3	5.0	18.2	19.3	3.1	22.8	4.4
3-3.5	8.8	6.2	22.8	12.3	2.0	29.4	7.4
3.5-4	8.2	4.6	13.8	9.1	1.6	3.0	3.7
4-4.5	10.5	0.7	14.4	6.5	1.1	7.0	5.8
4.5-5	4.6	9.5	13.9	9.0	1.3	15.3	3.2
5-5.5	9.2	0.4	12.4	3.4	3.4	61.9	3.5
5.5-6	2.3	1.0	10.4	11.7	4.3	3.9	9.4
6-6.5	5.2	33.1	7.4	26.2	4.2	0.4	7.5
6.5-7	9.0	56.0	13.1	18.3	11.2	1.0	4.1
7-7.5	16.0	0.9	5.4	12.4	2.9	1.0	8.5
7.5-8	40.5	0.18	14.1	10.0	10.4	3.5	33.6
8-8.5	0	0.32	1.0	0	7.6	0.5	3.6
8.5-9	0	0	0.1	3.2	48.0	2.0	12.2
9-9.5	0	0.21	1.2	0	0	0	3.7
$\overline{\%BE}$#	101	106	105	108	92	94	96

*Taken from RSIC Newsletter No. 58 (Sept. 1969) based on Ref. 91.

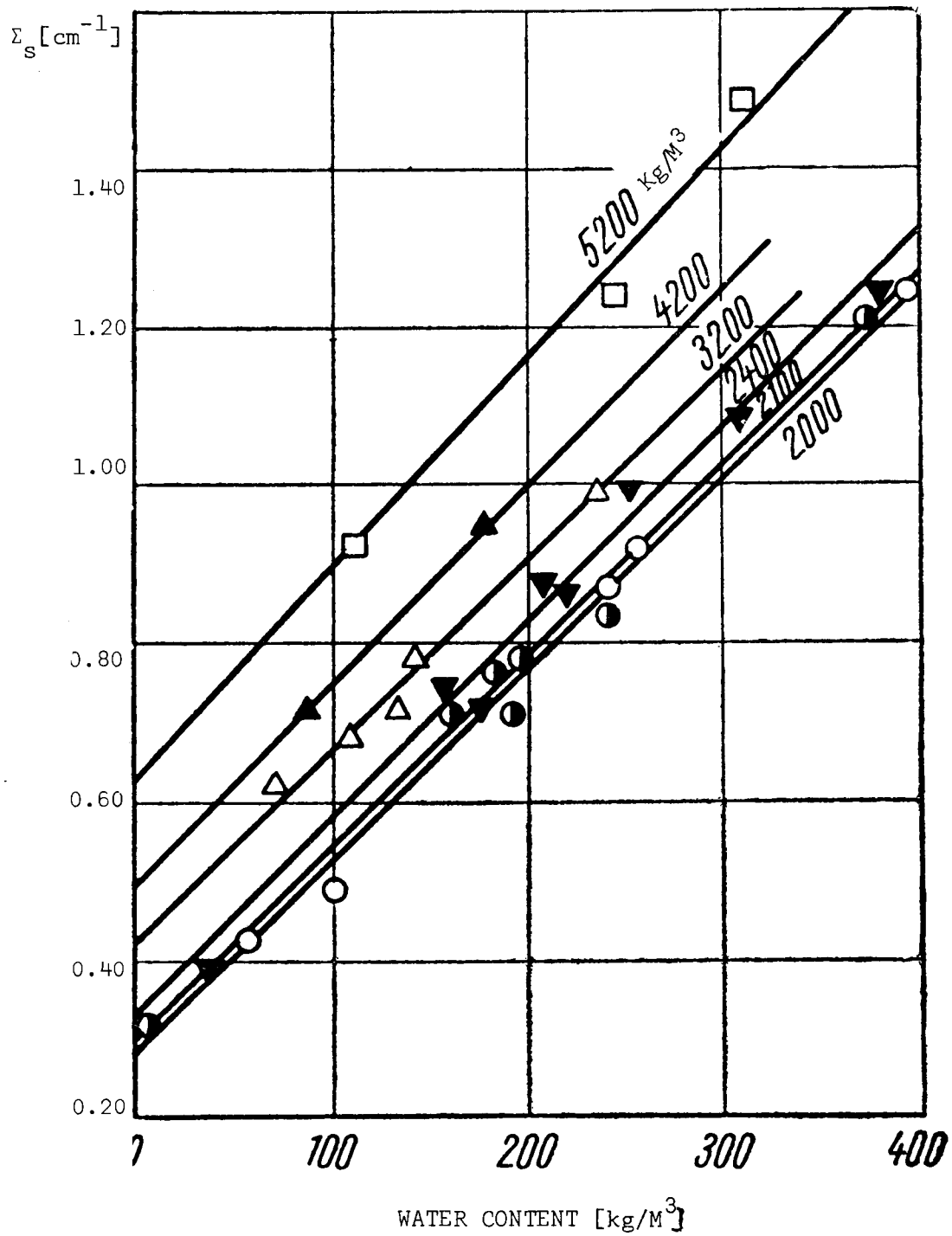

Fig. A-1. Thermal Neutron Elastic Scattering Cross Section for Different Concretes as a Function of the Water Content (From Ref. 17).

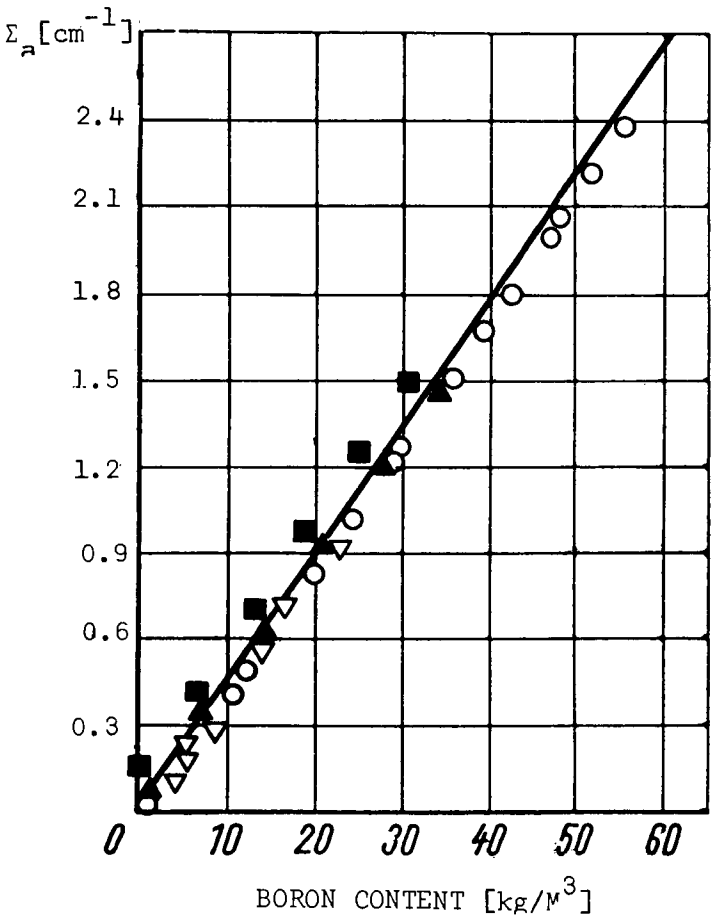

Fig. A-2. Thermal Neutron Absorption Cross Section for Different Concretes as a Function of Boron Centent (From Ref. 17).

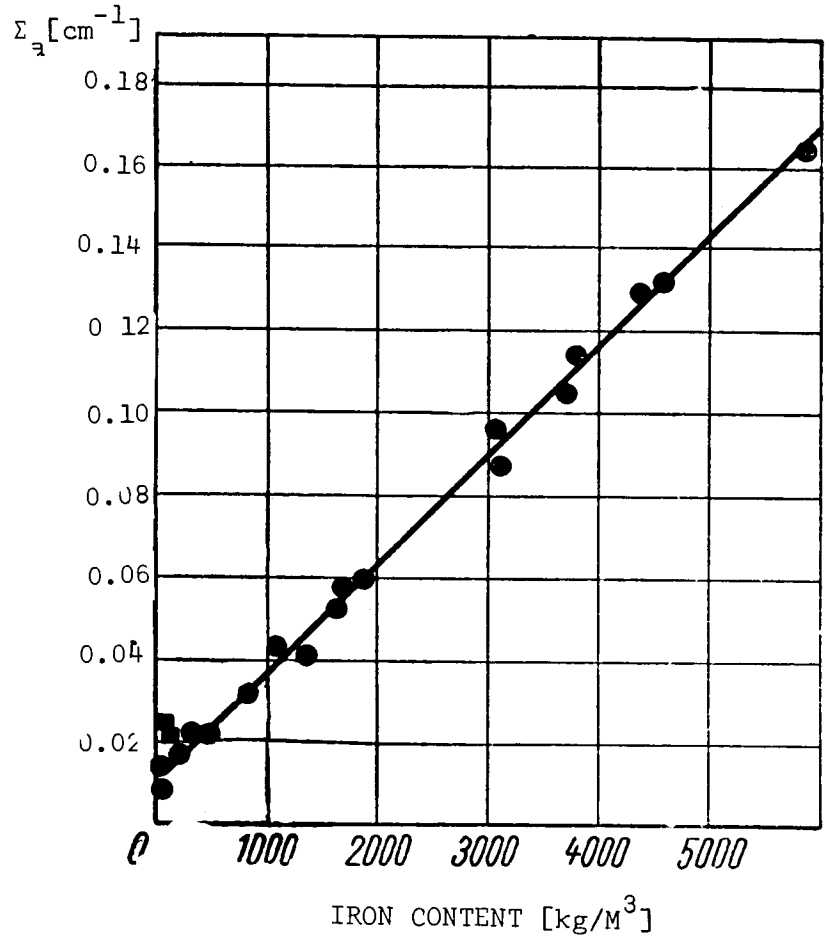

Fig. A-3. Thermal Neutron Absorption Cross Section for Different Concretes as a Function of Iron Content (From Ref. 17)

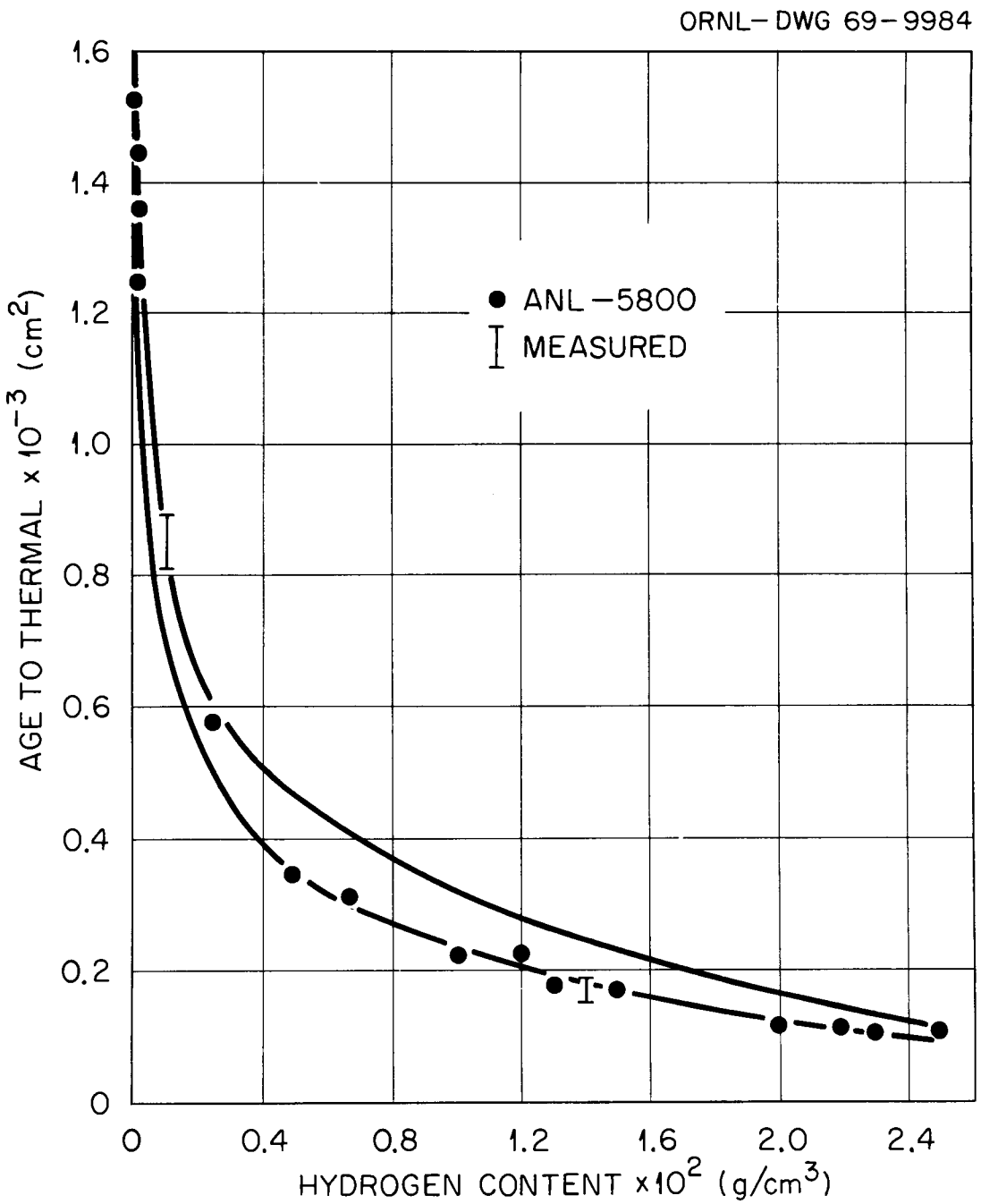

Fig. A-4. Fission Neutron Fermi Age to Thermal Energy for Concrete as a Function of Hydrogen Content (From Ref. 100). Curves Represent Upper and Lower Bounds for Various Concretes.

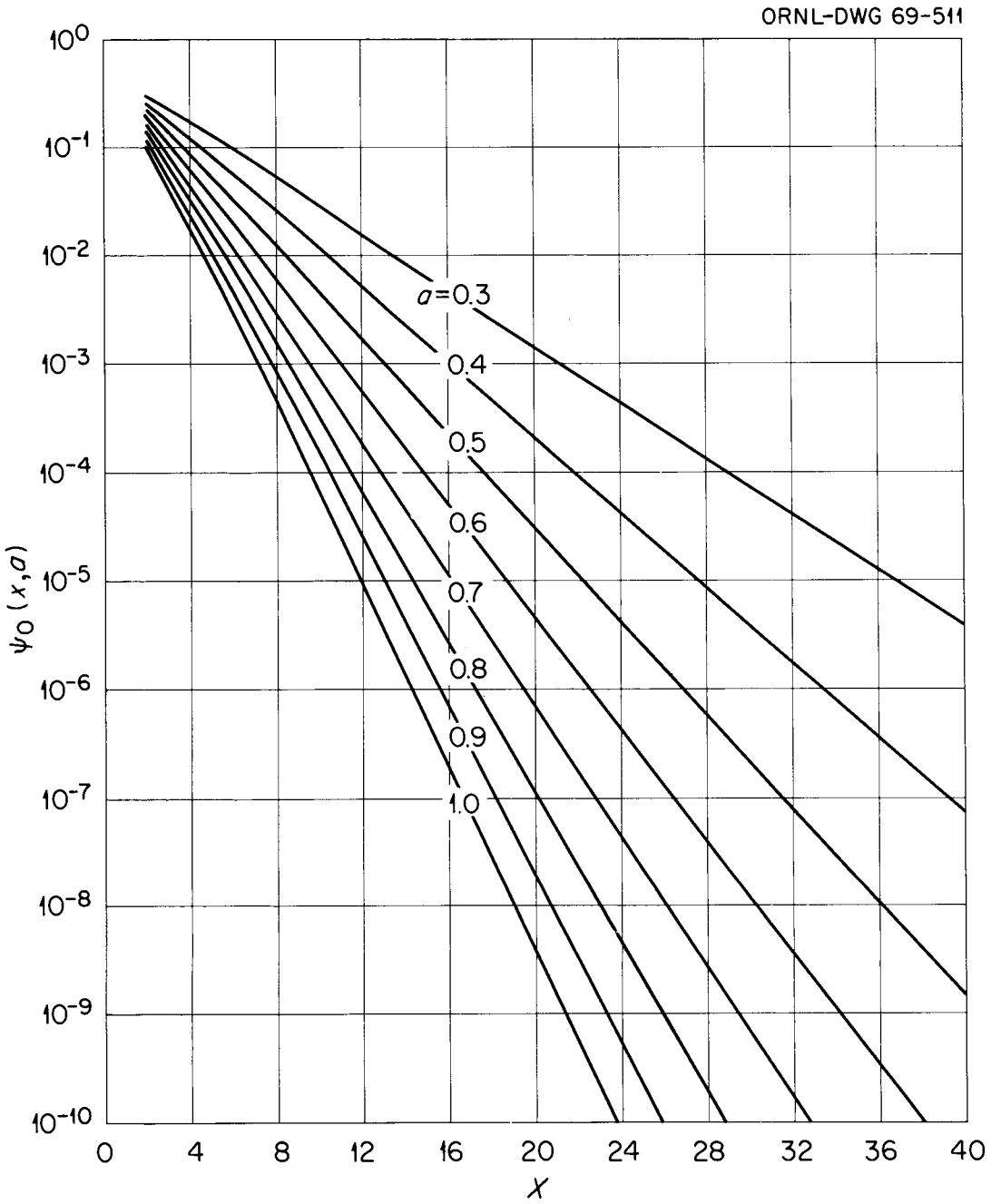

Fig. A-5. Slab Function $\psi_o(x,a)$ For $a \leq 1$.

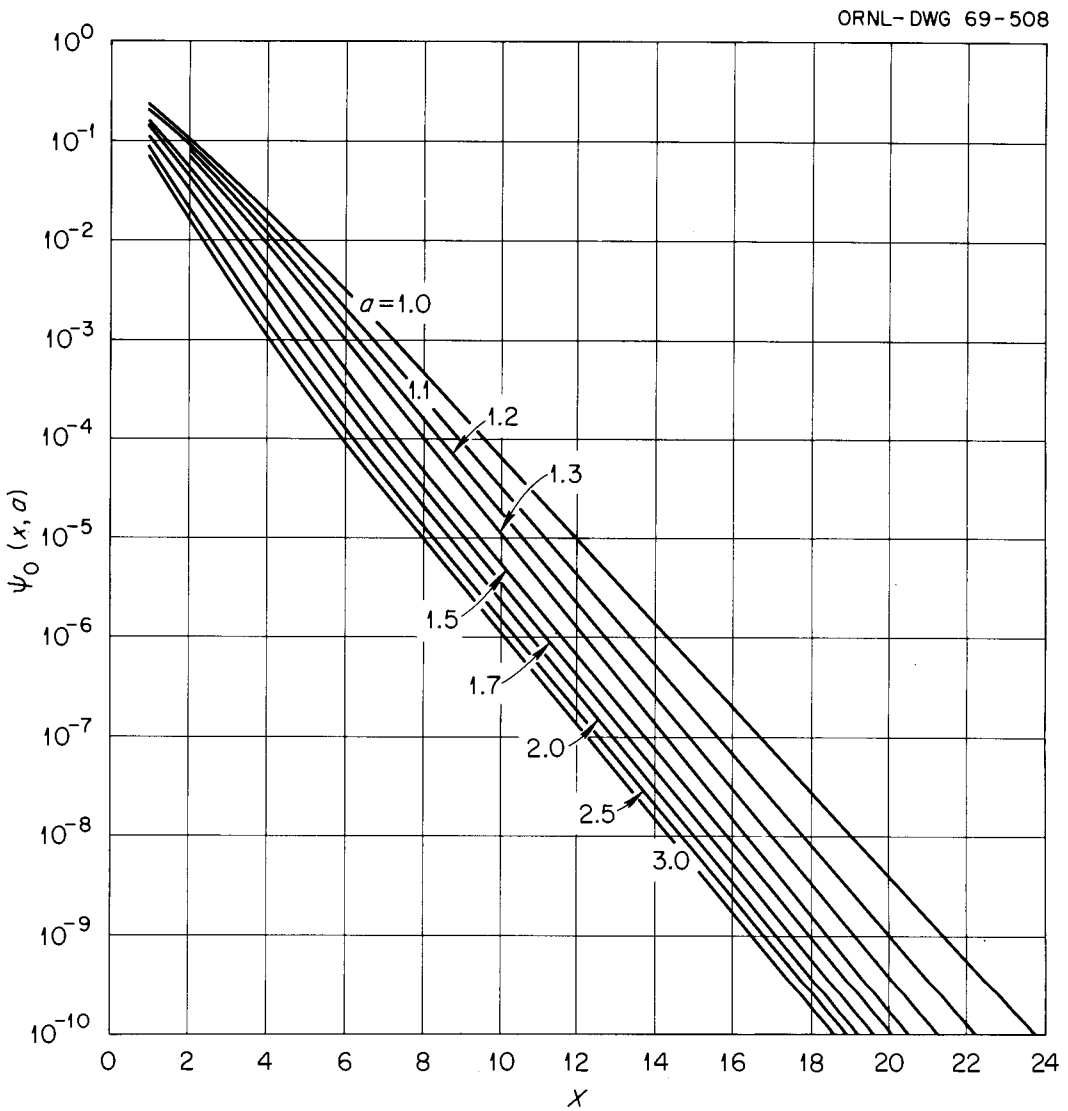

Fig. A-6. Slab Function $\psi_o(x,a)$ For $a \geq 1$.

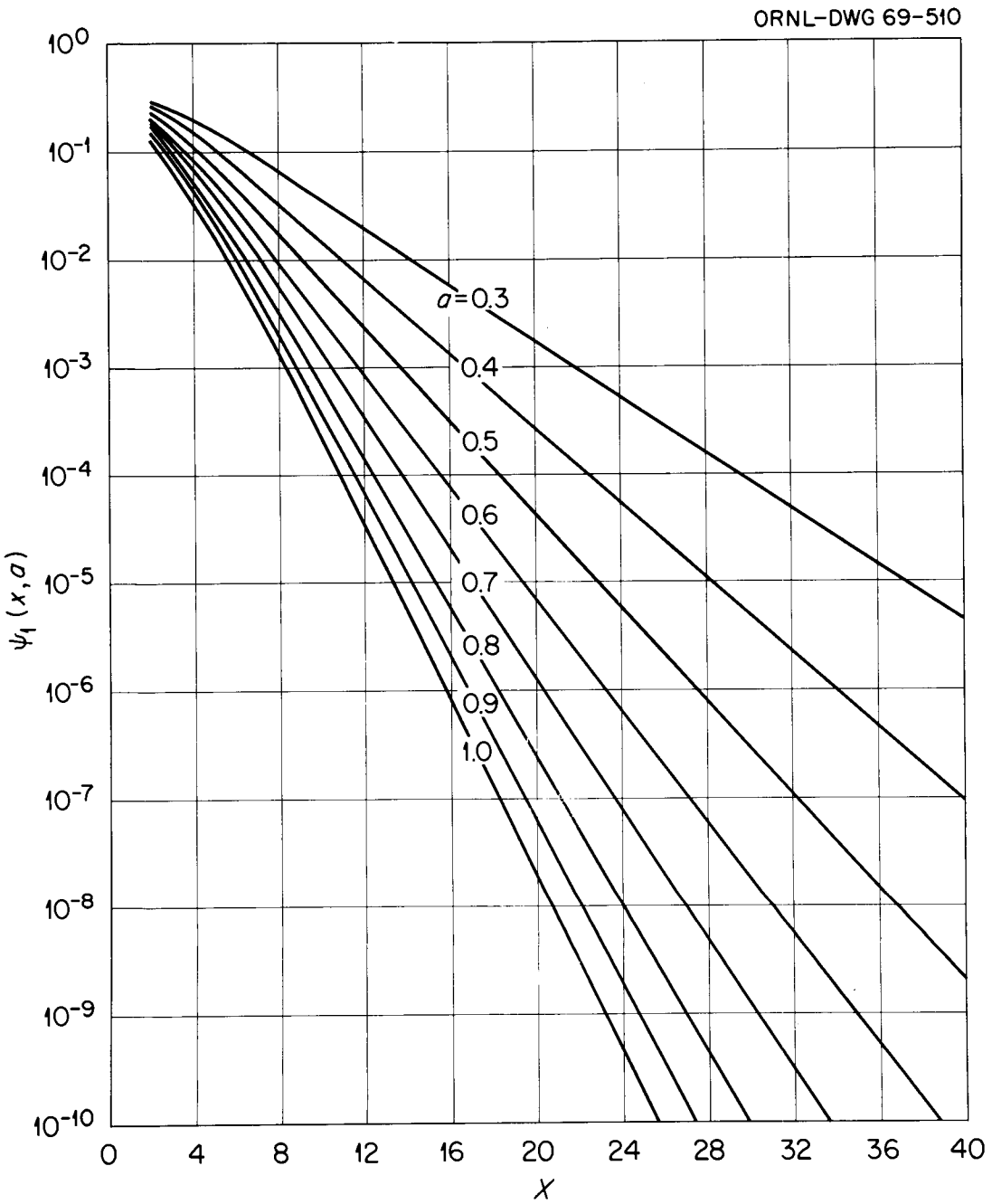

Fig. A-7. Slab Function $\psi_1(x,a)$ For $a \leq 1$.

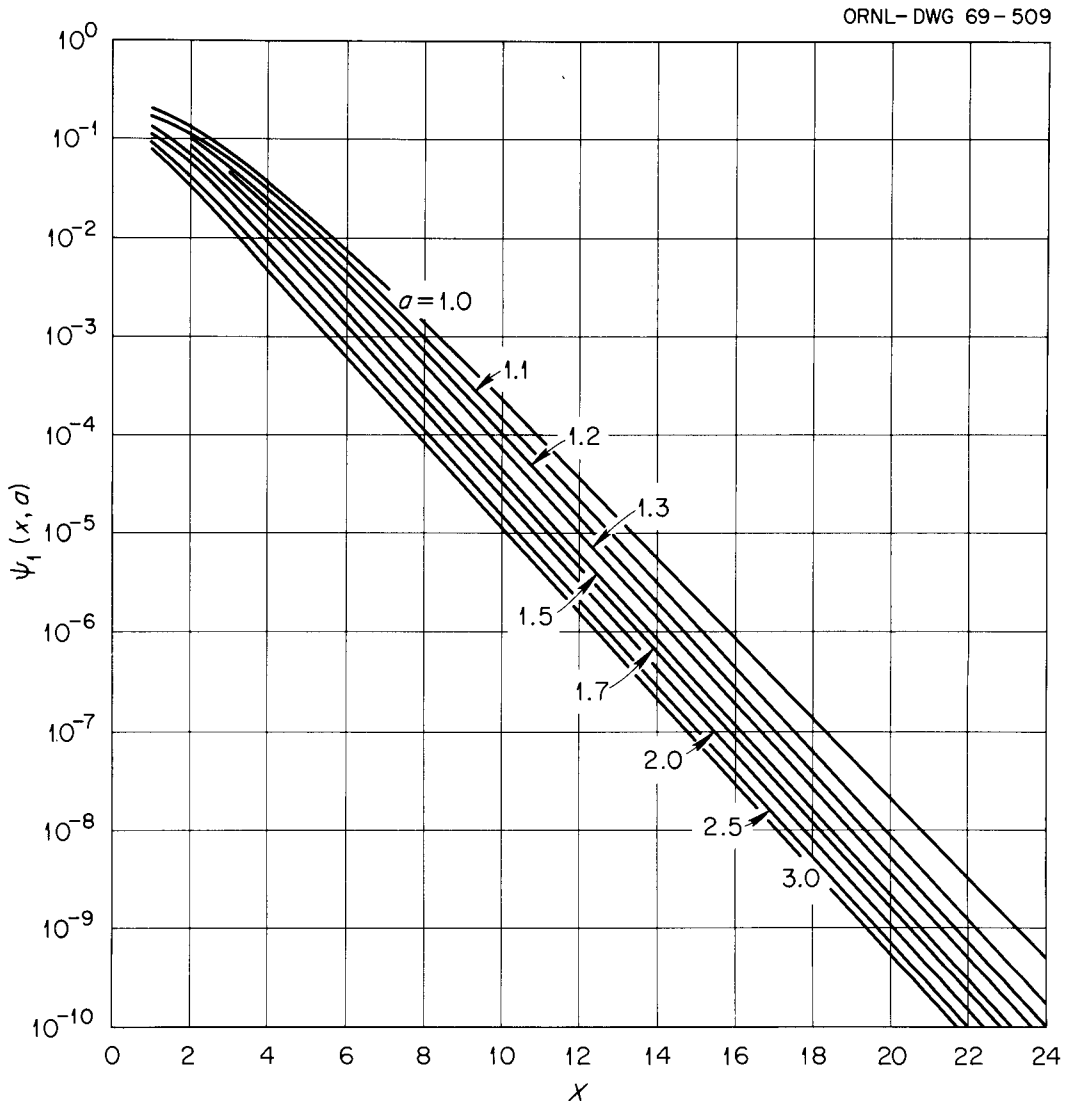

Fig. A-8. Slab Function $\psi_1(x,a)$ For $a \geq 1$.

APPENDIX B

DOSE EQUIVALENT TRANSMISSION FACTORS

TABLE B-1

ENERGY AND ANGULAR DEPENDENT TRANSMISSION FACTORS — NEUTRON DOSE EQUIVALENT 15 CM TSF CONCRETE SLAB

NEUTRON GROUPS (REMS/((SOURCE NEUTRON)/(CM**2)))

ENERGY GROUP (MEV)	ANGLE 1 MU= 0.9894	ANGLE 2 MU= 0.9446	ANGLE 3 MU= 0.8656	ANGLE 4 MU= 0.7550	ANGLE 5 MU= 0.6179	ANGLE 6 MU= 0.4580	ANGLE 7 MU= 0.2816	ANGLE 8 MU= 0.0950	SCALAR ADJOINT
1.22E 01---1.50E 01	3.058E-08	3.039E-08	2.991E-08	2.866E-08	2.573E-08	2.017E-08	1.295E-08	7.819E-09	2.025E-08
1.00E 01---1.22E 01	2.575E-08	2.560E-08	2.520E-08	2.415E-08	2.176E-08	1.734E-08	1.166E-08	7.409E-09	1.742E-08
8.19E 00---1.00E 01	2.495E-08	2.496E-08	2.481E-08	2.406E-08	2.200E-08	1.785E-08	1.211E-08	7.630E-09	1.756E-08
6.36E 00---8.19E 00	2.460E-08	2.462E-08	2.444E-08	2.363E-08	2.151E-08	1.742E-08	1.194E-08	7.662E-09	1.727E-08
4.97E 00---6.36E 00	2.461E-08	2.455E-08	2.423E-08	2.323E-08	2.100E-08	1.707E-08	1.214E-08	8.081E-09	1.718E-08
4.07E 00---4.97E 00	2.438E-08	2.407E-08	2.333E-08	2.186E-08	1.933E-08	1.563E-08	1.151E-08	7.846E-09	1.623E-08
3.01E 00---4.07E 00	2.021E-08	1.981E-08	1.896E-08	1.753E-08	1.540E-08	1.275E-08	1.002E-08	7.349E-09	1.345E-08
2.46E 00---3.01E 00	2.224E-08	2.191E-08	2.117E-08	1.980E-08	1.752E-08	1.425E-08	1.065E-08	7.553E-09	1.486E-08
2.35E 00---2.46E 00	2.434E-08	2.414E-08	2.362E-08	2.246E-08	2.018E-08	1.629E-08	1.122E-08	7.117E-09	1.638E-08
1.83E 00---2.35E 00	1.940E-08	1.896E-08	1.805E-08	1.651E-08	1.418E-08	1.116E-08	8.120E-09	5.600E-09	1.203E-08
1.11E 00---1.83E 00	1.319E-08	1.273E-08	1.184E-08	1.050E-08	8.737E-09	6.791E-09	5.056E-09	3.583E-09	7.644E-09
5.50E-01---1.11E 00	5.883E-09	5.591E-09	5.079E-09	4.385E-09	3.595E-09	2.835E-09	2.174E-09	1.580E-09	3.251E-09
1.11E-01---5.50E-01	1.589E-09	1.508E-09	1.372E-09	1.199E-09	1.013E-09	8.330E-10	6.625E-10	5.070E-10	9.265E-10
3.35E-03---1.11E-01	6.143E-10	5.911E-10	5.511E-10	4.980E-10	4.362E-10	3.697E-10	3.001E-10	2.298E-10	3.941E-10
5.83E-04---3.35E-03	5.205E-10	5.049E-10	4.773E-10	4.389E-10	3.912E-10	3.364E-10	2.758E-10	2.035E-10	3.500E-10
1.01E-04---5.83E-04	4.914E-10	4.761E-10	4.493E-10	4.121E-10	3.663E-10	3.141E-10	2.567E-10	1.956E-10	3.290E-10
2.90E-05---1.01E-04	4.596E-10	4.448E-10	4.190E-10	3.833E-10	3.398E-10	2.904E-10	2.366E-10	1.801E-10	3.051E-10
1.07E-05---2.90E-05	4.297E-10	4.156E-10	3.908E-10	3.567E-10	3.153E-10	2.685E-10	2.180E-10	1.655E-10	2.829E-10
3.06E-06---1.07E-05	3.904E-10	3.772E-10	3.540E-10	3.222E-10	2.837E-10	2.406E-10	1.945E-10	1.471E-10	2.544E-10
1.12E-06---3.06E-06	3.428E-10	3.306E-10	3.094E-10	2.805E-10	2.457E-10	2.070E-10	1.659E-10	1.245E-10	2.199E-10
4.14E-07---1.12E-06	2.844E-10	2.739E-10	2.556E-10	2.308E-10	2.010E-10	1.680E-10	1.330E-10	9.803E-11	1.792E-10
0.0 ---4.14E-07	1.612E-10	1.563E-10	1.476E-10	1.358E-10	1.214E-10	1.048E-10	8.633E-11	7.173E-11	1.103E-10

ENERGY AND ANGULAR DEPENDENT TRANSMISSION FACTORS — NEUTRON PLUS GAMMA-RAY DOSE EQUIVALENT 15 CM TSF CONCRETE SLAB

NEUTRON GROUPS (REMS/((SOURCE NEUTRON)/(CM**2)))

ENERGY GROUP (MEV)	ANGLE 1 MU= 0.9894	ANGLE 2 MU= 0.9446	ANGLE 3 MU= 0.8656	ANGLE 4 MU= 0.7550	ANGLE 5 MU= 0.6179	ANGLE 6 MU= 0.4580	ANGLE 7 MU= 0.2816	ANGLE 8 MU= 0.0950	SCALAR ADJOINT
1.22E 01---1.50E 01	3.096E-08	3.077E-08	3.030E-08	2.906E-08	2.614E-08	2.056E-08	1.329E-08	8.071E-09	2.061E-08
1.00E 01---1.22E 01	2.608E-08	2.593E-08	2.554E-08	2.450E-08	2.211E-08	1.767E-08	1.195E-08	7.625E-09	1.773E-08
8.19E 00---1.00E 01	2.523E-08	2.525E-08	2.510E-08	2.436E-08	2.230E-08	1.814E-08	1.236E-08	7.816E-09	1.782E-08
6.36E 00---8.19E 00	2.478E-08	2.480E-08	2.462E-08	2.382E-08	2.170E-08	1.760E-08	1.210E-08	7.783E-09	1.744E-08
4.97E 00---6.36E 00	2.469E-08	2.464E-08	2.431E-08	2.332E-08	2.108E-08	1.715E-08	1.221E-08	8.132E-09	1.725E-08
4.07E 00---4.97E 00	2.441E-08	2.409E-08	2.335E-08	2.189E-08	1.935E-08	1.566E-08	1.153E-08	7.861E-09	1.625E-08
3.01E 00---4.07E 00	2.022E-08	1.981E-08	1.897E-08	1.753E-08	1.541E-08	1.276E-08	1.002E-08	7.354E-09	1.346E-08
2.46E 00---3.01E 00	2.223E-08	2.190E-08	2.116E-08	1.979E-08	1.751E-08	1.425E-08	1.065E-08	7.552E-09	1.485E-08
2.35E 00---2.46E 00	2.431E-08	2.411E-08	2.359E-08	2.243E-08	2.016E-08	1.627E-08	1.121E-08	7.113E-09	1.637E-08
1.83E 00---2.35E 00	1.938E-08	1.893E-08	1.802E-08	1.649E-08	1.416E-08	1.115E-08	8.113E-09	5.597E-09	1.202E-08
1.11E 00---1.83E 00	1.319E-08	1.272E-08	1.184E-08	1.050E-08	8.742E-09	6.800E-09	5.068E-09	3.594E-09	7.650E-09
5.50E-01---1.11E 00	5.917E-09	5.626E-09	5.115E-09	4.422E-09	3.633E-09	2.871E-09	2.206E-09	1.605E-09	3.285E-09
1.11E-01---5.50E-01	1.668E-09	1.586E-09	1.448E-09	1.271E-09	1.080E-09	8.924E-10	7.126E-10	5.454E-10	9.862E-10
3.35E-03---1.11E-01	7.349E-10	7.095E-10	6.654E-10	6.060E-10	5.354E-10	4.575E-10	3.737E-10	2.863E-10	4.829E-10
5.83E-04---3.35E-03	6.546E-10	6.369E-10	6.051E-10	5.601E-10	5.032E-10	4.359E-10	3.595E-10	2.686E-10	4.503E-10
1.01E-04---5.83E-04	6.523E-10	6.343E-10	6.023E-10	5.570E-10	4.998E-10	4.325E-10	3.564E-10	2.654E-10	4.472E-10
2.90E-05---1.01E-04	6.477E-10	6.296E-10	5.975E-10	5.520E-10	4.948E-10	4.274E-10	3.516E-10	2.609E-10	4.424E-10
1.07E-05---2.90E-05	6.354E-10	6.175E-10	5.856E-10	5.405E-10	4.837E-10	4.170E-10	3.422E-10	2.534E-10	4.322E-10
3.06E-06---1.07E-05	6.054E-10	5.880E-10	5.571E-10	5.135E-10	4.586E-10	3.943E-10	3.224E-10	2.376E-10	4.092E-10
1.12E-06---3.06E-06	5.626E-10	5.461E-10	5.167E-10	4.752E-10	4.231E-10	3.621E-10	2.942E-10	2.147E-10	3.766E-10
4.14E-07---1.12E-06	4.961E-10	4.812E-10	4.547E-10	4.172E-10	3.701E-10	3.150E-10	2.535E-10	1.808E-10	3.279E-10
0.0 ---4.14E-07	3.186E-10	3.102E-10	2.954E-10	2.746E-10	2.484E-10	2.176E-10	1.827E-10	1.235E-10	2.210E-10

TABLE B-2

ENERGY AND ANGULAR DEPENDENT TRANSMISSION FACTORS — NEUTRON DOSE EQUIVALENT 30 CM TSF CONCRETE SLAB

NEUTRON GROUPS (REMS/((SOURCE NEUTRON)/(CM**2)))

ENERGY GROUP (MEV)	ANGLE 1 MU= 0.9894	ANGLE 2 MU= 0.9446	ANGLE 3 MU= 0.8656	ANGLE 4 MU= 0.7550	ANGLE 5 MU= 0.6179	ANGLE 6 MU= 0.4580	ANGLE 7 MU= 0.2816	ANGLE 8 MU= 0.0950	SCALAR ADJOINT
1.22E 01---1.50E 01	1.217E-08	1.160E-08	1.052E-08	8.901E-09	6.859E-09	4.800E-09	3.216E-09	2.076E-09	5.981E-09
1.00E 01---1.22E 01	1.021E-08	9.746E-09	8.875E-09	7.581E-09	5.960E-09	4.321E-09	3.013E-09	2.012E-09	5.228E-09
8.19E 00---1.00E 01	1.035E-08	9.923E-09	9.100E-09	7.833E-09	6.186E-09	4.460E-09	3.065E-09	2.025E-09	5.364E-09
6.36E 00---8.19E 00	1.012E-08	9.690E-09	8.873E-09	7.635E-09	6.056E-09	4.428E-09	3.106E-09	2.090E-09	5.292E-09
4.97E 00---6.36E 00	1.008E-08	9.632E-09	8.804E-09	7.593E-09	6.103E-09	4.588E-09	3.308E-09	2.252E-09	5.377E-09
4.07E 00---4.97E 00	8.953E-09	8.506E-09	7.714E-09	6.629E-09	5.374E-09	4.132E-09	3.034E-09	2.063E-09	4.781E-09
3.01E 00---4.07E 00	5.965E-09	5.669E-09	5.164E-09	4.509E-09	3.785E-09	3.072E-09	2.408E-09	1.768E-09	3.429E-09
2.46E 00---3.01E 00	7.080E-09	6.703E-09	6.043E-09	5.150E-09	4.137E-09	3.168E-09	2.354E-09	1.671E-09	3.728E-09
2.35E 00---2.46E 00	8.595E-09	8.141E-09	7.312E-09	6.121E-09	4.675E-09	3.241E-09	2.129E-09	1.349E-09	4.091E-09
1.83E 00---2.35E 00	4.767E-09	4.458E-09	3.932E-09	3.252E-09	2.525E-09	1.869E-09	1.344E-09	9.196E-10	2.300E-09
1.11E 00---1.83E 00	2.168E-09	2.014E-09	1.763E-09	1.458E-09	1.152E-09	8.834E-10	6.606E-10	4.693E-10	1.065E-09
5.50E-01---1.11E 00	6.070E-10	5.676E-10	5.053E-10	4.316E-10	3.572E-10	2.877E-10	2.240E-10	1.636E-10	3.277E-10
1.11E-01---5.50E-01	1.808E-10	1.732E-10	1.605E-10	1.443E-10	1.260E-10	1.066E-10	8.635E-11	6.498E-11	1.139E-10
3.35E-03---1.11E-01	1.152E-10	1.110E-10	1.039E-10	9.448E-11	8.327E-11	7.087E-11	5.765E-11	4.340E-11	7.490E-11
5.83E-04---3.35E-03	1.091E-10	1.053E-10	9.882E-11	9.004E-11	7.953E-11	6.781E-11	5.522E-11	4.158E-11	7.147E-11
1.01E-04---5.83E-04	9.554E-11	9.216E-11	8.637E-11	7.859E-11	6.931E-11	5.901E-11	4.799E-11	3.610E-11	6.230E-11
2.90E-05---1.01E-04	8.387E-11	8.084E-11	7.567E-11	6.873E-11	6.050E-11	5.140E-11	4.171E-11	3.132E-11	5.437E-11
1.07E-05---2.90E-05	7.531E-11	7.254E-11	6.782E-11	6.151E-11	5.404E-11	4.580E-11	3.707E-11	2.776E-11	4.854E-11
3.06E-06---1.07E-05	6.628E-11	6.381E-11	5.958E-11	5.394E-11	4.728E-11	3.995E-11	3.222E-11	2.403E-11	4.243E-11
1.12E-06---3.06E-06	5.641E-11	5.425E-11	5.057E-11	4.566E-11	3.988E-11	3.353E-11	2.685E-11	1.984E-11	3.571E-11
4.14E-07---1.12E-06	4.589E-11	4.410E-11	4.104E-11	3.696E-11	3.215E-11	2.685E-11	2.126E-11	1.538E-11	2.865E-11
0.0 ---4.14E-07	2.560E-11	2.481E-11	2.345E-11	2.157E-11	1.928E-11	1.665E-11	1.375E-11	1.053E-11	1.737E-11

ENERGY AND ANGULAR DEPENDENT TRANSMISSION FACTORS — NEUTRON PLUS GAMMA-RAY DOSE EQUIVALENT 30 CM TSF CONCRETE SLAB

NEUTRON GROUPS (REMS/((SOURCE NEUTRON)/(CM**2)))

ENERGY GROUP (MEV)	ANGLE 1 MU= 0.9894	ANGLE 2 MU= 0.9446	ANGLE 3 MU= 0.8656	ANGLE 4 MU= 0.7550	ANGLE 5 MU= 0.6179	ANGLE 6 MU= 0.4580	ANGLE 7 MU= 0.2816	ANGLE 8 MU= 0.0950	SCALAR ADJOINT
1.22E 01---1.50E 01	1.245E-08	1.187E-08	1.078E-08	9.148E-09	7.083E-09	4.992E-09	3.369E-09	2.188E-09	6.177E-09
1.00E 01---1.22E 01	1.045E-08	9.980E-09	9.102E-09	7.795E-09	6.155E-09	4.488E-09	3.149E-09	2.113E-09	5.398E-09
8.19E 00---1.00E 01	1.057E-08	1.014E-08	9.311E-09	8.034E-09	6.370E-09	4.619E-09	3.194E-09	2.120E-09	5.525E-09
6.36E 00---8.19E 00	1.028E-08	9.854E-09	9.034E-09	7.789E-09	6.199E-09	4.553E-09	3.208E-09	2.165E-09	5.416E-09
4.97E 00---6.36E 00	1.019E-08	9.747E-09	8.918E-09	7.703E-09	6.206E-09	4.680E-09	3.384E-09	2.307E-09	5.467E-09
4.07E 00---4.97E 00	9.052E-09	8.605E-09	7.812E-09	6.723E-09	5.463E-09	4.212E-09	3.100E-09	2.111E-09	4.858E-09
3.01E 00---4.07E 00	6.064E-09	5.767E-09	5.261E-09	4.602E-09	3.872E-09	3.151E-09	2.474E-09	1.818E-09	3.506E-09
2.46E 00---3.01E 00	7.201E-09	6.823E-09	6.161E-09	5.265E-09	4.247E-09	3.268E-09	2.438E-09	1.733E-09	3.825E-09
2.35E 00---2.46E 00	8.725E-09	8.273E-09	7.444E-09	6.253E-09	4.803E-09	3.359E-09	2.229E-09	1.420E-09	4.202E-09
1.83E 00---2.35E 00	4.905E-09	4.596E-09	4.068E-09	3.384E-09	2.648E-09	1.980E-09	1.435E-09	9.866E-10	2.408E-09
1.11E 00---1.83E 00	2.310E-09	2.154E-09	1.899E-09	1.587E-09	1.271E-09	9.884E-10	7.471E-10	5.332E-10	1.170E-09
5.50E-01---1.11E 00	7.424E-10	7.000E-10	6.321E-10	5.502E-10	4.646E-10	3.811E-10	3.008E-10	2.209E-10	4.232E-10
1.11E-01---5.50E-01	2.928E-10	2.823E-10	2.646E-10	2.412E-10	2.136E-10	1.828E-10	1.495E-10	1.130E-10	1.924E-10
3.35E-03---1.11E-01	2.331E-10	2.258E-10	2.132E-10	1.958E-10	1.745E-10	1.501E-10	1.231E-10	9.304E-11	1.567E-10
5.83E-04---3.35E-03	2.395E-10	2.323E-10	2.195E-10	2.019E-10	1.802E-10	1.551E-10	1.273E-10	9.623E-11	1.617E-10
1.01E-04---5.83E-04	2.271E-10	2.201E-10	2.079E-10	1.911E-10	1.704E-10	1.465E-10	1.201E-10	9.076E-11	1.529E-10
2.90E-05---1.01E-04	2.155E-10	2.088E-10	1.971E-10	1.810E-10	1.612E-10	1.384E-10	1.133E-10	8.543E-11	1.445E-10
1.07E-05---2.90E-05	2.047E-10	1.982E-10	1.870E-10	1.715E-10	1.525E-10	1.307E-10	1.068E-10	8.033E-11	1.367E-10
3.06E-06---1.07E-05	1.897E-10	1.836E-10	1.731E-10	1.586E-10	1.408E-10	1.204E-10	9.800E-11	7.345E-11	1.260E-10
1.12E-06---3.06E-06	1.710E-10	1.655E-10	1.558E-10	1.425E-10	1.262E-10	1.075E-10	8.703E-11	6.468E-11	1.127E-10
4.14E-07---1.12E-06	1.472E-10	1.424E-10	1.339E-10	1.223E-10	1.080E-10	9.158E-11	7.343E-11	5.355E-11	9.606E-11
0.0 ---4.14E-07	9.130E-11	8.882E-11	8.448E-11	7.841E-11	7.081E-11	6.187E-11	5.171E-11	4.005E-11	6.390E-11

TABLE B-3

ENERGY AND ANGULAR DEPENDENT TRANSMISSION FACTORS — NEUTRON DOSE EQUIVALENT 50 CM TSF CONCRETE SLAB

NEUTRON GROUPS (REMS/((SOURCE NEUTRON)/(CM**2)))

ENERGY GROUP (MEV)	ANGLE 1 MU= 0.9894	ANGLE 2 MU= 0.9446	ANGLE 3 MU= 0.8656	ANGLE 4 MU= 0.7550	ANGLE 5 MU= 0.6179	ANGLE 6 MU= 0.4580	ANGLE 7 MU= 0.2816	ANGLE 8 MU= 0.0950	SCALAR ADJOINT
1.22E 01---1.50E 01	3.027E-09	2.756E-09	2.312E-09	1.778E-09	1.265E-09	8.624E-10	5.805E-10	3.773E-10	1.208E-09
1.00E 01---1.22E 01	2.464E-09	2.253E-09	1.909E-09	1.494E-09	1.093E-09	7.712E-10	5.369E-10	3.605E-10	1.035E-09
8.19E 00---1.00E 01	2.609E-09	2.388E-09	2.023E-09	1.575E-09	1.136E-09	7.847E-10	5.363E-10	3.563E-10	1.076E-09
6.36E 00---8.19E 00	2.519E-09	2.310E-09	1.966E-09	1.547E-09	1.137E-09	8.048E-10	5.630E-10	3.815E-10	1.073E-09
4.97E 00---6.36E 00	2.391E-09	2.199E-09	1.886E-09	1.508E-09	1.136E-09	8.232E-10	5.825E-10	3.937E-10	1.059E-09
4.07E 00---4.97E 00	1.762E-09	1.625E-09	1.404E-09	1.143E-09	8.837E-10	6.573E-10	4.711E-10	3.159E-10	8.143E-10
3.01E 00---4.07E 00	9.023E-10	8.438E-10	7.507E-10	6.395E-10	5.261E-10	4.208E-10	3.267E-10	2.394E-10	4.831E-10
2.46E 00---3.01E 00	1.140E-09	1.044E-09	8.915E-10	7.151E-10	5.470E-10	4.067E-10	2.965E-10	2.083E-10	5.141E-10
2.35E 00---2.46E 00	1.580E-09	1.418E-09	1.157E-09	8.513E-10	5.689E-10	3.601E-10	2.259E-10	1.390E-10	5.610E-10
1.83E 00---2.35E 00	5.447E-10	4.912E-10	4.092E-10	3.182E-10	2.359E-10	1.703E-10	1.204E-10	8.154E-11	2.255E-10
1.11E 00---1.83E 00	1.672E-10	1.527E-10	1.309E-10	1.068E-10	8.426E-11	6.497E-11	4.881E-11	3.476E-11	7.890E-11
5.50E-01---1.11E 00	4.119E-11	3.889E-11	3.523E-11	3.080E-11	2.609E-11	2.141E-11	1.687E-11	1.238E-11	2.368E-11
1.11E-01---5.50E-01	1.668E-11	1.604E-11	1.495E-11	1.353E-11	1.187E-11	1.007E-11	8.179E-12	6.159E-12	1.070E-11
3.35E-03---1.11E-01	1.148E-11	1.105E-11	1.032E-11	9.356E-12	8.221E-12	6.977E-12	5.663E-12	4.258E-12	7.399E-12
5.83E-04---3.35E-03	1.044E-11	1.006E-11	9.410E-12	8.546E-12	7.525E-12	6.399E-12	5.200E-12	3.911E-12	6.769E-12
1.01E-04---5.83E-04	8.876E-12	8.551E-12	7.999E-12	7.262E-12	6.391E-12	5.431E-12	4.411E-12	3.316E-12	5.748E-12
2.90E-05---1.01E-04	7.640E-12	7.359E-12	6.879E-12	6.240E-12	5.486E-12	4.656E-12	3.776E-12	2.834E-12	4.933E-12
1.07E-05---2.90E-05	6.800E-12	6.546E-12	6.115E-12	5.542E-12	4.865E-12	4.121E-12	3.334E-12	2.496E-12	4.371E-12
3.06E-06---1.07E-05	5.956E-12	5.732E-12	5.349E-12	4.841E-12	4.241E-12	3.582E-12	2.888E-12	2.154E-12	3.807E-12
1.12E-06---3.06E-06	5.051E-12	4.856E-12	4.526E-12	4.086E-12	3.567E-12	2.999E-12	2.402E-12	1.774E-12	3.195E-12
4.14E-07---1.12E-06	4.103E-12	3.942E-12	3.669E-12	3.304E-12	2.874E-12	2.400E-12	1.900E-12	1.375E-12	2.561E-12
0.0 ---4.14E-07	2.287E-12	2.217E-12	2.095E-12	1.927E-12	1.723E-12	1.488E-12	1.229E-12	9.410E-13	1.552E-12

ENERGY AND ANGULAR DEPENDENT TRANSMISSION FACTORS — NEUTRON PLUS GAMMA-RAY DOSE EQUIVALENT 50 CM TSF CONCRETE SLAB

NEUTRON GROUPS (REMS/((SOURCE NEUTRON)/(CM**2)))

ENERGY GROUP (MEV)	ANGLE 1 MU= 0.9894	ANGLE 2 MU= 0.9446	ANGLE 3 MU= 0.8656	ANGLE 4 MU= 0.7550	ANGLE 5 MU= 0.6179	ANGLE 6 MU= 0.4580	ANGLE 7 MU= 0.2816	ANGLE 8 MU= 0.0950	SCALAR ADJOINT
1.22E 01---1.50E 01	3.167E-09	2.890E-09	2.438E-09	1.891E-09	1.362E-09	9.426E-10	6.430E-10	4.218E-10	1.294E-09
1.00E 01---1.22E 01	2.588E-09	2.373E-09	2.021E-09	1.596E-09	1.181E-09	8.445E-10	5.949E-10	4.024E-10	1.114E-09
8.19E 00---1.00E 01	2.733E-09	2.509E-09	2.136E-09	1.679E-09	1.226E-09	8.597E-10	5.951E-10	3.983E-10	1.156E-09
6.36E 00---8.19E 00	2.626E-09	2.413E-09	2.064E-09	1.636E-09	1.216E-09	8.711E-10	6.152E-10	4.186E-10	1.143E-09
4.97E 00---6.36E 00	2.485E-09	2.291E-09	1.974E-09	1.590E-09	1.208E-09	8.848E-10	6.313E-10	4.284E-10	1.123E-09
4.07E 00---4.97E 00	1.857E-09	1.717E-09	1.493E-09	1.224E-09	9.565E-10	7.190E-10	5.201E-10	3.506E-10	8.781E-10
3.01E 00---4.07E 00	9.888E-10	9.281E-10	8.310E-10	7.141E-10	5.931E-10	4.787E-10	3.741E-10	2.749E-10	5.428E-10
2.46E 00---3.01E 00	1.248E-09	1.149E-09	9.919E-10	8.079E-10	6.296E-10	4.771E-10	3.530E-10	2.497E-10	5.871E-10
2.35E 00---2.46E 00	1.708E-09	1.543E-09	1.277E-09	9.620E-10	6.670E-10	4.419E-10	2.889E-10	1.820E-10	6.456E-10
1.83E 00---2.35E 00	6.510E-10	5.943E-10	5.066E-10	4.075E-10	3.145E-10	2.362E-10	1.725E-10	1.188E-10	2.947E-10
1.11E 00---1.83E 00	2.513E-10	2.341E-10	2.075E-10	1.767E-10	1.459E-10	1.170E-10	9.041E-11	6.507E-11	1.336E-10
5.50E-01---1.11E 00	1.014E-10	9.721E-11	9.017E-11	8.107E-11	7.061E-11	5.933E-11	4.757E-11	3.514E-11	6.343E-11
1.11E-01---5.50E-01	5.705E-11	5.519E-11	5.198E-11	4.762E-11	4.233E-11	3.632E-11	2.976E-11	2.251E-11	3.804E-11
3.35E-03---1.11E-01	4.806E-11	4.651E-11	4.383E-11	4.017E-11	3.572E-11	3.064E-11	2.509E-11	1.895E-11	3.208E-11
5.83E-04---3.35E-03	4.794E-11	4.642E-11	4.379E-11	4.018E-11	3.576E-11	3.071E-11	2.516E-11	1.901E-11	3.211E-11
1.01E-04---5.83E-04	4.450E-11	4.309E-11	4.064E-11	3.728E-11	3.317E-11	2.848E-11	2.332E-11	1.761E-11	2.978E-11
2.90E-05---1.01E-04	4.159E-11	4.026E-11	3.796E-11	3.481E-11	3.095E-11	2.655E-11	2.171E-11	1.637E-11	2.777E-11
1.07E-05---2.90E-05	3.917E-11	3.792E-11	3.573E-11	3.274E-11	2.909E-11	2.492E-11	2.034E-11	1.530E-11	2.609E-11
3.06E-06---1.07E-05	3.611E-11	3.495E-11	3.292E-11	3.014E-11	2.674E-11	2.286E-11	1.861E-11	1.395E-11	2.395E-11
1.12E-06---3.06E-06	3.243E-11	3.137E-11	2.953E-11	2.700E-11	2.391E-11	2.037E-11	1.649E-11	1.226E-11	2.136E-11
4.14E-07---1.12E-06	2.786E-11	2.695E-11	2.535E-11	2.315E-11	2.045E-11	1.734E-11	1.391E-11	1.015E-11	1.819E-11
0.0 ---4.14E-07	1.729E-11	1.683E-11	1.601E-11	1.486E-11	1.343E-11	1.174E-11	9.818E-12	7.611E-12	1.212E-11

TABLE B-4

ENERGY AND ANGULAR DEPENDENT TRANSMISSION FACTORS — NEUTRON DOSE EQUIVALENT 75 CM TSF CONCRETE SLAB

NEUTRON GROUPS (REMS/((SOURCE NEUTRON)/(CM**2)))

ENERGY GROUP (MEV)	ANGLE 1 MU= 0.9894	ANGLE 2 MU= 0.9446	ANGLE 3 MU= 0.8656	ANGLE 4 MU= 0.7550	ANGLE 5 MU= 0.6179	ANGLE 6 MU= 0.4580	ANGLE 7 MU= 0.2816	ANGLE 8 MU= 0.0950	SCALAR ADJOINT
1.22E 01---1.50E 01	4.586E-10	4.009E-10	3.156E-10	2.267E-10	1.534E-10	1.018E-10	6.751E-11	4.377E-11	1.565E-10
1.00E 01---1.22E 01	3.538E-10	3.113E-10	2.485E-10	1.826E-10	1.274E-10	8.748E-11	6.018E-11	4.048E-11	1.279E-10
8.19E 00---1.00E 01	3.927E-10	3.442E-10	2.720E-10	1.961E-10	1.331E-10	8.890E-11	5.988E-11	3.992E-11	1.359E-10
6.36E 00---8.19E 00	3.721E-10	3.283E-10	2.629E-10	1.938E-10	1.354E-10	9.299E-11	6.404E-11	4.340E-11	1.356E-10
4.97E 00---6.36E 00	3.212E-10	2.858E-10	2.327E-10	1.757E-10	1.259E-10	8.786E-11	6.052E-11	4.039E-11	1.229E-10
4.07E 00---4.97E 00	1.832E-10	1.650E-10	1.376E-10	1.076E-10	8.021E-11	5.786E-11	4.052E-11	2.679E-11	7.600E-11
3.01E 00---4.07E 00	7.113E-11	6.594E-11	5.792E-11	4.867E-11	3.954E-11	3.131E-11	2.416E-11	1.768E-11	3.659E-11
2.46E 00---3.01E 00	9.423E-11	8.408E-11	6.920E-11	5.351E-11	3.980E-11	2.900E-11	2.081E-11	1.448E-11	3.845E-11
2.35E 00---2.46E 00	1.529E-10	1.291E-10	9.527E-11	6.218E-11	3.750E-11	2.218E-11	1.323E-11	7.841E-12	4.227E-11
1.83E 00---2.35E 00	3.020E-11	2.655E-11	2.137E-11	1.614E-11	1.174E-11	8.370E-12	5.865E-12	3.948E-12	1.151E-11
1.11E 00---1.83E 00	7.015E-12	6.408E-12	5.510E-12	4.532E-12	3.611E-12	2.807E-12	2.119E-12	1.512E-12	3.367E-12
5.50E-01---1.11E 00	1.914E-12	1.815E-12	1.656E-12	1.457E-12	1.241E-12	1.022E-12	8.073E-13	5.925E-13	1.122E-12
1.11E-01---5.50E-01	8.344E-13	8.020E-13	7.473E-13	6.756E-13	5.922E-13	5.019E-13	4.073E-13	3.066E-13	5.338E-13
3.35E-03---1.11E-01	5.679E-13	5.464E-13	5.098E-13	4.616E-13	4.052E-13	3.436E-13	2.787E-13	2.095E-13	3.648E-13
5.83E-04---3.35E-03	5.086E-13	4.900E-13	4.583E-13	4.161E-13	3.662E-13	3.113E-13	2.530E-13	1.903E-13	3.295E-13
1.01E-04---5.83E-04	4.311E-13	4.153E-13	3.884E-13	3.526E-13	3.103E-13	2.637E-13	2.142E-13	1.610E-13	2.791E-13
2.90E-05---1.01E-04	3.707E-13	3.570E-13	3.338E-13	3.028E-13	2.662E-13	2.259E-13	1.832E-13	1.375E-13	2.394E-13
1.07E-05---2.90E-05	3.299E-13	3.177E-13	2.968E-13	2.690E-13	2.361E-13	2.001E-13	1.619E-13	1.212E-13	2.122E-13
3.06E-06---1.07E-05	2.891E-13	2.783E-13	2.597E-13	2.351E-13	2.060E-13	1.740E-13	1.403E-13	1.046E-13	1.849E-13
1.12E-06---3.06E-06	2.454E-13	2.360E-13	2.199E-13	1.986E-13	1.734E-13	1.458E-13	1.168E-13	8.627E-14	1.553E-13
4.14E-07---1.12E-06	1.995E-13	1.917E-13	1.784E-13	1.607E-13	1.398E-13	1.168E-13	9.246E-14	6.689E-14	1.246E-13
0.0 ---4.14E-07	1.114E-13	1.079E-13	1.020E-13	9.385E-14	8.387E-14	7.245E-14	5.982E-14	7.909E-14	8.185E-14

ENERGY AND ANGULAR DEPENDENT TRANSMISSION FACTORS — NEUTRON PLUS GAMMA-RAY DOSE EQUIVALENT 75 CM TSF CONCRETE SLAB

NEUTRON GROUPS (REMS/((SOURCE NEUTRON)/(CM**2)))

ENERGY GROUP (MEV)	ANGLE 1 MU= 0.9894	ANGLE 2 MU= 0.9446	ANGLE 3 MU= 0.8656	ANGLE 4 MU= 0.7550	ANGLE 5 MU= 0.6179	ANGLE 6 MU= 0.4580	ANGLE 7 MU= 0.2816	ANGLE 8 MU= 0.0950	SCALAR ADJOINT
1.22E 01---1.50E 01	5.010E-10	4.413E-10	3.522E-10	2.582E-10	1.793E-10	1.223E-10	8.309E-11	5.464E-11	1.798E-10
1.00E 01---1.22E 01	3.917E-10	3.474E-10	2.813E-10	2.111E-10	1.512E-10	1.066E-10	7.485E-11	5.090E-11	1.493E-10
8.19E 00---1.00E 01	4.324E-10	3.821E-10	3.064E-10	2.259E-10	1.578E-10	1.085E-10	7.477E-11	5.034E-11	1.580E-10
6.36E 00---8.19E 00	4.076E-10	3.622E-10	2.939E-10	2.208E-10	1.580E-10	1.111E-10	7.780E-11	5.303E-11	1.558E-10
4.97E 00---6.36E 00	3.553E-10	3.183E-10	2.626E-10	2.021E-10	1.482E-10	1.059E-10	7.431E-11	5.003E-11	1.428E-10
4.07E 00---4.97E 00	2.158E-10	1.961E-10	1.663E-10	1.330E-10	1.019E-10	7.551E-11	5.408E-11	3.623E-11	9.523E-11
3.01E 00---4.07E 00	9.644E-11	9.029E-11	8.064E-11	6.920E-11	5.750E-11	4.647E-11	3.638E-11	2.677E-11	5.272E-11
2.46E 00---3.01E 00	1.263E-10	1.147E-10	9.742E-11	7.853E-11	6.114E-11	4.648E-11	3.448E-11	2.437E-11	5.755E-11
2.35E 00---2.46E 00	1.933E-10	1.676E-10	1.302E-10	9.241E-11	6.234E-11	4.153E-11	2.742E-11	1.730E-11	6.422E-11
1.83E 00---2.35E 00	5.669E-11	5.181E-11	4.454E-11	3.657E-11	2.906E-11	2.244E-11	1.672E-11	1.162E-11	2.696E-11
1.11E 00---1.83E 00	2.449E-11	2.315E-11	2.101E-11	1.840E-11	1.558E-11	1.274E-11	9.965E-12	7.202E-12	1.407E-11
5.50E-01---1.11E 00	1.267E-11	1.218E-11	1.135E-11	1.026E-11	8.970E-12	7.561E-12	6.073E-12	4.489E-12	8.041E-12
1.11E-01---5.50E-01	7.466E-12	7.224E-12	6.805E-12	6.234E-12	5.542E-12	4.757E-12	3.898E-12	2.949E-12	4.981E-12
3.35E-03---1.11E-01	6.300E-12	6.098E-12	5.748E-12	5.269E-12	4.687E-12	4.022E-12	3.294E-12	2.489E-12	4.209E-12
5.83E-04---3.35E-03	6.307E-12	6.109E-12	5.765E-12	5.293E-12	4.715E-12	4.053E-12	3.322E-12	2.511E-12	4.233E-12
1.01E-04---5.83E-04	5.886E-12	5.702E-12	5.382E-12	4.941E-12	4.401E-12	3.782E-12	3.100E-12	2.342E-12	3.951E-12
2.90E-05---1.01E-04	5.537E-12	5.364E-12	5.062E-12	4.646E-12	4.137E-12	3.552E-12	2.908E-12	2.194E-12	3.711E-12
1.07E-05---2.90E-05	5.245E-12	5.080E-12	4.793E-12	4.397E-12	3.912E-12	3.355E-12	2.742E-12	2.064E-12	3.507E-12
3.06E-06---1.07E-05	4.861E-12	4.707E-12	4.439E-12	4.070E-12	3.616E-12	3.096E-12	2.524E-12	1.893E-12	3.239E-12
1.12E-06---3.06E-06	4.393E-12	4.253E-12	4.009E-12	3.671E-12	3.256E-12	2.779E-12	2.253E-12	1.676E-12	2.909E-12
4.14E-07---1.12E-06	3.799E-12	3.677E-12	3.463E-12	3.169E-12	2.805E-12	2.383E-12	1.915E-12	1.399E-12	2.494E-12
0.0 ---4.14E-07	2.392E-12	2.329E-12	2.217E-12	2.061E-12	1.865E-12	1.633E-12	1.369E-12	1.063E-12	1.684E-12

TABLE B-5

ENERGY AND ANGULAR DEPENDENT TRANSMISSION FACTORS — NEUTRON DOSE EQUIVALENT 100 CM TSF CONCRETE SLAB

NEUTRON GROUPS (REMS/((SOURCE NEUTRON)/(CM**2)))

ENERGY GROUP (MEV)	ANGLE 1 MU= 0.9894	ANGLE 2 MU= 0.9446	ANGLE 3 MU= 0.8656	ANGLE 4 MU= 0.7550	ANGLE 5 MU= 0.6179	ANGLE 6 MU= 0.4580	ANGLE 7 MU= 0.2816	ANGLE 8 MU= 0.0950	SCALAR ADJOINT
1.22E 01---1.50E 01	6.335E-11	5.381E-11	4.058E-11	2.789E-11	1.822E-11	1.178E-11	7.709E-12	4.977E-12	1.948E-11
1.00E 01---1.22E 01	4.601E-11	3.941E-11	3.022E-11	2.132E-11	1.441E-11	9.695E-12	6.613E-12	4.459E-12	1.508E-11
8.19E 00---1.00E 01	5.337E-11	4.530E-11	3.409E-11	2.337E-11	1.525E-11	9.921E-12	6.608E-12	4.419E-12	1.643E-11
6.36E 00---8.19E 00	4.931E-11	4.231E-11	3.249E-11	2.292E-11	1.544E-11	1.032E-11	6.998E-12	4.728E-12	1.615E-11
4.97E 00---6.36E 00	3.792E-11	3.292E-11	2.583E-11	1.873E-11	1.294E-11	8.756E-12	5.894E-12	3.882E-12	1.310E-11
4.07E 00---4.97E 00	1.656E-11	1.467E-11	1.194E-11	9.093E-12	6.613E-12	4.669E-12	3.215E-12	2.102E-12	6.397E-12
3.01E 00---4.07E 00	5.113E-12	4.720E-12	4.120E-12	3.437E-12	2.775E-12	2.186E-12	1.682E-12	1.230E-12	2.578E-12
2.46E 00---3.01E 00	6.989E-12	6.141E-12	4.951E-12	3.759E-12	2.756E-12	1.986E-12	1.412E-12	9.757E-13	2.703E-12
2.35E 00---2.46E 00	1.312E-11	1.051E-11	7.143E-12	4.279E-12	2.417E-12	1.361E-12	7.763E-13	4.429E-13	3.041E-12
1.83E 00---2.35E 00	1.552E-12	1.348E-12	1.069E-12	7.988E-13	5.773E-13	4.098E-13	2.862E-13	1.921E-13	5.717E-13
1.11E 00---1.83E 00	3.171E-13	2.907E-13	2.514E-13	2.081E-13	1.668E-13	1.302E-13	9.855E-14	7.036E-14	1.549E-13
5.50E-01---1.11E 00	9.350E-14	8.872E-14	8.097E-14	7.131E-14	6.076E-14	5.006E-14	3.955E-14	2.903E-14	5.493E-14
1.11E-01---5.50E-01	4.106E-14	3.946E-14	3.677E-14	3.324E-14	2.914E-14	2.469E-14	2.004E-14	1.509E-14	2.627E-14
3.35E-03---1.11E-01	2.794E-14	2.688E-14	2.509E-14	2.272E-14	1.994E-14	1.691E-14	1.372E-14	1.032E-14	1.796E-14
5.83E-04---3.35E-03	2.507E-14	2.415E-14	2.259E-14	2.051E-14	1.806E-14	1.536E-14	1.248E-14	9.386E-15	1.625E-14
1.01E-04---5.83E-04	2.128E-14	2.050E-14	1.917E-14	1.741E-14	1.532E-14	1.302E-14	1.058E-14	7.952E-15	1.378E-14
2.90E-05---1.01E-04	1.832E-14	1.764E-14	1.650E-14	1.497E-14	1.316E-14	1.117E-14	9.059E-15	6.800E-15	1.183E-14
1.07E-05---2.90E-05	1.632E-14	1.571E-14	1.468E-14	1.330E-14	1.168E-14	9.896E-15	8.008E-15	5.995E-15	1.049E-14
3.06E-06---1.07E-05	1.430E-14	1.377E-14	1.285E-14	1.163E-14	1.019E-14	8.610E-15	6.943E-15	5.176E-15	9.147E-15
1.12E-06---3.06E-06	1.214E-14	1.168E-14	1.088E-14	9.827E-15	8.581E-15	7.214E-15	5.778E-15	4.269E-15	7.685E-15
4.14E-07---1.12E-06	9.873E-15	9.487E-15	8.829E-15	7.953E-15	6.917E-15	5.777E-15	4.574E-15	3.309E-15	6.164E-15
0.0 ---4.14E-07	5.507E-15	5.338E-15	5.044E-15	4.641E-15	4.148E-15	3.583E-15	2.959E-15	3.936E-15	4.053E-15

ENERGY AND ANGULAR DEPENDENT TRANSMISSION FACTORS — NEUTRON PLUS GAMMA-RAY DOSE EQUIVALENT 100 CM TSF CONCRETE SLAB

NEUTRON GROUPS (REMS/((SOURCE NEUTRON)/(CM**2)))

ENERGY GROUP (MEV)	ANGLE 1 MU= 0.9894	ANGLE 2 MU= 0.9446	ANGLE 3 MU= 0.8656	ANGLE 4 MU= 0.7550	ANGLE 5 MU= 0.6179	ANGLE 6 MU= 0.4580	ANGLE 7 MU= 0.2816	ANGLE 8 MU= 0.0950	SCALAR ADJOINT
1.22E 01---1.50E 01	7.383E-11	6.350E-11	4.904E-11	3.493E-11	2.385E-11	1.613E-11	1.093E-11	7.197E-12	2.463E-11
1.00E 01---1.22E 01	5.516E-11	4.792E-11	3.772E-11	2.763E-11	1.952E-11	1.369E-11	9.626E-12	6.579E-12	1.975E-11
8.19E 00---1.00E 01	6.313E-11	5.436E-11	4.203E-11	2.998E-11	2.053E-11	1.399E-11	9.627E-12	6.512E-12	2.126E-11
6.36E 00---8.19E 00	5.811E-11	5.051E-11	3.974E-11	2.901E-11	2.035E-11	1.413E-11	9.841E-12	6.705E-12	2.062E-11
4.97E 00---6.36E 00	4.630E-11	4.078E-11	3.284E-11	2.470E-11	1.781E-11	1.257E-11	8.752E-12	5.864E-12	1.750E-11
4.07E 00---4.97E 00	2.385E-11	2.156E-11	1.815E-11	1.446E-11	1.107E-11	8.212E-12	5.893E-12	3.951E-12	1.039E-11
3.01E 00---4.07E 00	1.013E-11	9.518E-12	8.548E-12	7.391E-12	6.191E-12	5.040E-12	3.968E-12	2.926E-12	5.660E-12
2.46E 00---3.01E 00	1.341E-11	1.220E-11	1.043E-11	8.507E-12	6.723E-12	5.181E-12	3.882E-12	2.756E-12	6.289E-12
2.35E 00---2.46E 00	2.164E-11	1.842E-11	1.406E-11	1.001E-11	6.937E-12	4.770E-12	3.226E-12	2.060E-12	7.144E-12
1.83E 00---2.35E 00	6.266E-12	5.803E-12	5.102E-12	4.303E-12	3.507E-12	2.765E-12	2.090E-12	1.464E-12	3.204E-12
1.11E 00---1.83E 00	3.183E-12	3.028E-12	2.774E-12	2.454E-12	2.097E-12	1.728E-12	1.358E-12	9.833E-13	1.885E-12
5.50E-01---1.11E 00	1.792E-12	1.725E-12	1.611E-12	1.459E-12	1.279E-12	1.081E-12	8.695E-13	6.433E-13	1.146E-12
1.11E-01---5.50E-01	1.082E-12	1.048E-12	9.881E-13	9.065E-13	8.071E-13	6.937E-13	5.690E-13	4.307E-13	7.252E-13
3.35E-03---1.11E-01	9.277E-13	8.985E-13	8.479E-13	7.783E-13	6.932E-13	5.958E-13	4.884E-13	3.693E-13	6.225E-13
5.83E-04---3.35E-03	9.458E-13	9.167E-13	8.660E-13	7.961E-13	7.101E-13	6.111E-13	5.015E-13	3.792E-13	6.374E-13
1.01E-04---5.83E-04	8.919E-13	8.646E-13	8.168E-13	7.509E-13	6.698E-13	5.764E-13	4.728E-13	3.574E-13	6.011E-13
2.90E-05---1.01E-04	8.474E-13	8.214E-13	7.759E-13	7.132E-13	6.359E-13	5.468E-13	4.481E-13	3.383E-13	5.704E-13
1.07E-05---2.90E-05	8.084E-13	7.834E-13	7.399E-13	6.798E-13	6.057E-13	5.203E-13	4.257E-13	3.206E-13	5.429E-13
3.06E-06---1.07E-05	7.537E-13	7.303E-13	6.895E-13	6.331E-13	5.635E-13	4.832E-13	3.943E-13	2.959E-13	5.045E-13
1.12E-06---3.06E-06	6.859E-13	6.645E-13	6.271E-13	5.753E-13	5.111E-13	4.370E-13	3.548E-13	2.642E-13	4.566E-13
4.14E-07---1.12E-06	5.971E-13	5.783E-13	5.454E-13	4.999E-13	4.433E-13	3.774E-13	3.039E-13	2.222E-13	3.942E-13
0.0 ---4.14E-07	3.811E-13	3.712E-13	3.537E-13	3.292E-13	2.983E-13	2.616E-13	2.195E-13	1.708E-13	2.695E-13

TABLE B-6

ENERGY AND ANGULAR DEPENDENT TRANSMISSION FACTORS — NEUTRON DOSE EQUIVALENT 150 CM TSF CONCRETE SLAB

NEUTRON GROUPS (REMS/((SOURCE NEUTRON)/(CM**2)))

ENERGY GROUP (MEV)	ANGLE 1 MU= 0.9894	ANGLE 2 MU= 0.9446	ANGLE 3 MU= 0.8656	ANGLE 4 MU= 0.7550	ANGLE 5 MU= 0.6179	ANGLE 6 MU= 0.4580	ANGLE 7 MU= 0.2816	ANGLE 8 MU= 0.0950	SCALAR ADJOINT
1.22E 01---1.50E 01	1.042E-12	8.506E-13	6.060E-13	3.940E-13	2.459E-13	1.536E-13	9.794E-14	6.224E-14	2.805E-13
1.00E 01---1.22E 01	6.700E-13	5.536E-13	4.038E-13	2.717E-13	1.772E-13	1.166E-13	7.869E-14	5.314E-14	1.956E-13
8.19E 00---1.00E 01	8.380E-13	6.803E-13	4.805E-13	3.095E-13	1.921E-13	1.207E-13	7.889E-14	5.271E-14	2.229E-13
6.36E 00---8.19E 00	7.226E-13	5.963E-13	4.330E-13	2.882E-13	1.843E-13	1.182E-13	7.788E-14	5.197E-14	2.055E-13
4.97E 00---6.36E 00	4.273E-13	3.586E-13	2.678E-13	1.842E-13	1.210E-13	7.833E-14	5.086E-14	3.272E-14	1.292E-13
4.07E 00---4.97E 00	1.082E-13	9.389E-14	7.416E-14	5.467E-14	3.855E-14	2.649E-14	1.784E-14	1.149E-14	3.833E-14
3.01E 00---4.07E 00	2.359E-14	2.171E-14	1.886E-14	1.564E-14	1.256E-14	9.857E-15	7.571E-15	5.546E-15	1.172E-14
2.46E 00---3.01E 00	3.361E-14	2.907E-14	2.301E-14	1.722E-14	1.249E-14	8.919E-15	6.289E-15	4.315E-15	1.240E-14
2.35E 00---2.46E 00	8.137E-14	5.978E-14	3.609E-14	1.953E-14	1.024E-14	5.364E-15	2.828E-15	1.490E-15	1.504E-14
1.83E 00---2.35E 00	3.805E-15	3.272E-15	2.570E-15	1.907E-15	1.371E-15	9.697E-16	6.751E-16	4.521E-16	1.367E-15
1.11E 00---1.83E 00	7.066E-16	6.494E-16	5.637E-16	4.681E-16	3.761E-16	2.941E-16	2.229E-16	1.591E-16	3.484E-16
5.50E-01---1.11E 00	2.166E-16	2.055E-16	1.875E-16	1.650E-16	1.405E-16	1.157E-16	9.142E-17	6.709E-17	1.271E-16
1.11E-01---5.50E-01	9.462E-17	9.093E-17	8.471E-17	7.655E-17	6.709E-17	5.684E-17	4.612E-17	3.472E-17	6.048E-17
3.35E-03---1.11E-01	6.418E-17	6.173E-17	5.760E-17	5.215E-17	4.576E-17	3.880E-17	3.147E-17	2.366E-17	4.120E-17
5.83E-04---3.35E-03	5.735E-17	5.525E-17	5.167E-17	4.691E-17	4.129E-17	3.509E-17	2.851E-17	2.144E-17	3.714E-17
1.01E-04---5.83E-04	4.857E-17	4.679E-17	4.376E-17	3.972E-17	3.495E-17	2.970E-17	2.412E-17	1.813E-17	3.144E-17
2.90E-05---1.01E-04	4.173E-17	4.019E-17	3.757E-17	3.408E-17	2.996E-17	2.542E-17	2.062E-17	1.547E-17	2.694E-17
1.07E-05---2.90E-05	3.712E-17	3.574E-17	3.338E-17	3.025E-17	2.655E-17	2.249E-17	1.820E-17	1.362E-17	2.386E-17
3.06E-06---1.07E-05	3.250E-17	3.128E-17	2.919E-17	2.642E-17	2.314E-17	1.955E-17	1.576E-17	1.175E-17	2.077E-17
1.12E-06---3.06E-06	2.756E-17	2.650E-17	2.469E-17	2.229E-17	1.946E-17	1.636E-17	1.310E-17	9.681E-18	1.743E-17
4.14E-07---1.12E-06	2.239E-17	2.151E-17	2.002E-17	1.803E-17	1.568E-17	1.309E-17	1.037E-17	7.502E-18	1.397E-17
0.0 ---4.14E-07	1.248E-17	1.210E-17	1.143E-17	1.052E-17	9.400E-18	8.120E-18	6.707E-18	5.135E-18	8.468E-18

ENERGY AND ANGULAR DEPENDENT TRANSMISSION FACTORS — NEUTRON PLUS GAMMA-RAY DOSE EQUIVALENT 150 CM TSF CONCRETE SLAB

NEUTRON GROUPS (REMS/((SOURCE NEUTRON)/(CM**2)))

ENERGY GROUP (MEV)	ANGLE 1 MU= 0.9894	ANGLE 2 MU= 0.9446	ANGLE 3 MU= 0.8656	ANGLE 4 MU= 0.7550	ANGLE 5 MU= 0.6179	ANGLE 6 MU= 0.4580	ANGLE 7 MU= 0.2816	ANGLE 8 MU= 0.0950	SCALAR ADJOINT
1.22E 01---1.50E 01	1.493E-12	1.259E-12	9.506E-13	6.695E-13	4.582E-13	3.134E-13	2.156E-13	1.440E-13	4.810E-13
1.00E 01---1.22E 01	1.044E-12	8.949E-13	6.956E-13	5.088E-13	3.633E-13	2.593E-13	1.857E-13	1.288E-13	3.702E-13
8.19E 00---1.00E 01	1.245E-12	1.048E-12	7.907E-13	5.568E-13	3.822E-13	2.635E-13	1.840E-13	1.259E-13	4.029E-13
6.36E 00---8.19E 00	1.087E-12	9.280E-13	7.152E-13	5.158E-13	3.611E-13	2.520E-13	1.765E-13	1.205E-13	3.713E-13
4.97E 00---6.36E 00	7.538E-13	6.586E-13	5.272E-13	3.974E-13	2.895E-13	2.073E-13	1.461E-13	9.833E-14	2.848E-13
4.07E 00---4.97E 00	3.544E-13	3.239E-13	2.786E-13	2.284E-13	1.805E-13	1.382E-13	1.016E-13	6.909E-14	1.668E-13
3.01E 00---4.07E 00	1.776E-13	1.686E-13	1.540E-13	1.359E-13	1.162E-13	9.629E-14	7.673E-14	5.684E-14	1.054E-13
2.46E 00---3.01E 00	2.320E-13	2.153E-13	1.900E-13	1.610E-13	1.320E-13	1.050E-13	8.047E-14	5.776E-14	1.210E-13
2.35E 00---2.46E 00	3.562E-13	3.102E-13	2.497E-13	1.924E-13	1.447E-13	1.063E-13	7.534E-14	4.936E-14	1.395E-13
1.83E 00---2.35E 00	1.413E-13	1.331E-13	1.201E-13	1.043E-13	8.724E-14	7.027E-14	5.394E-14	3.806E-14	7.855E-14
1.11E 00---1.83E 00	8.479E-14	8.110E-14	7.494E-14	6.694E-14	5.778E-14	4.800E-14	3.794E-14	2.754E-14	5.174E-14
5.50E-01---1.11E 00	5.165E-14	4.982E-14	4.668E-14	4.245E-14	3.738E-14	3.169E-14	2.557E-14	1.894E-14	3.345E-14
1.11E-01---5.50E-01	3.244E-14	3.144E-14	2.970E-14	2.731E-14	2.437E-14	2.098E-14	1.724E-14	1.306E-14	2.188E-14
3.35E-03---1.11E-01	2.846E-14	2.759E-14	2.607E-14	2.398E-14	2.140E-14	1.842E-14	1.512E-14	1.144E-14	1.920E-14
5.83E-04---3.35E-03	2.972E-14	2.883E-14	2.727E-14	2.510E-14	2.243E-14	1.933E-14	1.588E-14	1.202E-14	2.013E-14
1.01E-04---5.83E-04	2.838E-14	2.753E-14	2.604E-14	2.398E-14	2.142E-14	1.846E-14	1.517E-14	1.147E-14	1.922E-14
2.90E-05---1.01E-04	2.728E-14	2.646E-14	2.503E-14	2.304E-14	2.058E-14	1.772E-14	1.454E-14	1.099E-14	1.845E-14
1.07E-05---2.90E-05	2.624E-14	2.545E-14	2.406E-14	2.214E-14	1.976E-14	1.700E-14	1.393E-14	1.050E-14	1.771E-14
3.06E-06---1.07E-05	2.463E-14	2.388E-14	2.258E-14	2.077E-14	1.851E-14	1.590E-14	1.300E-14	9.762E-15	1.657E-14
1.12E-06---3.06E-06	2.259E-14	2.190E-14	2.070E-14	1.902E-14	1.693E-14	1.450E-14	1.179E-14	8.790E-15	1.512E-14
4.14E-07---1.12E-06	1.980E-14	1.920E-14	1.813E-14	1.665E-14	1.480E-14	1.262E-14	1.018E-14	7.455E-15	1.315E-14
0.0 ---4.14E-07	1.283E-14	1.250E-14	1.192E-14	1.111E-14	1.008E-14	8.856E-15	7.444E-15	5.801E-15	9.110E-15

TABLE B-7

ENERGY AND ANGULAR DEPENDENT TRANSMISSION FACTORS — NEUTRON DOSE EQUIVALENT 200 CM TSF CONCRETE SLAB

NEUTRON GROUPS (REMS/((SOURCE NEUTRON)/(CM**2)))

ENERGY GROUP (MEV)	ANGLE 1 MU= 0.9894	ANGLE 2 MU= 0.9446	ANGLE 3 MU= 0.8656	ANGLE 4 MU= 0.7550	ANGLE 5 MU= 0.6179	ANGLE 6 MU= 0.4580	ANGLE 7 MU= 0.2816	ANGLE 8 MU= 0.0950	SCALAR ADJOINT
1.22E 01---1.50E 01	1.536E-14	1.224E-14	8.433E-15	5.301E-15	3.211E-15	1.957E-15	1.225E-15	7.701E-16	3.823E-15
1.00E 01---1.22E 01	8.826E-15	7.154E-15	5.086E-15	3.341E-15	2.138E-15	1.390E-15	9.345E-16	6.331E-16	2.431E-15
8.19E 00---1.00E 01	1.170E-14	9.243E-15	6.289E-15	3.903E-15	2.345E-15	1.436E-15	9.255E-16	6.166E-16	2.858E-15
6.36E 00---8.19E 00	9.262E-15	7.455E-15	5.229E-15	3.356E-15	2.073E-15	1.289E-15	8.297E-16	5.458E-16	2.415E-15
4.97E 00---6.36E 00	4.140E-15	3.402E-15	2.467E-15	1.645E-15	1.049E-15	6.604E-16	4.185E-16	2.644E-16	1.159E-15
4.07E 00---4.97E 00	6.039E-16	5.182E-16	4.027E-16	2.917E-16	2.023E-16	1.369E-16	9.099E-17	5.809E-17	2.044E-16
3.01E 00---4.07E 00	1.040E-16	9.569E-17	8.307E-17	6.886E-17	5.526E-17	4.338E-17	3.335E-17	2.448E-17	5.160E-17
2.46E 00---3.01E 00	1.520E-16	1.309E-16	1.032E-16	7.709E-17	5.591E-17	3.990E-17	2.810E-17	1.926E-17	5.560E-17
2.35E 00---2.46E 00	4.511E-16	3.111E-16	1.752E-16	9.043E-17	4.567E-17	2.286E-17	1.138E-17	5.622E-18	7.340E-17
1.83E 00---2.35E 00	9.103E-18	7.812E-18	6.124E-18	4.538E-18	3.261E-18	2.305E-18	1.604E-18	1.074E-18	3.256E-18
1.11E 00---1.83E 00	1.660E-18	1.527E-18	1.326E-18	1.102E-18	8.862E-19	6.931E-19	5.254E-19	3.752E-19	8.205E-19
5.50E-01---1.11E 00	5.133E-19	4.870E-19	4.443E-19	3.911E-19	3.331E-19	2.743E-19	2.167E-19	1.590E-19	3.012E-19
1.11E-01---5.50E-01	2.242E-19	2.155E-19	2.008E-19	1.814E-19	1.590E-19	1.347E-19	1.093E-19	8.228E-20	1.433E-19
3.35E-03---1.11E-01	1.521E-19	1.463E-19	1.365E-19	1.236E-19	1.085E-19	9.196E-20	7.459E-20	5.607E-20	9.766E-20
5.83E-04---3.35E-03	1.359E-19	1.309E-19	1.225E-19	1.112E-19	9.786E-20	8.318E-20	6.759E-20	5.083E-20	8.803E-20
1.01E-04---5.83E-04	1.151E-19	1.109E-19	1.037E-19	9.416E-20	8.285E-20	7.039E-20	5.717E-20	4.297E-20	7.452E-20
2.90E-05---1.01E-04	9.893E-20	9.528E-20	8.907E-20	8.079E-20	7.102E-20	6.027E-20	4.887E-20	3.668E-20	6.385E-20
1.07E-05---2.90E-05	8.799E-20	8.472E-20	7.914E-20	7.171E-20	6.295E-20	5.332E-20	4.314E-20	3.230E-20	5.657E-20
3.06E-06---1.07E-05	7.706E-20	7.416E-20	6.921E-20	6.263E-20	5.487E-20	4.635E-20	3.737E-20	2.786E-20	4.925E-20
1.12E-06---3.06E-06	6.534E-20	6.283E-20	5.855E-20	5.286E-20	4.615E-20	3.879E-20	3.107E-20	2.295E-20	4.133E-20
4.14E-07---1.12E-06	5.308E-20	5.100E-20	4.746E-20	4.274E-20	3.717E-20	3.104E-20	2.458E-20	1.778E-20	3.313E-20
0.0 ---4.14E-07	2.958E-20	2.867E-20	2.709E-20	2.493E-20	2.228E-20	1.925E-20	1.590E-20	1.217E-20	2.007E-20

ENERGY AND ANGULAR DEPENDENT TRANSMISSION FACTORS — NEUTRON PLUS GAMMA-RAY DOSE EQUIVALENT 200 CM TSF CONCRETE SLAB

NEUTRON GROUPS (REMS/((SOURCE NEUTRON)/(CM**2)))

ENERGY GROUP (MEV)	ANGLE 1 MU= 0.9894	ANGLE 2 MU= 0.9446	ANGLE 3 MU= 0.8656	ANGLE 4 MU= 0.7550	ANGLE 5 MU= 0.6179	ANGLE 6 MU= 0.4580	ANGLE 7 MU= 0.2816	ANGLE 8 MU= 0.0950	SCALAR ADJOINT
1.22E 01---1.50E 01	3.256E-14	2.771E-14	2.141E-14	1.563E-14	1.118E-14	7.990E-15	5.700E-15	3.909E-15	1.140E-14
1.00E 01---1.22E 01	2.264E-14	1.969E-14	1.576E-14	1.200E-14	8.951E-15	6.646E-15	4.900E-15	3.460E-15	8.849E-15
8.19E 00---1.00E 01	2.666E-14	2.267E-14	1.751E-14	1.281E-14	9.191E-15	6.602E-15	4.745E-15	3.291E-15	9.379E-15
6.36E 00---8.19E 00	2.241E-14	1.934E-14	1.527E-14	1.141E-14	8.322E-15	6.025E-15	4.329E-15	2.981E-15	8.307E-15
4.97E 00---6.36E 00	1.545E-14	1.377E-14	1.141E-14	8.990E-15	6.864E-15	5.124E-15	3.723E-15	2.543E-15	6.538E-15
4.07E 00---4.97E 00	8.939E-15	8.321E-15	7.362E-15	6.239E-15	5.093E-15	4.007E-15	3.008E-15	2.068E-15	4.620E-15
3.01E 00---4.07E 00	5.445E-15	5.200E-15	4.795E-15	4.279E-15	3.700E-15	3.095E-15	2.482E-15	1.842E-15	3.340E-15
2.46E 00---3.01E 00	7.018E-15	6.599E-15	5.936E-15	5.136E-15	4.294E-15	3.468E-15	2.688E-15	1.939E-15	3.894E-15
2.35E 00---2.46E 00	9.888E-15	8.940E-15	7.599E-15	6.177E-15	4.846E-15	3.673E-15	2.657E-15	1.760E-15	4.483E-15
1.83E 00---2.35E 00	4.948E-15	4.690E-15	4.269E-15	3.740E-15	3.158E-15	2.563E-15	1.977E-15	1.399E-15	2.831E-15
1.11E 00---1.83E 00	3.130E-15	3.000E-15	2.781E-15	2.494E-15	2.161E-15	1.801E-15	1.427E-15	1.036E-15	1.932E-15
5.50E-01---1.11E 00	1.963E-15	1.895E-15	1.778E-15	1.619E-15	1.428E-15	1.213E-15	9.795E-16	7.258E-16	1.277E-15
1.11E-01---5.50E-01	1.252E-15	1.214E-15	1.147E-15	1.056E-15	9.427E-16	8.125E-16	6.678E-16	5.061E-16	8.466E-16
3.35E-03---1.11E-01	1.108E-15	1.074E-15	1.016E-15	9.347E-16	8.347E-16	7.192E-16	5.907E-16	4.471E-16	7.492E-16
5.83E-04---3.35E-03	1.167E-15	1.133E-15	1.072E-15	9.874E-16	8.827E-16	7.614E-16	6.258E-16	4.737E-16	7.921E-16
1.01E-04---5.83E-04	1.120E-15	1.087E-15	1.029E-15	9.476E-16	8.472E-16	7.306E-16	6.003E-16	4.543E-16	7.600E-16
2.90E-05---1.01E-04	1.081E-15	1.049E-15	9.929E-16	9.145E-16	8.173E-16	7.044E-16	5.782E-16	4.369E-16	7.329E-16
1.07E-05---2.90E-05	1.043E-15	1.012E-15	9.575E-16	8.817E-16	7.874E-16	6.779E-16	5.557E-16	4.190E-16	7.057E-16
3.06E-06---1.07E-05	9.819E-16	9.525E-16	9.009E-16	8.290E-16	7.397E-16	6.358E-16	5.199E-16	3.906E-16	6.621E-16
1.12E-06---3.06E-06	9.033E-16	8.761E-16	8.283E-16	7.617E-16	6.786E-16	5.817E-16	4.733E-16	3.529E-16	6.060E-16
4.14E-07---1.12E-06	7.941E-16	7.701E-16	7.278E-16	6.687E-16	5.948E-16	5.079E-16	4.100E-16	3.003E-16	5.288E-16
0.0 ---4.14E-07	5.174E-16	5.043E-16	4.812E-16	4.486E-16	4.073E-16	3.580E-16	3.011E-16	2.348E-16	3.681E-16

TABLE B-8

ENERGY AND ANGULAR DEPENDENT TRANSMISSION FACTORS GAMMA-RAY DOSE EQUIVALENT 15 CM TSF CONCRETE SLAB

GAMMA-RAY GROUPS (REMS/((SOURCE GAMMA-RAY)/(CM**2)))

ENERGY GROUP (MEV)	ANGLE 1 MU= 0.9894	ANGLE 2 MU= 0.9446	ANGLE 3 MU= 0.8656	ANGLE 4 MU= 0.7550	ANGLE 5 MU= 0.6179	ANGLE 6 MU= 0.4580	ANGLE 7 MU= 0.2816	ANGLE 8 MU= 0.0950	SCALAR ADJOINT
8.00E 00---1.00E 01	1.397E-09	1.405E-09	1.431E-09	1.473E-09	1.487E-09	1.349E-09	8.305E-10	1.410E-10	1.074E-09
6.50E 00---8.00E 00	1.186E-09	1.193E-09	1.212E-09	1.241E-09	1.238E-09	1.099E-09	6.519E-10	1.233E-10	8.901E-10
5.00E 00---6.50E 00	9.890E-10	9.936E-10	1.007E-09	1.021E-09	1.001E-09	8.617E-10	4.859E-10	1.043E-10	7.158E-10
4.00E 00---5.00E 00	8.139E-10	8.165E-10	8.228E-10	8.244E-10	7.896E-10	6.530E-10	3.478E-10	8.531E-11	5.622E-10
3.00E 00---4.00E 00	6.603E-10	6.606E-10	6.606E-10	6.512E-10	6.061E-10	4.784E-10	2.409E-10	6.830E-11	4.316E-10
2.50E 00---3.00E 00	5.312E-10	5.296E-10	5.246E-10	5.073E-10	4.571E-10	3.437E-10	1.658E-10	5.392E-11	3.276E-10
2.00E 00---2.50E 00	4.389E-10	4.357E-10	4.273E-10	4.058E-10	3.553E-10	2.566E-10	1.213E-10	4.417E-11	2.573E-10
1.66E 00---2.00E 00	3.581E-10	3.535E-10	3.425E-10	3.184E-10	2.701E-10	1.871E-10	8.791E-11	3.567E-11	1.989E-10
1.33E 00---1.66E 00	2.878E-10	2.824E-10	2.702E-10	2.462E-10	2.026E-10	1.357E-10	6.480E-11	2.892E-11	1.523E-10
1.00E 00---1.33E 00	2.183E-10	2.124E-10	1.998E-10	1.773E-10	1.407E-10	9.101E-11	4.520E-11	2.222E-11	1.092E-10
8.00E-01---1.00E 00	1.562E-10	1.506E-10	1.392E-10	1.204E-10	9.257E-11	5.889E-11	3.119E-11	1.672E-11	7.454E-11
6.00E-01---8.00E-01	1.126E-10	1.076E-10	9.789E-11	8.270E-11	6.205E-11	3.932E-11	2.214E-11	1.259E-11	5.174E-11
4.00E-01---6.00E-01	7.006E-11	6.629E-11	5.925E-11	4.884E-11	3.586E-11	2.299E-11	1.385E-11	8.283E-12	3.111E-11
3.00E-01---4.00E-01	3.788E-11	3.544E-11	3.107E-11	2.502E-11	1.806E-11	1.178E-11	7.483E-12	4.682E-12	1.626E-11
2.00E-01---3.00E-01	2.058E-11	1.909E-11	1.651E-11	1.310E-11	9.435E-12	6.330E-12	4.200E-12	2.717E-12	8.715E-12
1.00E-01---2.00E-01	6.727E-12	6.178E-12	5.274E-12	4.176E-12	3.112E-12	2.271E-12	1.658E-12	1.143E-12	2.959E-12
5.00E-02---1.00E-01	4.546E-14	3.758E-14	2.736E-14	1.866E-14	1.282E-14	3.001E-14	1.520E-14	9.503E-15	2.007E-14
2.00E-02---5.00E-02	1.390E-18	1.006E-18	5.508E-19	2.243E-19	7.281E-20	2.724E-20	1.590E-20	1.137E-20	2.013E-19

TABLE B-9

ENERGY AND ANGULAR DEPENDENT TRANSMISSION FACTORS — GAMMA-RAY DOSE EQUIVALENT 30 CM TSF CONCRETE SLAB

GAMMA-RAY GROUPS (REMS/((SOURCE GAMMA-RAY)/(CM**2)))

ENERGY GROUP (MEV)	ANGLE 1 MU= 0.9894	ANGLE 2 MU= 0.9446	ANGLE 3 MU= 0.8656	ANGLE 4 MU= 0.7550	ANGLE 5 MU= 0.6179	ANGLE 6 MU= 0.4580	ANGLE 7 MU= 0.2816	ANGLE 8 MU= 0.0950	SCALAR ADJOINT
8.00E 00---1.00E 01	7.236E-10	7.082E-10	6.773E-10	6.173E-10	5.011E-10	3.072E-10	9.359E-11	1.461E-11	3.519E-10
6.50E 00---8.00E 00	5.992E-10	5.849E-10	5.557E-10	5.001E-10	3.972E-10	2.357E-10	7.117E-11	1.270E-11	2.826E-10
5.00E 00---6.50E 00	4.792E-10	4.657E-10	4.381E-10	3.870E-10	2.980E-10	1.693E-10	5.097E-11	1.057E-11	2.165E-10
4.00E 00---5.00E 00	3.716E-10	3.588E-10	3.329E-10	2.868E-10	2.125E-10	1.148E-10	3.499E-11	8.454E-12	1.591E-10
3.00E 00---4.00E 00	2.781E-10	2.663E-10	2.428E-10	2.030E-10	1.439E-10	7.402E-11	2.346E-11	6.546E-12	1.121E-10
2.50E 00---3.00E 00	2.029E-10	1.924E-10	1.718E-10	1.389E-10	9.407E-11	4.644E-11	1.565E-11	5.004E-12	7.688E-11
2.00E 00---2.50E 00	1.519E-10	1.426E-10	1.250E-10	9.827E-11	6.415E-11	3.099E-11	1.119E-11	3.947E-12	5.477E-11
1.66E 00---2.00E 00	1.097E-10	1.018E-10	8.742E-11	6.662E-11	4.197E-11	2.007E-11	7.839E-12	3.048E-12	3.762E-11
1.33E 00---1.66E 00	7.740E-11	7.109E-11	5.983E-11	4.436E-11	2.722E-11	1.314E-11	5.550E-12	2.338E-12	2.550E-11
1.00E 00---1.33E 00	4.874E-11	4.417E-11	3.631E-11	2.612E-11	1.568E-11	7.779E-12	3.588E-12	1.645E-12	1.541E-11
8.00E-01---1.00E 00	2.809E-11	2.513E-11	2.022E-11	1.422E-11	8.487E-12	4.420E-12	2.226E-12	1.112E-12	8.658E-12
6.00E-01---8.00E-01	1.621E-11	1.436E-11	1.138E-11	7.896E-12	4.759E-12	2.609E-12	1.405E-12	7.449E-13	4.952E-12
4.00E-01---6.00E-01	7.481E-12	6.562E-12	5.130E-12	3.542E-12	2.186E-12	1.269E-12	7.244E-13	4.039E-13	2.292E-12
3.00E-01---4.00E-01	2.666E-12	2.313E-12	1.783E-12	1.226E-12	7.753E-13	4.753E-13	2.901E-13	1.738E-13	8.212E-13
2.00E-01---3.00E-01	1.012E-12	8.770E-13	6.792E-13	4.771E-13	3.151E-13	2.033E-13	1.297E-13	8.051E-14	3.267E-13
1.00E-01---2.00E-01	1.704E-13	1.504E-13	1.219E-13	9.336E-14	6.972E-14	5.161E-14	3.788E-14	2.701E-14	6.841E-14
5.00E-02---1.00E-01	8.890E-18	6.587E-18	4.288E-18	2.754E-18	1.825E-18	1.254E-18	8.880E-19	1.124E-18	2.263E-18
2.00E-02---5.00E-02	3.193E-28	1.470E-28	3.947E-29	1.015E-29	4.587E-30	2.749E-30	1.830E-30	1.332E-30	2.458E-29

TABLE B-10

ENERGY AND ANGULAR DEPENDENT TRANSMISSION FACTORS — GAMMA-RAY DOSE EQUIVALENT 50 CM TSF CONCRETE SLAB

GAMMA-RAY GROUPS (REMS/((SOURCE GAMMA-RAY)/(CM**2)))

ENERGY GROUP (MEV)	ANGLE 1 MU= 0.9894	ANGLE 2 MU= 0.9446	ANGLE 3 MU= 0.8656	ANGLE 4 MU= 0.7550	ANGLE 5 MU= 0.6179	ANGLE 6 MU= 0.4580	ANGLE 7 MU= 0.2816	ANGLE 8 MU= 0.0950	SCALAR ADJOINT
8.00E 00---1.00E 01	2.900E-10	2.712E-10	2.361E-10	1.825E-10	1.124E-10	4.372E-11	7.555E-12	4.915E-13	9.566E-11
6.50E 00---8.00E 00	2.294E-10	2.132E-10	1.833E-10	1.387E-10	8.284E-11	3.120E-11	5.671E-12	4.760E-13	7.303E-11
5.00E 00---6.50E 00	1.709E-10	1.574E-10	1.329E-10	9.768E-11	5.593E-11	2.030E-11	3.963E-12	4.305E-13	5.187E-11
4.00E 00---5.00E 00	1.200E-10	1.092E-10	9.009E-11	6.376E-11	3.472E-11	1.216E-11	2.597E-12	3.771E-13	3.437E-11
3.00E 00---4.00E 00	7.902E-11	7.090E-11	5.687E-11	3.857E-11	1.994E-11	6.848E-12	1.626E-12	2.999E-13	2.127E-11
2.50E 00---3.00E 00	4.929E-11	4.350E-11	3.382E-11	2.192E-11	1.078E-11	3.693E-12	9.858E-13	2.346E-13	1.246E-11
2.00E 00---2.50E 00	3.172E-11	2.759E-11	2.090E-11	1.307E-11	6.234E-12	2.181E-12	6.428E-13	1.788E-13	7.648E-12
1.66E 00---2.00E 00	1.904E-11	1.630E-11	1.201E-11	7.251E-12	3.381E-12	1.230E-12	4.033E-13	1.303E-13	4.391E-12
1.33E 00---1.66E 00	1.106E-11	9.337E-12	6.717E-12	3.953E-12	1.835E-12	7.045E-13	2.537E-13	9.133E-14	2.471E-12
1.00E 00---1.33E 00	5.341E-12	4.438E-12	3.115E-12	1.795E-12	8.441E-13	3.484E-13	1.390E-13	5.596E-14	1.163E-12
8.00E-01---1.00E 00	2.232E-12	1.830E-12	1.262E-12	7.228E-13	3.526E-13	1.591E-13	7.099E-14	3.192E-14	4.834E-13
6.00E-01---8.00E-01	9.458E-13	7.701E-13	5.285E-13	3.074E-13	1.582E-13	7.747E-14	3.756E-14	1.810E-14	2.093E-13
4.00E-01---6.00E-01	2.892E-13	2.354E-13	1.633E-13	9.867E-14	5.447E-14	2.873E-14	1.477E-14	7.424E-15	6.746E-14
3.00E-01---4.00E-01	5.782E-14	4.659E-14	3.212E-14	1.972E-14	1.142E-14	6.508E-15	3.710E-15	2.102E-15	1.387E-14
2.00E-01---3.00E-01	1.384E-14	1.138E-14	8.204E-15	5.425E-15	3.432E-15	2.123E-15	1.292E-15	7.649E-16	3.794E-15
1.00E-01---2.00E-01	1.140E-15	9.937E-16	7.982E-16	6.112E-16	4.574E-16	3.389E-16	2.488E-16	1.774E-16	4.498E-16
5.00E-02---1.00E-01	1.537E-22	1.169E-22	8.052E-23	5.461E-23	3.767E-23	7.976E-23	4.269E-23	2.728E-23	5.801E-23
2.00E-02---5.00E-02	1.422E-37	4.695E-38	9.149E-39	2.937E-39	1.557E-39	9.497E-40	6.346E-40	4.630E-40	8.619E-39

TABLE B-11

ENERGY AND ANGULAR DEPENDENT TRANSMISSION FACTORS

GAMMA-RAY DOSE EQUIVALENT 75 CM TSF CONCRETE SLAB

GAMMA-RAY GROUPS (REMS/((SOURCE GAMMA-RAY)/(CM**2)))

ENERGY GROUP (MEV)	ANGLE 1 MU= 0.9894	ANGLE 2 MU= 0.9446	ANGLE 3 MU= 0.8656	ANGLE 4 MU= 0.7550	ANGLE 5 MU= 0.6179	ANGLE 6 MU= 0.4580	ANGLE 7 MU= 0.2816	ANGLE 8 MU= 0.0950	SCALAR ADJOINT
8.00E 00---1.00E 01	8.824E-11	7.816E-11	6.044E-11	3.805E-11	1.699E-11	4.147E-12	4.596E-13	-3.270E-14	2.108E-11
6.50E 00---8.00E 00	6.510E-11	5.712E-11	4.341E-11	2.656E-11	1.133E-11	2.611E-12	3.093E-13	3.617E-14	1.496E-11
5.00E 00---6.50E 00	4.382E-11	3.791E-11	2.807E-11	1.651E-11	6.692E-12	1.517E-12	2.055E-13	2.910E-14	9.579E-12
4.00E 00---5.00E 00	2.679E-11	2.275E-11	1.630E-11	9.119E-12	3.490E-12	7.895E-13	1.248E-13	2.085E-14	5.513E-12
3.00E 00---4.00E 00	1.482E-11	1.233E-11	8.507E-12	4.516E-12	1.642E-12	3.804E-13	6.957E-14	1.349E-14	2.867E-12
2.50E 00---3.00E 00	7.454E-12	6.057E-12	4.008E-12	2.013E-12	7.013E-13	1.707E-13	3.642E-14	8.125E-15	1.354E-12
2.00E 00---2.50E 00	3.923E-12	3.127E-12	2.003E-12	9.690E-13	3.335E-13	8.665E-14	2.075E-14	5.126E-15	6.819E-13
1.66E 00---2.00E 00	1.842E-12	1.439E-12	8.916E-13	4.175E-13	1.446E-13	4.095E-14	1.107E-14	3.035E-15	3.076E-13
1.33E 00---1.66E 00	8.298E-13	6.372E-13	3.855E-13	1.780E-13	6.368E-14	1.969E-14	5.878E-15	1.768E-15	1.353E-13
1.00E 00---1.33E 00	2.859E-13	2.159E-13	1.280E-13	5.921E-14	2.240E-14	7.659E-15	2.556E-15	8.673E-16	4.604E-14
8.00E-01---1.00E 00	7.843E-14	5.841E-14	3.426E-14	1.618E-14	6.636E-15	2.585E-15	1.004E-15	3.944E-16	1.273E-14
6.00E-01---8.00E-01	2.260E-14	1.685E-14	1.006E-14	5.032E-15	2.279E-15	9.958E-16	4.316E-16	1.853E-16	3.871E-15
4.00E-01---6.00E-01	4.144E-15	3.162E-15	2.002E-15	1.107E-15	5.638E-16	2.719E-16	1.261E-16	5.669E-17	8.020E-16
3.00E-01---4.00E-01	3.935E-16	2.975E-16	1.881E-16	1.063E-16	5.697E-17	2.997E-17	1.584E-17	8.413E-18	7.843E-17
2.00E-01---3.00E-01	5.497E-17	4.360E-17	3.020E-17	1.935E-17	1.190E-17	7.140E-18	4.190E-18	2.381E-18	1.370E-17
1.00E-01---2.00E-01	2.169E-18	1.887E-18	1.515E-18	1.160E-18	8.686E-19	6.436E-19	4.726E-19	3.370E-19	8.541E-19
5.00E-02---1.00E-01	1.264E-28	9.589E-29	6.606E-29	4.480E-29	3.091E-29	6.540E-29	3.503E-29	2.239E-29	4.760E-29
2.00E-02---5.00E-02	4.304E-51	8.895E-52	1.594E-52	6.777E-53	3.742E-53	2.293E-53	1.533E-53	1.121E-53	2.103E-52

TABLE B-12

ENERGY AND ANGULAR DEPENDENT TRANSMISSION FACTORS — GAMMA-RAY DOSE EQUIVALENT 100 CM TSF CONCRETE SLAB

GAMMA-RAY GROUPS (REMS/((SOURCE GAMMA-RAY)/(CM**2)))

ENERGY GROUP (MEV)	ANGLE 1 MU= 0.9894	ANGLE 2 MU= 0.9446	ANGLE 3 MU= 0.8656	ANGLE 4 MU= 0.7550	ANGLE 5 MU= 0.6179	ANGLE 6 MU= 0.4580	ANGLE 7 MU= 0.2816	ANGLE 8 MU= 0.0950	SCALAR ADJOINT
8.00E 00---1.00E 01	2.607E-11	2.178E-11	1.500E-11	7.761E-12	2.528E-12	3.919E-13	3.053E-14	4.461E-15	4.909E-12
6.50E 00---8.00E 00	1.785E-11	1.471E-11	9.881E-12	4.926E-12	1.534E-12	2.367E-13	2.157E-14	3.347E-15	3.228E-12
5.00E 00---6.50E 00	1.078E-11	8.722E-12	5.669E-12	2.693E-12	7.957E-13	1.244E-13	1.344E-14	2.222E-15	1.854E-12
4.00E 00---5.00E 00	5.684E-12	4.493E-12	2.800E-12	1.254E-12	3.505E-13	5.669E-14	7.332E-15	1.233E-15	9.203E-13
3.00E 00---4.00E 00	2.626E-12	2.023E-12	1.205E-12	5.086E-13	1.365E-13	2.341E-14	3.544E-15	6.307E-16	4.004E-13
2.50E 00---3.00E 00	1.052E-12	7.867E-13	4.451E-13	1.767E-13	4.611E-14	8.624E-15	1.529E-15	2.862E-16	1.506E-13
2.00E 00---2.50E 00	4.507E-13	3.293E-13	1.796E-13	6.890E-14	1.819E-14	3.737E-15	7.420E-16	1.494E-16	6.193E-14
1.66E 00---2.00E 00	1.640E-13	1.170E-13	6.155E-14	2.306E-14	6.324E-15	1.463E-15	3.287E-16	7.293E-17	2.173E-14
1.33E 00---1.66E 00	5.700E-14	3.996E-14	2.062E-14	7.763E-15	2.274E-15	5.876E-16	1.460E-16	3.591E-17	7.438E-15
1.00E 00---1.33E 00	1.398E-14	9.668E-15	4.953E-15	1.925E-15	6.153E-16	1.780E-16	5.001E-17	1.433E-17	1.827E-15
8.00E-01---1.00E 00	2.480E-15	1.692E-15	8.651E-16	3.514E-16	1.258E-16	4.316E-17	1.480E-17	5.184E-18	3.286E-16
6.00E-01---8.00E-01	4.870E-16	3.376E-16	1.814E-16	8.152E-17	3.342E-17	1.326E-17	5.263E-18	2.081E-18	7.026E-17
4.00E-01---6.00E-01	5.403E-17	3.955E-17	2.380E-17	1.260E-17	6.132E-18	2.801E-18	1.218E-18	5.074E-19	9.474E-18
3.00E-01---4.00E-01	2.382E-18	1.722E-18	1.032E-18	5.539E-19	2.806E-19	1.383E-19	6.820E-20	3.396E-20	4.234E-19
2.00E-01---3.00E-01	1.996E-19	1.554E-19	1.056E-19	6.664E-20	4.039E-20	2.381E-20	1.368E-20	7.579E-21	4.745E-20
1.00E-01---2.00E-01	4.089E-21	3.557E-21	2.856E-21	2.187E-21	1.637E-21	1.213E-21	8.906E-22	6.351E-22	1.610E-21
5.00E-02---1.00E-01	1.012E-34	7.696E-35	5.314E-35	3.610E-35	2.494E-35	5.416E-35	2.874E-35	1.831E-35	3.870E-35
2.00E-02---5.00E-02	3.495E-64	5.046E-65	1.048E-65	4.849E-66	2.700E-66	1.658E-66	1.109E-66	8.111E-67	1.527E-65

TABLE B-13

ENERGY AND ANGULAR DEPENDENT TRANSMISSION FACTORS

GAMMA-RAY DOSE EQUIVALENT 150 CM TSF CONCRETE SLAB

GAMMA-RAY GROUPS (REMS/((SOURCE GAMMA-RAY)/(CM**2)))

ENERGY GROUP (MEV)	ANGLE 1 MU= 0.9894	ANGLE 2 MU= 0.9446	ANGLE 3 MU= 0.8656	ANGLE 4 MU= 0.7550	ANGLE 5 MU= 0.6179	ANGLE 6 MU= 0.4580	ANGLE 7 MU= 0.2816	ANGLE 8 MU= 0.0950	SCALAR ADJOINT
8.00E 00---1.00E 01	2.146E-12	1.592E-12	8.702E-13	3.085E-13	5.672E-14	4.164E-15	4.975E-16	1.194E-16	2.880E-13
6.50E 00---8.00E 00	1.249E-12	9.087E-13	4.794E-13	1.618E-13	2.840E-14	2.184E-15	2.798E-16	4.779E-17	1.610E-13
5.00E 00---6.50E 00	6.024E-13	4.271E-13	2.154E-13	6.851E-14	1.153E-14	9.634E-16	1.304E-16	1.186E-17	7.389E-14
4.00E 00---5.00E 00	2.334E-13	1.602E-13	7.635E-14	2.264E-14	3.688E-15	3.531E-16	4.318E-17	-7.520E-19	2.702E-14
3.00E 00---4.00E 00	7.491E-14	4.968E-14	2.238E-14	6.250E-15	1.016E-15	1.123E-16	1.174E-17	-1.935E-18	8.208E-15
2.50E 00---3.00E 00	1.866E-14	1.188E-14	4.997E-15	1.301E-15	2.127E-16	2.820E-17	2.477E-18	-7.274E-19	1.921E-15
2.00E 00---2.50E 00	5.272E-15	3.266E-15	1.323E-15	3.388E-16	5.900E-17	9.062E-18	7.654E-19	-2.292E-19	5.251E-16
1.66E 00---2.00E 00	1.136E-15	6.835E-16	2.672E-16	6.847E-17	1.318E-17	2.399E-18	2.534E-19	-2.591E-20	1.098E-16
1.33E 00---1.66E 00	2.348E-16	1.395E-16	5.464E-17	1.485E-17	3.255E-18	6.716E-19	9.331E-20	3.939E-21	2.273E-17
1.00E 00---1.33E 00	2.919E-17	1.747E-17	7.164E-18	2.176E-18	5.434E-19	1.220E-19	2.410E-20	4.111E-21	2.940E-18
8.00E-01---1.00E 00	2.119E-18	1.250E-18	5.156E-19	1.675E-19	4.849E-20	1.363E-20	3.680E-21	1.003E-21	2.157E-19
6.00E-01---8.00E-01	1.947E-19	1.218E-19	5.730E-20	2.252E-20	7.958E-21	2.696E-21	9.285E-22	3.208E-22	2.301E-20
4.00E-01---6.00E-01	8.259E-21	5.809E-21	3.364E-21	1.727E-21	8.124E-22	3.556E-22	1.468E-22	5.756E-23	1.341E-21
3.00E-01---4.00E-01	7.457E-23	5.123E-23	2.903E-23	1.475E-23	6.987E-24	3.154E-24	1.395E-24	6.172E-25	1.177E-23
2.00E-01---3.00E-01	2.387E-24	1.829E-24	1.225E-24	7.636E-25	4.570E-25	2.654E-25	1.496E-25	8.094E-26	5.464E-25
1.00E-01---2.00E-01	1.463E-26	1.273E-26	1.022E-26	7.825E-27	5.857E-27	4.340E-27	3.187E-27	2.272E-27	5.760E-27
5.00E-02---1.00E-01	6.672E-47	5.075E-47	3.507E-47	2.384E-47	1.648E-47	3.610E-47	1.910E-47	1.215E-47	2.564E-47
2.00E-02---5.00E-02	0.0	0.0	0.0	0.0	0.0	0.0	0.0	0.0	0.0

TABLE B-14

ENERGY AND ANGULAR DEPENDENT TRANSMISSION FACTORS

GAMMA-RAY DOSE EQUIVALENT 200 CM TSF CONCRETE SLAB

GAMMA-RAY GROUPS (REMS/((SOURCE GAMMA-RAY)/(CM**2)))

ENERGY GROUP (MEV)	ANGLE 1 MU= 0.9894	ANGLE 2 MU= 0.9446	ANGLE 3 MU= 0.8656	ANGLE 4 MU= 0.7550	ANGLE 5 MU= 0.6179	ANGLE 6 MU= 0.4580	ANGLE 7 MU= 0.2816	ANGLE 8 MU= 0.0950	SCALAR ADJOINT
8.00E 00---1.00E 01	1.679E-13	1.107E-13	4.828E-14	1.193E-14	1.303E-15	6.503E-17	8.553E-18	-9.452E-18	1.774E-14
6.50E 00---8.00E 00	8.250E-14	5.308E-14	2.214E-14	5.156E-15	5.445E-16	3.498E-17	8.491E-19	-6.086E-18	8.380E-15
5.00E 00---6.50E 00	3.162E-14	1.972E-14	7.794E-15	1.701E-15	1.780E-16	1.560E-17	-1.175E-18	-3.143E-18	3.068E-15
4.00E 00---5.00E 00	8.928E-15	5.352E-15	1.978E-15	4.002E-16	4.274E-17	5.096E-18	-8.696E-19	-1.048E-18	8.206E-16
3.00E 00---4.00E 00	1.991E-15	1.150E-15	4.007E-16	7.711E-17	8.800E-18	1.372E-18	-3.465E-19	-2.980E-19	1.748E-16
2.50E 00---3.00E 00	3.034E-16	1.662E-16	5.321E-17	9.401E-18	1.136E-18	2.205E-19	-6.596E-20	-4.495E-20	2.501E-17
2.00E 00---2.50E 00	5.663E-17	3.024E-17	9.415E-18	1.683E-18	2.278E-19	4.819E-20	-1.366E-20	-9.113E-21	4.564E-18
1.66E 00---2.00E 00	7.156E-18	3.698E-18	1.116E-18	2.050E-19	3.236E-20	7.238E-21	-1.541E-21	-1.046E-21	5.618E-19
1.33E 00---1.66E 00	8.831E-19	4.566E-19	1.434E-19	3.011E-20	5.582E-21	1.215E-21	-7.870E-23	-1.056E-22	7.081E-20
1.00E 00---1.33E 00	5.597E-20	3.023E-20	1.079E-20	2.838E-21	6.112E-22	1.220E-22	1.547E-23	-7.423E-25	4.897E-21
8.00E-01---1.00E 00	1.632E-21	8.633E-22	3.086E-22	8.574E-23	2.113E-23	5.205E-24	1.063E-24	1.786E-25	1.424E-22
6.00E-01---8.00E-01	7.103E-23	4.187E-23	1.845E-23	6.761E-24	2.174E-24	6.537E-25	1.997E-25	6.001E-26	7.616E-24
4.00E-01---6.00E-01	1.208E-24	8.387E-25	4.817E-25	2.457E-25	1.148E-25	4.978E-26	2.032E-26	7.877E-27	1.923E-25
3.00E-01---4.00E-01	2.133E-27	1.432E-27	7.935E-28	3.942E-28	1.810E-28	7.806E-29	3.238E-29	1.317E-29	3.204E-28
2.00E-01---3.00E-01	2.735E-29	2.086E-29	1.391E-29	8.635E-30	5.148E-30	2.975E-30	1.667E-30	8.950E-31	6.188E-30
1.00E-01---2.00E-01	5.281E-32	4.593E-32	3.688E-32	2.824E-32	2.114E-32	1.566E-32	1.150E-32	8.201E-33	2.079E-32
5.00E-02---1.00E-01	4.588E-59	3.482E-59	2.400E-59	1.629E-59	1.124E-59	2.398E-59	1.281E-59	8.176E-60	1.735E-59
2.00E-02---5.00E-02	0.0	0.0	0.0	0.0	0.0	0.0	0.0	0.0	0.0

ORNL-RSIC-26
UC-34 — Physics

INTERNAL DISTRIBUTION

1-3. L. S. Abbott
4. R. G. Alsmiller, Jr.
5. T. W. Armstrong
6. J. A. Auxier
7. J. R. Buchanan
8. C. E. Burgart
9. V. R. Cain
10. H. C. Claiborne
11. C. E. Clifford
12. F. C. Maienschein
13. F. R. Mynatt, CTC
14. R. W. Peelle
15. R. W. Roussin
16. W. S. Snyder
17. E. A. Straker
18. D. K. Trubey
19. E. R. Cohen (consultant)
20. H. Feshbach (consultant)
21. H. Goldstein (consultant)
22-23. Central Research Library
24. ORNL Y-12 Technical Library, Document Reference Section
25-124. Laboratory Records (RSIC)
125. Laboratory Records ORNL RC
126. ORNL Patent Office

EXTERNAL DISTRIBUTION

127. Z. G. Burson, EG&G, 680 E. Sunset Rd., Las Vegas, Nev. 89101
128. A. B. Chilton, 207 Nuclear Engineering Lab., University of Illinois Urbana, Ill. 61801
129. Charles Eisenhauer, Radiation Physics Division, National Bureau of Standards, Gaithersburg, Md. 20760
130. Major R. W. Enz, Radiation Physics Branch, DASA, Washington, D. C. 20301
131. W. H. Hannum, Division of Reactor Development & Technology, U. S. Atomic Energy Commission, Washington, D. C. 20545
132. P. B. Hemmig, Division of Reactor Development & Technology, U. S. Atomic Energy Commission, Washington, D. C. 20545
133-137. F. A. R. Schmidt, Institut fur Kernenergetik, 7000 Stuttgart 80, Pfaffenwaldring 31, Germany
138. L. V. Spencer, National Bureau of Standards, Washington, D. C. 20234
139-148. Division of Technical Information Extension (DTIE)
149. Laboratory and University Division (ORO). Attn: Kermit O. Laughon
150-383. Given Distribution as shown in TID-4500 under Physics Category (25 copies - CFSTI)